

DETERMINISTIC CHANNEL EQUALIZATION FOR  
SPATIAL MULTIPLEXING AND SPACE-TIME CODED  
TRANSMISSIONS

by

Zhan Zhang

Submitted in partial fulfillment of the  
requirements for the degree of

DOCTOR OF PHILOSOPHY

Major Subject: Electrical and Computer Engineering

at

DALHOUSIE UNIVERSITY

Halifax, Nova Scotia

September, 2003

© Copyright by Zhan Zhang, 2003



National Library  
of Canada

Bibliothèque nationale  
du Canada

Acquisitions and  
Bibliographic Services

Acquisitions et  
services bibliographiques

395 Wellington Street  
Ottawa ON K1A 0N4  
Canada

395, rue Wellington  
Ottawa ON K1A 0N4  
Canada

*Your file   Votre référence*

*ISBN: 0-612-89102-X*

*Our file   Notre référence*

*ISBN: 0-612-89102-X*

The author has granted a non-exclusive licence allowing the National Library of Canada to reproduce, loan, distribute or sell copies of this thesis in microform, paper or electronic formats.

L'auteur a accordé une licence non exclusive permettant à la Bibliothèque nationale du Canada de reproduire, prêter, distribuer ou vendre des copies de cette thèse sous la forme de microfiche/film, de reproduction sur papier ou sur format électronique.

The author retains ownership of the copyright in this thesis. Neither the thesis nor substantial extracts from it may be printed or otherwise reproduced without the author's permission.

L'auteur conserve la propriété du droit d'auteur qui protège cette thèse. Ni la thèse ni des extraits substantiels de celle-ci ne doivent être imprimés ou autrement reproduits sans son autorisation.

---

In compliance with the Canadian Privacy Act some supporting forms may have been removed from this dissertation.

Conformément à la loi canadienne sur la protection de la vie privée, quelques formulaires secondaires ont été enlevés de ce manuscrit.

While these forms may be included in the document page count, their removal does not represent any loss of content from the dissertation.

Bien que ces formulaires aient inclus dans la pagination, il n'y aura aucun contenu manquant.

**Canada**

**Dalhousie University**  
**Faculty of Engineering**

The undersigned hereby certify that they have examined, and recommend to the Faculty of Graduate Studies for acceptance, the thesis entitled "**Deterministic Channel Equalization for Spatial Multiplexing and Space-Time Coded Transmissions**" by **Zhan Zhang** in partial fulfillment of the requirements for the degree of **Doctor of Philosophy**.

Dated: Oct 3<sup>rd</sup> 2003

/

Supervisor:

/ Dr. Jacek Ilow

External Examiner:

Dr. Brent R. Petersen

Examiners:

Dr. Ezz El-Masry

^


Dr. William J. Phillips

**Dalhousie University**  
**Faculty of Engineering**

Date: Oct. 6<sup>th</sup>, 2003

Author: **Zhan Zhang**  
Title: **Deterministic Channel Equalization for Spatial Multiplexing and  
Space-Time Coded Transmissions**  
Major Subject: **Electrical and Computer Engineering**  
Degree: **Doctor of Philosophy**  
Convocation: **May, 2004**

Permission is herewith granted to Dalhousie University to circulate and to have copied for non-commercial purposes, at its discretion, the above thesis upon the request of individuals or institutions.

  
\_\_\_\_\_  
Signature of Author

The author reserves other publication rights, and neither the thesis nor extensive extracts from it may be printed or otherwise reproduced without the author's written permission.

The author attests that permission has been obtained for the use of any copyrighted material appearing in this thesis (other than brief excerpts requiring only proper acknowledgement in scholarly writing), and that all such use is clearly acknowledged.

*To my parents and my wife*

# Contents

<b>List of Figures</b>	<b>viii</b>
<b>List of Abbreviations</b>	<b>xi</b>
<b>Notations and Symbols</b>	<b>xiv</b>
<b>Acknowledgements</b>	<b>xvi</b>
<b>Abstract</b>	<b>xvii</b>
<b>1 Introduction</b>	<b>1</b>
1.1 Dissertation Objectives, Contributions and Outline . . . . .	4
1.1.1 Objectives and Organization . . . . .	4
1.1.2 Research Impact . . . . .	7
1.2 Evolution and Characteristics of Wireless Communications . . . . .	9
1.2.1 Channel Capacity . . . . .	9
1.2.2 Challenges in Wireless Communications . . . . .	13
1.2.3 Advanced Digital Signal Processing . . . . .	14
1.3 Spatial Diversity and MIMO Systems . . . . .	15
1.3.1 Spatial Multiplexing and Beamforming Schemes . . . . .	15
1.3.2 Space-Time Coded Schemes . . . . .	18
1.4 Multipath Propagation Environment . . . . .	19

1.4.1	Multipath Characteristics . . . . .	19
1.4.2	Time-Dispersive Channel Modeling . . . . .	20
1.5	MIMO Channel Characterization . . . . .	22
1.5.1	MIMO Flat-Fading Channel Modeling . . . . .	23
1.5.2	MIMO Time-Dispersive Fading Channel Characterization . . . . .	25
1.6	Channel Identification and Equalization . . . . .	30
<b>2</b>	<b>Frequency Domain Equalization for MIMO Space-Time Transmissions with Single Carrier Signaling</b>	<b>34</b>
2.1	Motivations . . . . .	35
2.2	Transmission Signaling . . . . .	36
2.3	Receiver Algorithm for SIMO Cases . . . . .	38
2.4	MIMO: Spatial Multiplexing Cases . . . . .	42
2.5	Performance Simulations . . . . .	46
2.6	Summary . . . . .	48
<b>3</b>	<b>Blind Channel Equalization for DSTM Signaling Transmissions over Rich-Multipath Channels</b>	<b>53</b>
3.1	Introduction . . . . .	54
3.2	Review of the Differential Space-Time Modulation . . . . .	55
3.3	New Receiver Algorithm for Transmission over FIR Rich-Multipath Fading Channels . . . . .	56
3.3.1	Basis Representations of the Transmitted Signals . . . . .	56
3.3.2	Column Rank Assumption of Channel Matrices and Oversampling .	61
3.3.3	Estimation of the Multiple Transmitted Signals from Received Data in Presence of Noise and Rich Multipath Channels . . . . .	64
3.4	Performance Simulations . . . . .	69
3.5	Summary . . . . .	70

<b>4</b>	<b>Differential Space-Time Modulation for Transmissions Over Unknown Time-Dispersive Channels</b>	<b>76</b>
4.1	Motivation and Methodology . . . . .	77
4.2	DSTT's Signal Frame and Modulation . . . . .	78
4.2.1	Encoding the Information Bits to the ST Frames . . . . .	78
4.2.2	Extending the ST Frame Circularly and Modulating the Symbols . .	80
4.3	The Receiver Algorithm . . . . .	81
4.3.1	The Received Signal Structure . . . . .	81
4.3.2	Signal Detection . . . . .	83
4.4	Performance Simulations . . . . .	85
4.5	Summary . . . . .	87
<b>5</b>	<b>Conclusions</b>	<b>91</b>
5.1	Dissertation Summary . . . . .	92
5.2	Future Directions . . . . .	93
	<b>Appendix</b>	<b>98</b>
	<b>Bibliography</b>	<b>98</b>



# List of Figures

1.1	A System Modeling in Shannon's Channel Capacity Research. . . . .	10
1.2	Multi-Element Antenna Transceiver System Modeling. . . . .	11
1.3	Modeling of a General Wireless Communication System. . . . .	13
1.4	Channel Impulse Response Illustration. . . . .	19
1.5	Equivalent Discrete-Time Linear Filter Model of FIR Channel. . . . .	20
1.6	Visualization of the MIMO Scatter Modeling. . . . .	24
1.7	Visualization of the Multipath Propagation and Scattering. . . . .	26
1.8	MIMO System Input-Output Relations in the $z$ -domain. . . . .	28
1.9	Mathematical Modeling of a MIMO System with $K$ Transmit and $M$ Re- ceive Antennas. . . . .	30
2.1	The Timing of the Transmitted and Received Signal Streams. . . . .	37
2.2	Single-Input Multiple-Output System. . . . .	38
2.3	Spatial Multiplexing Transceiver. . . . .	43
2.4	The BER Performance over Multipath Fading Channel (MIMO cases: QPSK- SCFDE, QPSK-OFDM). . . . .	49
2.5	Symbol Constellations Before and After Equalization (MIMO cases: QPSK- SCFDE, $M=4$ , $K=4$ , $SNR=15.2$ dB for upper figures, $SNR=20$ dB for lower figures). . . . .	49
2.6	The BER Performance over Multipath Fading Channel (MIMO cases: 16QAM- SCFDE, 16QAM-OFDM). . . . .	50

2.7	Symbol Constellations Before and After Equalization (MIMO cases: 16-ary QAM SCFDE, $M=4$ , $K=4$ , SNR=18 dB for Upper Figures, SNR=22.2 dB for Lower Figures).	50
2.8	The BER Performance over Multipath Fading Channel (SIMO Cases: QPSK-SCFDE, QPSK-OFDM).	51
2.9	The BER Performance over Multipath Fading Channel (SIMO Cases: 16QAM-SCFDE, 16QAM-OFDM).	51
2.10	Symbol Constellation Before and After Channel Equalization (SIMO Cases: QPSK-SCFDE, 16QAM-SCFDE).	52
3.1	Transmitted Signal Frame Structure and Timing.	57
3.2	Received Signal Constellation Diagram { $L=7$ , $M=6$ , $K=4$ , $P=1$ , SNR = 18.5 dB. }	71
3.3	Signal Constellation Diagram After Equalization { $L=7$ , $M=6$ , $K=4$ , $P=1$ , SNR= 18.5 dB. }	71
3.4	Received Signal Constellation Diagram { $L=7$ , $M=6$ , $K=4$ , $P=1$ , SNR =19.3 dB. }	71
3.5	Signal Constellation Diagram After Equalization { $L=7$ , $M=6$ , $K=4$ , $P=1$ , SNR= 19.3 dB. }	71
3.6	Received Signal Constellation Diagram { $L=7$ , $M=6$ , $K=4$ , $P=1$ , SNR = 21.4 dB. }	72
3.7	Signal Constellation Diagram After Equalization { $L=7$ , $M=6$ , $K=4$ , $P=1$ , SNR= 21.4 dB. }	72
3.8	System BER Performance in Time-Dispersive Fading Channel ( $L=3$ , $K=4$ , $P=1$ ).	72
3.9	System BER Performance in Time-Dispersive Fading Channel ( $L=5$ , $K=4$ , $P=1$ ).	73
3.10	System BER Performance in Time-Dispersive Fading Channel ( $L=7$ , $K=4$ , $P=1$ ).	73

3.11	System Bit Error Rate Performance in Time-Dispersive Fading Channel ( $L=5, K=4, M=5, 6, P=1$ ). . . . .	74
3.12	System Bit Error Rate Performance in Time-Dispersive Fading Channel ( $L=6, K=4, M=5, 6, P=1$ ). . . . .	74
3.13	System Bit Error Rate Performance in Time-Dispersive Fading Channel ( $L=7, K=4, M=5, 6, P=1$ ). . . . .	75
4.1	The Timing of the Symbol Stream in the Transmitted Frame. . . . .	80
4.2	The DSTT BER Performance ( $\mathcal{M} = 8, K = 3, M = 1, J = 12$ ). . . . .	88
4.3	The DSTT BER Performance ( $\mathcal{M} = 8, K = 3, M = 2, J = 12$ ). . . . .	88
4.4	The DSTM BER Performance in Frequency-Selective Fading Channels ( $\mathcal{M} = 4, K = 4, M = 1$ ). . . . .	89
4.5	The DSTT BER Performance ( $\mathcal{M} = 4, K = 4, M = 1, J = 4$ ). . . . .	89
4.6	The DSTM BER Performance in Frequency-Selective Fading Channels ( $\mathcal{M} = 4, K = 4, M = 2$ ). . . . .	90
4.7	The DSTT BER Performance ( $\mathcal{M} = 4, K = 4, M = 2, J = 4$ ). . . . .	90

# Abbreviations and Acronyms

AWGN	Additive White Gaussian Noise
BER	Bit Error Rate
BLAST	Bell Laboratory Layered Space Time
BPSK	Binary Phase Shift Keying
BWA	Broadband Wireless Access
$bps/Hz$	Bit Per Second Per Hertz
CIR	Channel Impulse Response
CCI	Co-Channel Interference
CDMA	Code Division Multiple Access
CM	Constant Modulus
CMA	Constant Modulus Algorithm
DFT	Discrete Fourier Transform
DFE	Decision-Feed-back Equalizer
DOA	Direction of Arrival
DPSK	Differential Phase Shift Keying
DSP	Digital Signal Processing
DS-SS	Direct Sequence Spread Spectrum
DSTM	Differential Space Time Modulation
$E_b/N_0$	Bit Energy-to-Noise Density Ratio

FA	Finite Alphabet
FIR	Finite Impulse Response
LSE	Least Square Estimation
LOS	Line of Sight
HOS	Higher-Order Statistics
IDFT	Inverse Discrete Fourier Transform
ISI	Inter-Symbol Interference
MAI	Multiple Access Interference
MAP	Maximum A Posteriori Probability
MCMA	Multiple-Constant-Modulus Algorithm
MEA	Multiple-Element Antenna
MIMO	Multiple-Input and Multiple-Output
ML	Maximum Likelihood
MLSE	Maximum Likelihood Sequence Estimation
MRC	Maximum-Ratio Combining
MSE	Mean Square Error Criterion
MMSE	Minimum Mean Square Error
MUD	Multi-User Detection
OFDM	Orthogonal Frequency Division Multiplexing
PA	Power Amplifier
PAPR	Peak-to-Average Power Ratio
PCS	Personal Communication System
PDA	Personal Digital Assistant
PDF	Probability Density Function
PSK	Phase Shift Keying

QAM	Quadrature Amplitude Modulation
QPSK	Quadrature Phase Shift Keying
QoS	Quality of Service
RF	Radio Frequency
SCFDE	Single-Carrier Frequency Domain Equalization
SDMA	Space-Division Multiple Access
SIMO	Single Input and Multiple Output
SIR	Signal-to-Interference Ratio
SINR	Signal-to-Interference-plus-Noise-Ratio
SNR	Signal-to-Noise Ratio
SS	Spread Spectrum
ST	Space-Time
STBC	Space-Time Block Code
STC	Space-Time Code
STT	Space-Time Trellis
STTC	Space-Time Trellis Code
SVD	Singular Value Decomposition
TCM	Trellis Coded Modulation
TDMA	Time Division Multiple Access
ULA	Uniform Linear Antenna Array
VA	Viterbi Algorithm

# Notations and Symbols

In this dissertation, bold-face letters denote matrices and vectors whereas the scalar variables are in plain lower-case letters. The most of notations adopted in this dissertation are standard algebraic representations. The others conform to the Matlab® notations for descriptions of the matrices or vectors. All the computer simulations in this dissertation were conducted in the Matlab® computing environment. Some definition and concepts used in the following chapters, such as channel capacity, complex Gaussian random variable, and singular value decomposition (SVD), are described in Appendix. The notations and symbols used in this dissertation are listed as follows.

$(\cdot)^H$	Hermitian Transpose (Complex Conjugate Transpose)
$(\cdot)^T$	Matrix Transpose
$(\cdot)^*$	Complex Conjugate
$(\cdot)^{-1}$	Matrix Inverse
$(\cdot)^\dagger$	Matrix Pseudo-Inverse
$\mathbf{I}_{n \times n}$	$n \times n$ Identity matrix
$\ \cdot\ $	Norm of Vector or Matrix
$\ \cdot\ _{Frob}$	Frobenius Norm
$[\mathbf{A}, \mathbf{B}]$	Concatenation of Matrix A and Matrix B
$\mathbf{A}_{[:, m]}$	$m^{th}$ Column of Matrix A
$\mathbf{A}_{[j, :]}$	$j^{th}$ Row of Matrix A
$\mathbf{A}_{[i:j, :]}$	Rows from $i^{th}$ to $j^{th}$ of Matrix A

$\mathbf{A}_{[:, i:j]}$	Columns from $i^{th}$ to $j^{th}$ of Matrix $\mathbf{A}$
$\mathbf{A}_{(i,j)}$	The Element at $i^{th}$ Row and $j^{th}$ Column of Matrix $\mathbf{A}$
$\text{Trace}(\mathbf{A})$	Trace of Matrix $\mathbf{A}$
$\text{diag} \{a_1, a_2, \dots, a_q\}$	An $n \times n$ Diagonal Matrix with Diagonal Elements $\{a_1, a_2, \dots, a_q\}$
$\hat{\mathbf{A}}$	Estimate of Matrix $\mathbf{A}$
$\Re\{\cdot\}$	Real Part of Complex Matrix or Scalar Value
$\Im\{\cdot\}$	Imaginary Part of Complex Matrix or Scalar Value
$E(\cdot)$	Statistical Expectation
$\mathcal{CN}$	Complex Normal Distribution
$\arg \max_c (\mathbf{A}(c))$	Argument Maximizing the Function $\mathbf{A}(c)$ over the Set $c$
$\arg \min_c (\mathbf{A}(c))$	Argument Minimizing the Function $\mathbf{A}(c)$ over the Set $c$
$\exp(\cdot)$	Exponential Function
$M$	The Number of Receiver Antennas
$K$	The Number of Transmitter Antennas
$f_c$	Carrier Frequency
$T_s$	Symbol Duration



# Acknowledgements

Firstly, I would like to express gratitude to supervisor Dr. Jacek Ilow for his stimulating advice and encouragement during my Ph.D. studies and research at Dalhousie University. It has been very rewarding to work with his research group. I would like to thank Dr. Ilow for his time for me to present and discuss on my research subject and progress. I also like to thank the following professors: Dr. Qi-Ming He for his discussions on the stochastic process; Dr. William J. Phillips for his insightful and helpful explanations on wavelet theory and filter-banks; Dr. Zhizhang Chen for his instruction regarding wireless link signal power budgeting and wireless channel characteristics; Dr. Ezz El-Masry and Dr. Brent R. Petersen for their valuable suggestions for improvement on my dissertation.

I also wish to thank my colleagues: Rex Antony, Tong Wang, Helen (Congying) Xia, Mingli You, Mohan Baro, Xin Liao, Yang Liu for discussions on the topics of channel coding, signal modulation and detection, and channel equalization for wireless communications.

I would like to express my appreciation to Natural Sciences and Engineering Research Council of Canada (NSERC), *Faculty of Graduate Studies*, and *Department of Electrical and Computer Engineering* for the financial support I received during my studies.

A thanks to the staff who have been assisting my Ph.D. studies and research at the *Department of Electrical and Computer Engineering*; *Faculty of Engineering*; *Killam Library*; and *Design & Technology Library* at Dalhousie University.

# Abstract

This dissertation is concerned with the use of multiple antennas in advanced wireless communication systems. In particular, investigations are focused on the equalization approaches for the multiple-input and multiple-output (MIMO) finite impulse response (FIR) fading channels. New transceiver strategies are derived and compared to existing ones using theoretical derivations and simulation results.

Two major challenges in developing wireless networks are bandwidth efficiency and the system resilience to channel distortions. By transmitting multiple signal streams simultaneously in the same frequency band via the multiple spatial subchannels, a MIMO transceiver can significantly increase bandwidth utilization over that of the conventional single-input single-output (SISO) transceiver. In general, multi-antenna techniques (i) will enable high data rate services in band-limited systems; or (ii) will provide increased fading resistance in power-limited systems. In this dissertation, we deal with both kinds of MIMO systems which are referred to as spatial multiplexing and space-time coded systems, respectively.

To accommodate the higher data rates exceeding the channel coherence bandwidth, the frequency selective MIMO channels have to be compensated. The proposed equalization algorithms exploit the signal structure which is either induced at the transmitter by design or is built into the received signal by the multipath channel. The signal structures, such as block-Toeplitz, constant modulus and circulant characteristics, enable spatial-temporal data processing to efficiently recover transmitted information either with or without channel estimation. The deterministic methodology presented can operate on a small number of signal samples obtained within short time duration. This is in contrast with the statistic approaches that rely on the statistics of a large number of received signal samples.

The dissertation introduces three equalization schemes which operate in one of the two modes: the training-aided and the blind. The first frequency domain scheme with the single carrier signaling achieves MIMO spatial multiplexing. It offers the advantage of reduced constraints on the power amplifier linearity over MIMO orthogonal frequency division multiplexing (OFDM) while offering a comparable performance. The second scheme is applicable to unitary differential space-time modulations. It can operate blindly with quasi-static time-varying channels where channel estimation is costly. The third scheme combats inter-symbol-interference (ISI) with a new space-time modulation. It has the feature that, by delegating the signal processing to the transmitter, the ISI mitigation at the receiver is simplified dramatically. Therefore, the receiver algorithm is computationally efficient, which is favorable for forward-link communications.

The simulation results demonstrate the robust performance of the developed schemes. In particular, the influence of different system parameters, such as the number of transmit and receive antennas, frame length, as well as the different maximum channel lengths, on the BER performance are documented. With the contribution of the three new MIMO equalization schemes, this dissertation demonstrates how the space dimension, in addition to time and frequency, can be taken into account when exploring the MIMO signal structure for channel equalization using algebraic methods of signal processing.

# Chapter 1

## Introduction

**W**IRELESS networks offer the convenience of mobility and flexible access beyond the reach of any wire-line network. With the increasing acceptance of wireless services, the goal of the next generation digital radio systems is to provide broadband multimedia communications with improved performance over that of the existing systems. In provisioning the high-data rate services, the main challenges arise from the harsh wireless signal propagation environment, which is characterized by (i) the time-varying random fading; (ii) the convolution distortions due to the multipath propagation; and (iii) the information signal being corrupted by thermal noise and in-band interference [1]- [4]. Traditionally, the digital communication systems assume a classic setup of radio interface equipped with single transmit and single receive antenna, and in order to mitigate channel propagation impairments, signal processing algorithms in time/frequency domains are deployed. However, these approaches are becoming incapable of accommodating the increasing demands for channel capacity in the congested spectrum which is a finite resource.

Digital communications using multiple transmit and receive antennas has recently emerged as one of the most significant technical breakthroughs in modern communications [5]-[7]. These multiple-input multiple-output (MIMO) systems are widely considered to be the most promising avenue for significantly increasing bandwidth efficiency of wireless data transmission systems as they have the potential to break the capacity limit described

in Shannon's theory on single-antenna systems [8]-[11]. The multi-antenna systems accommodate multiple bit streams in the same frequency band, and in order to recover them, the transceiver exploits the unique spatial signatures of the received information bearing waveforms. With this feature, by adding '*space*' as the third domain or dimension, MIMO systems established a new paradigm in digital signal processing (DSP) for wireless communications. This new degree of freedom motivates innovative transceiver designs (i) to gain benefits from increased MIMO system bandwidth efficiency without sacrificing power efficiency; and (ii) to overcome the unreliable radio environments [12]-[14]. In particular, the space dimension in MIMO systems not only creates a diversity gain, but also is a key feature to turn multipath propagation, traditionally a pitfall of wireless transmission, into a benefit for the user [15].

The general MIMO system theory has been investigated for a number of years, e.g., in control theory and circuit design. However, substantial advances in MIMO space-time communications have only emerged for about ten years. Currently, the research in MIMO transceivers concentrates on flat fading channels, which assumes that the signals only experience the random attenuation of the envelope and are not affected by the memory effects in the channel. This assumption is valid if the transmission rate is less than the channel coherence bandwidth. However, in future wireless networks, the real-time multimedia services, such as video conferencing, require data rates on the order of 2-20 Mb/s. After the time division multiplexing to accommodate multiple users, the symbol rate is even much higher than this data rate for each user, and as a result of this high symbol transmission rate, the channel exhibits time-dispersive effects, which have to be taken into account in the transceiver design. This is because the transmitted symbol duration in this case is becoming comparable to or much smaller than the delay difference of the signal copies received along multiple paths [16], [17]. The assumption for the flat fading characteristics on the channel modeling will not hold any longer. Therefore, it is critical to focus further investigations into MIMO radio systems to compensate for the time-dispersive fading channels. This process is referred to as MIMO channel equalization.

This dissertation contributes three effective schemes and algorithms for MIMO channel equalization within several typical transmission scenarios. The main theme for these algorithms is *deterministic* channel equalization which does not impose any assumption on the statistical properties of the signal sources at the multi-element antenna transmitter. This differs from the statistical methods, which take advantage of some statistical properties of the signal sources. The MIMO channel considered in this dissertation is finite impulse response (FIR) and may be viewed a limitation of the algorithms developed. We feel, however, that since the proposed algorithms are computationally efficient, the channel length in the channel identification stages can be adjusted so as to capture the most significant characteristics of the channel.

In one of the proposed algorithms, to take advantage of three dimensions for signal processing, the induced circulant signal structure is exploited in the context of MIMO setup to accomplish the ISI mitigation and separation of the spatially multiplexed signals. In a space-time coded scheme, we demonstrated how to connect the equalization for the FIR time dispersive channels with the known solutions for flat fading channels by applying direct signal subspace estimation.

The increase in the capacity of MIMO transceivers comes at the expense of the complexity of the terminals, when compared to traditional modems offering similar data rates with a larger bandwidth. The motivating factor when developing the algorithms in this dissertation was to keep this complexity at a minimum. Despite the implementation costs, it has been suggested that at some point in the future, multi-antenna techniques may also enable high data rate services for those systems that do not have bandwidth in abundance. On the other hand, if high data rates are not required, the increased fading resistance or diversity inherent in multi-antenna transceiver concepts can be used to increase system coverage. It is expected that the results obtained in this dissertation will be valuable in the design of future MIMO transceivers.

Because of the profoundness of the wireless communication theory and the broad range of its applications, it is impossible to touch on all the areas related to this dissertation

within a short background introduction. The remainder of this chapter emphasizes only the theoretical advances and research trends in channel equalization which are critical in the development of the main ideas in this work. The first section of this chapter, Section 1.1, presents the objectives and contributions of this dissertation as well as the outline. Section 1.2, highlights the issues in channel capacity, the challenges of wireless communications at the physical layer, and the significance of advanced digital signal processing. Section 1.3, reviews briefly the two main types of signaling schemes in MIMO systems, namely spatial multiplexing and space-time coding. It also contrasts MIMO systems with beamforming approaches. The mathematical underpinnings for modeling fading and time-dispersive channels in both the single-input single-output (SISO) and the MIMO systems are given in Sections 1.4 and 1.5. Section 1.6, lays out the state-of-art in channel equalization for frequency selective fading channels.

## **1.1 Dissertation Objectives, Contributions and Outline**

### **1.1.1 Objectives and Organization**

The main contributions are now briefly presented. The overall objective of this dissertation is to find the efficient methods for the transmission over frequency selective fading channels with multiple antennas on both sides of the transceiver. Novel transmission strategies are pursued in two cases: (1) when the MIMO channel impulse response (CIR) is available at the receiver; and (2) when the MIMO channel effects have to be mitigated in a blind fashion. The equalization schemes for both spatial multiplexing transceivers and space-time coded communications are sought. The investigated approaches exploit space-time channel diversity and signal structures so that the deterministic solutions for the estimation of the transmitted data could be evoked.

The performance metric for comparing different schemes in the dissertation is the bit error rate (BER). The BER curves as a function of signal-to-noise ratio (SNR) considered in this dissertation are demonstrating the power efficiency of the analyzed schemes. In

addition to this performance measure, similarly as in conventional digital communications, one should be concerned with bandwidth efficiency, i.e., the bit rate supported in 1 Hz of bandwidth. In this dissertation, when comparing different schemes in terms of power efficiency in the simulations, we ensured that the bandwidth efficiency was the same.

When necessary, we discuss the computational complexity of different algorithms so better insight into the operation of algorithms could be obtained. The combination of different signaling schemes and assumptions about the MIMO CIR knowledge offer the communication system engineers the design choices that will affect the final performance of the overall system.

Because of the increasing size and complexity of the new transceiver schemes, it becomes extremely difficult or even impossible to only use analytical methods for evaluating the overall performance of the new transmission link [18], [19]. On the other hand, at an initial design of the system prototype, it is cumbersome to construct all the candidate schemes with possible numerous parameter changes for verifying the functionality. However, the flexible software-based simulations can expeditiously handle this challenging task. In this dissertation, all the proposed schemes and algorithms were validated and compared through a large number of computer simulations in the Matlab® computing environment.

Next, an overview of the dissertation is given chapter by chapter.

## **Chapter 2**

The second chapter studies a frequency domain equalization method with single carrier signaling communications for MIMO spatial multiplexing. The main feature of this scheme is to fully exploit the induced signal structure to mitigate ISI at the receiver using efficient processing. OFDM has a high peak-to-average power ratio (PAPR) and demands the use of highly linear power amplifiers (PA). The proposed scheme offers the advantage of reduced constraints on the PA linearity. It is shown, via Monte-Carlo simulations, that this approach is able to achieve comparable performance to that of MIMO-OFDM schemes. This scheme is suitable for multiple-path rich-scattering and high SNR environments, in

which the transceiver simultaneously transmits the multiple data streams within the same frequency bandwidth, and the receiver makes use of the unique spatial signature to separate the different streams. The multiple spatial subchannels achieve a high total capacity.

### **Chapter 3**

The third chapter presents a blind channel equalization algorithm for unitary differential space-time modulated transmissions (DSTM). This transceiver system differs from that in the second chapter in that it is a differential space-time coded system. The focus is on a non-coherent receiver scheme exploiting the block Toeplitz signal structures and the constant modulus property to recover the transmitted signal without prior knowledge of channel impulse response. The new scheme falls into the category of the deterministic algebraic algorithms and it can accommodate the quasi-static time-varying channels for mobile transmission links.

### **Chapter 4**

The fourth chapter considers a space-time modulation to combat the time-dispersive effects. The major concern in this chapter is to accomplish the ISI mitigation in the same time as maintaining the spatial diversity for fading resistance. By inducing a special space-time signal structure on the transmitted signal frames at the transmitter, this scheme substantially relieves the equalization burden of the receiver. It is especially suitable for forward-link communication, where the base-station conducts sophisticated processing and coding, and the receiver structure of mobile devices should be relatively simple. This scheme builds into the transmitted symbol frame a unique circular structure so that ISI mitigation processing is integrated with the detection of the differential space-time codes. The new, low complexity, transceiver is based on cyclic group codes and a non-coherent reception.



## Chapter 5

The fifth chapter concludes this dissertation. It emphasizes the major features and impacts of the algorithms and schemes developed in this dissertation.

### 1.1.2 Research Impact

The results from this dissertation in the form of research papers are submitted for publications in refereed journals and their conference versions were already published in the respectful research conferences as follows:

#### Refereed Conference Proceeding Publications

- [C-1] Zhan Zhang and Jacek Ilow, Frequency Domain Equalization for MIMO space-time transmission with single carrier signaling, to appear in the *IEEE International Symposium on Personal, Indoor, and Mobile Radio Communications, PIMRC 2003*, Beijing, Sep, 7-11, 2003.
- [C-2] Zhan Zhang and Jacek Ilow, A receiver algorithm for unitary space-time differentially encoded transmissions of FIR multipath channels, the *4th IEEE International Workshop on Mobile and Wireless Communications Network*, Stockholm, Sweden, Page(s): 429 -433, 2002.
- [C-3] Zhan Zhang and Jacek Ilow, Frequency Domain Equalization with Multiple Receiving Antennas for Single Carrier Signaling, *Communication Networks & Services Research (CNSR) 2003 Conference*, Moncton, New Brunswick, Canada, Page(s): 10-13, May, 15-16, 2003.
- [C-4] Zhan Zhang and Jacek Ilow, Multiwavelet-based fractal modulation, *Proceedings of the IASTED International Conference Wireless and Optical Communications*, Banff, Canada, Pages: 267-271, July, 17-19, 2002.
- [SC-1] Zhan Zhang and Jacek Ilow, Differential Space-time Transceiver for Unknown Multi-path Time-Dispersive Channels, Submitted to *IEEE ISSPIT*

2003, Darmstadt, Germany, Aug. 2003.

### **Papers Submitted to Refereed Journals**

[SJ-1] Zhan Zhang and Jacek Ilow, MIMO Channel Equalization based on the Induced Signal Structure of Block Circulant Matrix, being submitted to *IEEE Trans. Veh. Technol.*, 2003.

[SJ-2] Zhan Zhang and Jacek Ilow, Signal reception for Space-Time Differentially Encoded Transmissions over FIR Rich-Multipath Channels, submitted to *EURASIP Journal on Applied Signal Processing*, Dec., 2002. and its revised version submitted in Aug. 2003.

In each of the publications mentioned above, the author of this dissertation initiated and carried out the research and was the principle author during composition of the papers.

The research contributions from this dissertation can be classified into three areas corresponding to three main chapters of the dissertation. The specific papers and the chapters are listed below:

#### **Chapter 2 Frequency Domain Equalization for MIMO Space-Time Transmission with Single Carrier Signaling**

The frequency domain equalization approach for spatial multiplexing schemes in Chapter 2 is described in: [SJ-1], [C-1] and [C-3];

#### **Chapter 3 Blind Channel Equalization for DSTM Signaling Transmissions over Rich-Multipath Channels**

The blind channel equalization receiver algorithm for DSTM signaling in Chapter 3 is described in: [SJ-2] and [C-2];

#### **Chapter 4 Differential Space-Time Modulation for Transmissions Over Unknown Time-Dispersive Channels**

A differential space-time coded modulation scheme in Chapter 4 is presented in: [SJ-1] and [SC-1];

In addition, as a special modulation scheme, a multiple-fractal modulation is introduced and discussed in [C-4]. This contribution is not included in this dissertation but it is in the area of radio interface techniques that is the same general subject as that of this dissertation.

## 1.2 Evolution and Characteristics of Wireless Communications

The demands for the ubiquitous personal communications, mobility and multimedia support, drive the development of new radio systems with claiming capacities. This results in a congested spectrum and puts high requirements on the transceiver designs. Within the framework of the conventional SISO transceiver design, we have almost reached the theoretical limits, and the new designs in this area arrive at the phase of diminishing returns for performance improvement.

This section describes the channel capacity for single-antenna systems and shows how the multiple-antenna transceivers break this barrier. It also points out the challenges for communication system designs associated with the provisioning of increasing data rates. At the end of the section, it is argued that advanced DSP is a tool that has to be used to achieve the limits promised by the MIMO capacity theorems and to overcome the radio channel challenges.

### 1.2.1 Channel Capacity

A new era of information theory and wireless communication begun when Dr. Claude Shannon published his paper titled: “*A mathematical theory of communication*”, in 1948. In this paper, he first proved the following theory, which applies to SISO systems, where a communication link is modeled as illustrated in Fig. 1.1.

**Theorem 1** [20] *The capacity of a channel of band  $W$  perturbed by white thermal noise with power  $N$  when the average transmitter power is limited to  $P$ , is given by*

$$C = W \log \frac{P + N}{N}.$$

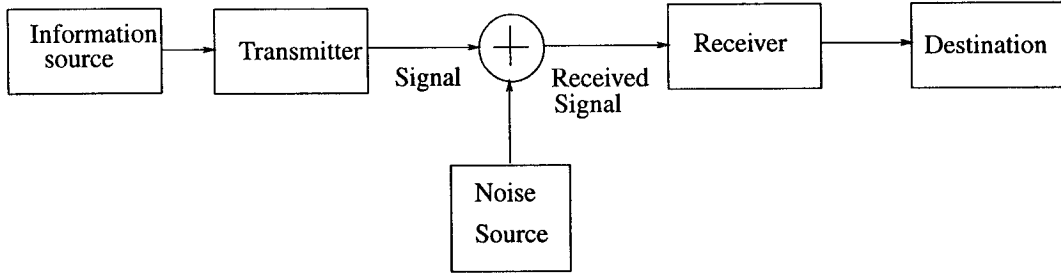


Figure 1.1: A System Modeling in Shannon's Channel Capacity Research.

Shannon first pointed out this theoretical limit of channel capacity that single antenna systems can achieve. Since then, the research has been conducted in an effort to approach this capacity limit. A variety of advances in coding/decoding, modulation/demodulation, noise suppression and signal detection have been made to reduce gaps between the transmission rate and the 'Shannon limit'.

Nowadays, more potential wireless applications are emerging in a larger scale, such as virtual navigation, tele-medicine, crisis management, distance learning [21]. Wireless local area networks (LAN) and multimedia personal digital assistants (PDA) are deployed with a higher density of terminals than ever. This results in severe spectrum congestion. The contradiction between limited frequency bandwidth resource and the increasing number of wireless users is a rigorous challenge that the wireless system design has to face. At present, the effort in approaching the Shannon capacity at the cost of higher processing complexity has reached a point of diminishing returns as the achieved transmission rate gets gradually closer to the capacity limit. Hence, the progress within the framework of single-antenna radio interface is slowing down.

Encouragingly, the recent research indicates multiple-antenna systems at certain conditions are able to achieve much higher bandwidth efficiency than that of single antenna

systems assumed by Shannon. The rest of this section presents a mathematical formulation of this capacity increase.

Spatial-temporal MIMO transceiver systems have multiple antennas in both sides of the transmission link. The relation between the generic received signal vector  $\mathbf{Y}$  and the

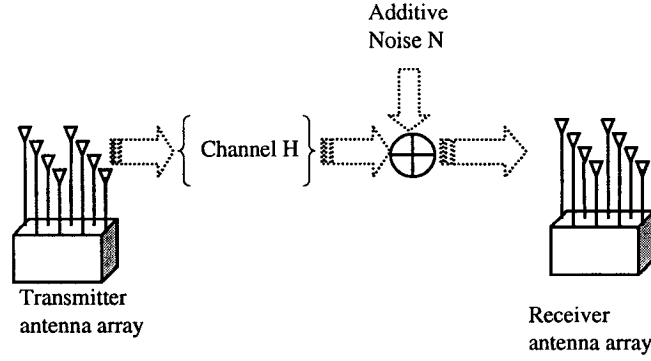


Figure 1.2: Multi-Element Antenna Transceiver System Modeling.

transmitted signal vector  $\mathbf{X}$  over a flat fading channel, in systems with the  $K$  transmitter antenna elements and the  $M$  receiver antenna elements, can be expressed as follows:

$$\mathbf{Y}_{M \times 1} = \mathbf{H}(t)_{M \times K} \mathbf{X}_{K \times 1} + \mathbf{N}_{M \times 1} \quad (1.1)$$

where

$$\mathbf{H}(t) = \begin{bmatrix} h_{11}(t) & h_{12}(t) & \cdots & h_{1K}(t) \\ h_{21}(t) & h_{22}(t) & \cdots & h_{2K}(t) \\ \vdots & \vdots & \vdots & \vdots \\ h_{M1}(t) & h_{M2}(t) & \cdots & h_{MK}(t) \end{bmatrix} \quad (1.2)$$

The matrix  $\mathbf{H}(t)$  captures the time-varying channel gain information at the time instant  $t$ . In the discrete-time domain, after matched filtering and sampling, the generic

$\mathbf{Y}_{M \times 1}$  is replaced by  $\mathbf{Y}(i)$ , and  $\mathbf{X}_{K \times 1}$  is replaced by  $\mathbf{X}(i)$  where

$$\mathbf{Y}(i) = \begin{bmatrix} Y_1(i) \\ Y_2(i) \\ \vdots \\ Y_M(i) \end{bmatrix}, \quad \mathbf{X}(i) = \begin{bmatrix} X_1(i) \\ X_2(i) \\ \vdots \\ X_K(i) \end{bmatrix}, \quad \mathbf{N}(i) = \begin{bmatrix} n_1(i) \\ n_2(i) \\ \vdots \\ n_M(i) \end{bmatrix},$$

The vectors  $\mathbf{Y}(i)$  and  $\mathbf{X}(i)$  respectively are the received and transmitted vector at the  $i^{th}$  symbol timing slot of a data stream, the vector  $\mathbf{N}(i)$  is a noise component vector. Usually, the element of transfer matrix  $\mathbf{H}$  is assumed to have an i.i.d circularly symmetric complex Gaussian distribution  $h_{ij} = (x_{ij} + jy_{ij}) \sim \mathcal{CN}(0, \delta^2)$  [8]. In addition, the noise vector  $\mathbf{N}$  also is assumed to have the same distribution.

A spatial multiplexing or space-time modulated transmitter simultaneously transmits multiple streams in the same time and frequency band. The signals arrive at the receiver antenna array along different propagation paths. The receiver gathers multiple copies of the signals from every antenna element.

For a MIMO channel with the aforementioned flat fading modeling, the ergodic capacity of the channel is calculated by [8]-[11]:

$$C = \mathbf{E}_H \{ \log_2 [\det(\mathbf{I}_M + \frac{\rho}{K} \mathbf{H} \mathbf{H}^H)] \} \text{ bps/Hz} \quad (1.3)$$

where  $\rho$  is average transmission power.

By examining this formula, it can be deduced that the MIMO channel has the lowest capacity when all the subchannels are completely correlated [14]:

$$C_{low} \cong \log_2(1 + M\rho) \text{ bps/Hz} \quad (1.4)$$

The maximum capacity of the channel occurs when all the subchannels are of full rank and SINR is high [14], and it achieves the value:

$$C_{high} \cong \min(M, K) \log_2(1 + \frac{M\rho}{K}) \text{ bps/Hz} \quad (1.5)$$

The full-rank cases happen normally when the multipath scattering is rich at the location of the receiver array. This equation indicates that the MIMO capacity has the potential to

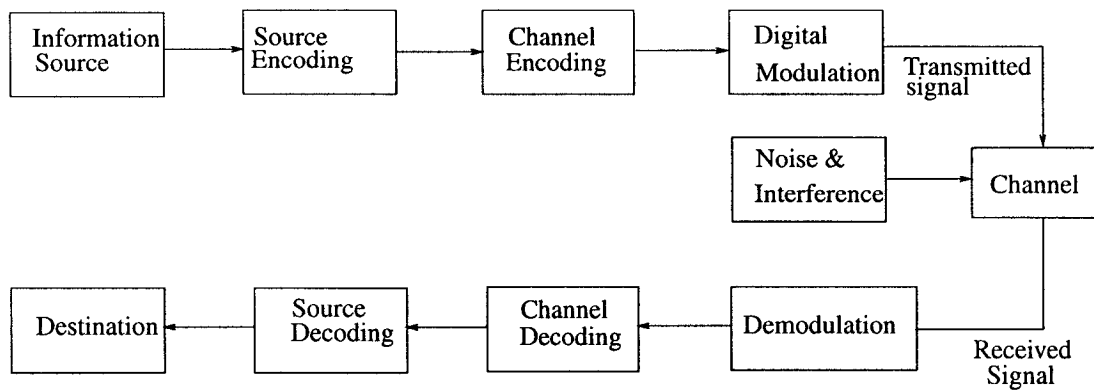


Figure 1.3: Modeling of a General Wireless Communication System.

achieve an increase with a multiplicative factor proportional to the smaller of the transmitter and receiver antenna numbers. This definitely is a huge capacity enhancement that other signaling techniques are unable to offer.

### 1.2.2 Challenges in Wireless Communications

A digital wireless communication link normally consists of a digital source, a source encoder/decoder, a channel encoder/decoder, a digital modulator/demodulator, and a channel contaminated by noise and interference. Figure 1.3 illustrates a radio communication link including these essential elements. The error rate of the symbol detection over a time-dispersive fading channel is one of the most important factors considered in this dissertation.

The following are the challenges that wireless communication design is facing:

- In mobile communications, the mobility of the transceiver and the multi-path propagation of the signal cause a time-varying frequency-selective environment for the wireless transmission. Channel linear or nonlinear distortion on the signals, multiple access interference (MAI) and noise contamination pose severe difficulties in term of achieving a low detection error rate. In this aspect, radio interface is of enormous significance and the high performance of the wireless networking is provided at the

cost of the complexity of its radio-interface.

- The wireless resources such as available bandwidth are more and more becoming a limiting factor due to an increasing number of users.
- Mobile devices are required to be designed with limited battery capacity and small portable sizes.
- Synchronization of the timing, phase, and frequency has to be accomplished without reducing the transmission efficiency in a multipath fading environment impaired by time-dispersive characteristics, multi-access interference, low SNR and Doppler effects.
- Security, flexible and reliable networking, and optimization of resource allocation are also the main concerns of wireless systems.

### **1.2.3 Advanced Digital Signal Processing**

Digital signal processing is an enabling factor to advance the wireless techniques. The signal envelope fading, MAI, ISI, Doppler effects, inter-channel interference (ICI) and noise perturbation constitute the main causes of the errors in signal detection at the receiver. Signal processing approaches in a mathematical theory framework are the most effective leverages to mitigate the channel distortion, to increase the SNR, to achieve signal synchronization, so as to improve the overall network performance.

“The fundamental theory behind detection, classification, and estimation has its home in mathematical statistics and decision theory” [22]. The progress of digital signal processing in channel coding, statistics, optimization, adaptive theory, and detection theory have brought a variety of technical solutions and enhancements to wireless systems. The thriving wireless applications are embodiments of the success of the underlying signal processing algorithms.



## 1.3 Spatial Diversity and MIMO Systems

This section highlights the recent developments in MIMO channel coding and signal processing. Some breakthroughs in the MIMO system research are also reviewed. A comparison between beamforming and MIMO schemes is conducted to clarify their unique performance advantages and implementation feasibility in the different scenarios.

There have been many significant advances in channel coding and signal processing in the last fifty years, such as the development of convolution code and Viterbi algorithm (VA) [23] [24]. Particularly, the invention of the turbo code and turbo-processing theories due to the excellent work of Claude Berrou in 1993 [25] [26], have been widely regarded as a groundbreaking progress in the coding theory in the last ten years, which is a ‘near optimum error correcting coding and decoding’. All of these are representatives of the successful breakthroughs in the research to reduce the gap to Shannon’s capacity limit against noise and interference.

However, there is much more to be achieved in the design of communication transceivers, specifically, the development on space-time signal processing and MIMO channel verifies that spatial characteristics of the channel and signals can be exploited along with their time and frequency patterns to substantially enhance the transceiver capacity and system resilience to the signal fading effect [8]-[11].

### 1.3.1 Spatial Multiplexing and Beamforming Schemes

This section reviews the spatial multiplexing and beamforming systems. A brief comparison between them is presented to highlight their different characteristics.

As a typical example of the spatial multiplexing systems, BLAST (Bell Laboratories Layered Space-Time) experiments demonstrated a 20-40 bps/Hz transmission with a realistic SNR (22 dB to 34 dB) and error rate in an indoor experiment in 1998 [5], [7], [27]. By exploiting the spatial-temporal signature of subchannels and receive diversity, BLAST

successfully verified that the spatial characteristics of the received signals can be taken advantage of to divide the channel into multiple spatial subchannels. Moreover, it also clearly indicates that simultaneous transmitting of multiple signal streams through different low-powered subchannels is more beneficial than using only a single high-powered channel [4].

Optimal cancellation and detection processing techniques enable the MIMO channel to be layered into several subchannels allowing simultaneous parallel transmissions of multiple data streams [28]. In spatial multiplexing, a multiplicative capacity increase as compared to that of single antenna systems can be achieved, provided the channel is of rich multipath scattering.

The recent research on MIMO channels has its origin from beamforming techniques [29]-[31] and spatial filtering. A variety of algorithms of array signal processing emerged in the last 20 years [32]. The latest research exploits both the array structure and the signal space-time-frequency characteristics. The investigation aspects include array manifold, time manifold, constant modulus, source independence, finite alphabet, and block Toeplitz structure [12], [13]. This leads to receive diversity algorithms for multiple access interference (MAI) cancellation, channel equalization [33]- [36], and blind beamforming [37], [38].

As pointed out in the paper [10], ‘smart antenna’ or beamforming normally refers to the techniques exploiting the signaling or processing of data at one side of the transmission link. ‘Smart antenna’ normally is employed at base stations because of the limitations of size, complexity, power and cost of the mobile devices.

Later research and engineering development indicated that, in rich multi-path scattering environments, MIMO schemes, which process at the both sides of the communication links, are able to provide higher capacity and fading resistance than what ‘smart antenna’ can offer. The other aspects of the difference between ‘smart antenna’ and MIMO schemes are enumerated as follows:

1. MIMO techniques stem from the ‘smart antenna’, but they may establish multiple

spatial sub-channels to gain higher capacity increase. The magnitude of the capacity increase through spatial multiplexing of MIMO channels depends on the channel scattering environment. In the cases where the channel exhibits high-rank characteristics, a maximal capacity increase can be achieved. The key point of 'smart antenna' is 'beamforming', which normally focuses the beam to the desired direction in order to maximize the signal SNR. This processing is conducted at either the transmitter or receiver through optimal weighting on the signals to be transmitted from each element of transmit MEA or by optimally combining the signals from each element of the receive MEA.

2. 'MIMO' normally needs uncorrelated antennas which should be spaced as far as the space limitation allows while 'smart antenna' usually tends to use closely spaced antennas as an array with certain geometric characteristics.
3. 'MIMO' usually has a small number of antennas while 'smart antenna' MEA typically has a large number of antennas for better beamforming aperture.
4. 'MIMO' concentrates on data stream spatial multiplexing or diversity maximization while 'smart antenna' focuses on the average SNR improvement and spatial filtering to reject the interference.
5. 'Smart antenna' has superior performance for open space or line-of-sight (LOS) propagation dominated environments. On the other hand, 'MIMO' needs a rich-scattering environment, which imposes distinct spatial signatures to the signals transmitted from every single antenna.

Therefore, for different transmission scenarios, a proper scheme of beamforming and MIMO should be chosen by taking advantage of the different characteristics of 'MIMO' and 'smart antenna' to achieve the optimal effects.

In summary, transmit and receive diversity achieved by multiple antennas will improve the signal quality by the diversity gain and array gain [39] which are effective in both mobile and fixed broadband wireless access (BWA), especially for the multi-user interference

suppression and equalization. “ Whichever multiple access technique is employed, the ultimate performance limitation is the system’s susceptibility to interference” [40]. Hence, the spatial-temporal methodologies, including beamforming and MIMO, enhance the overall wireless network performance.

### 1.3.2 Space-Time Coded Schemes

“ Space-time trellis and block codes enjoy a rich structure that should be exploited in a multi-user broadband wireless modem to enhance its performance and reduce the complexity of receiver signal processing functions”. [41].

While Foschini has been focusing on the spatial multiplexing for higher capacity [5], Alamouti started a new field of space-time transmit diversity coding to achieve higher fading resistance for lower bit error rate in low SNR situations [42]. From then on, transmit diversity and space-time channel coding became important subjects to combine both spatial and temporal dependencies of a channel to maximize the fading resistance, and at the same time, to maintain as low as possible a receiver complexity. This area also has been attracting intensified research interest.

The discussion on ST coding design criteria was initialized in [43], [44], which pointed out the crucial rank criterion and determinant criterion to achieve the maximum diversity. Space-time block code, ST trellis code and the concatenated codes based on ST codes have good performances with low-complexity signal reception schemes, especially for the codes with unitary ST constellation [45]-[50]. Based on the unitary ST block code, the differential group code and unitary differential ST modulation (DSTM) were proposed for noncoherent detection so that the signal could be detected without the knowledge of channel impulse responses (CIR) [51]-[54]. The modified version of DSTM was discussed in [55], [56] for better interference suppression.

Space-time coding is an effective method in increasing both bandwidth and power efficiency to exploit full spatial diversity. The theoretical and experimental investigations show

that the large diversity gain could be achieved by unitary ST code in the fading channels provided the SNR is mild to high [47].

## 1.4 Multipath Propagation Environment

### 1.4.1 Multipath Characteristics

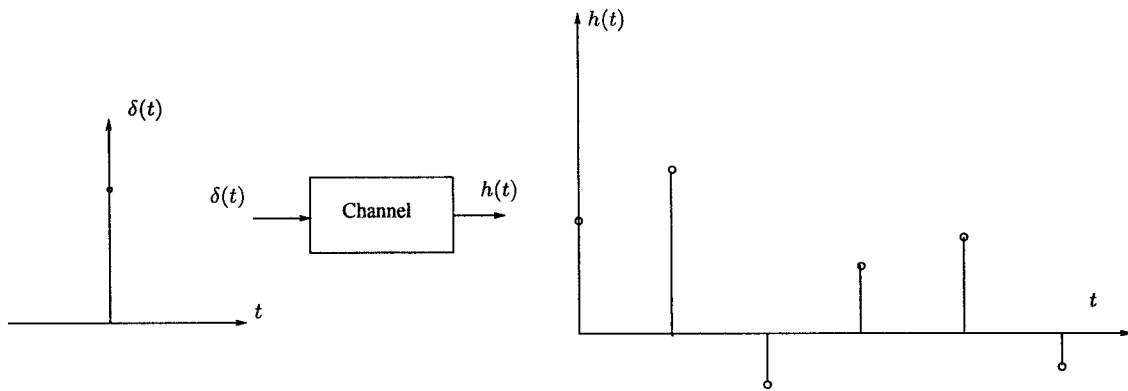


Figure 1.4: Channel Impulse Response Illustration.

In wireless communications, each transmitted symbol generates a large number of echoes because of the numerous electromagnetic scatters in the environment of the signal wave propagation. The multiple signal echoes arrive at the receiver along different propagation paths with a different delay. For high-speed transmissions driven by the immense throughput demanding, the symbol duration is comparable to or even much smaller than the multipath delay difference of the echoes. Therefore, the echoes have a delay large enough to collide with the subsequent symbols. The received symbols at the receiver are not the original symbols sent by the transmitter with only a magnitude attenuation but are the superposition of the transmitted symbols and their echoes. Hence, the multipath causes the symbols to overlap in time domain. This phenomena is called “time-dispersive channel” effect, which generates inter-symbol-interference (ISI) and is the major channel distortion

on the signals and results in poor signal quality. Fig. 1.4 illustrates the discrete time impulse response of a time-dispersive channel, which could be modeled as a discrete-time linear filter, as demonstrated in Fig. 1.5. The output of the channel is a convolution of input signal with channel impulse response. Section 1.4.2 presents more detail in regard to the mathematical modeling of time-dispersive channels.

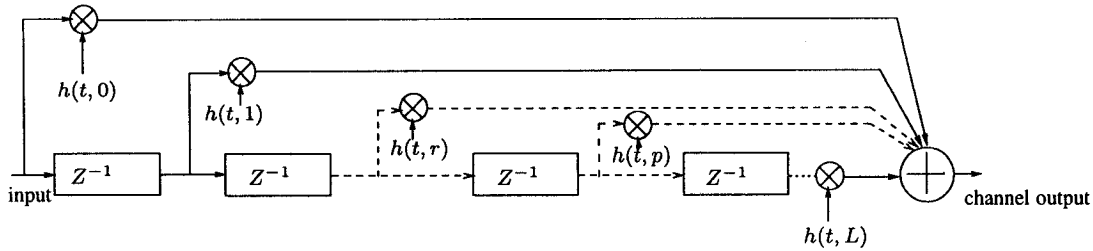


Figure 1.5: Equivalent Discrete-Time Linear Filter Model of FIR Channel.

For MIMO systems, there is more than one source of input into the channel so that not only the ISI exists but also multiple-source interferences appear. Hence, it is more difficult to mitigate the ISI at the receiver. The main focus of this dissertation is on the approaches in removing ISI within the framework of MIMO systems.

## 1.4.2 Time-Dispersive Channel Modeling

“Fading dispersive channels are usually best described as random linear time-varying filters.” [2]

This section considers the time-dispersive channel modeling and classification, which are the theoretical basis in the discussion of MIMO equalization schemes later on in this dissertation. As a dominant barrier to support high bit rates, the time-dispersive channel is the most critical problem to be tackled when introducing high data rate services, and hence is of tremendous research interest.

Time-spread due to the multiple propagation paths (scattering echoes) of the signal wave results in severe ISI effects and frequency selective fading channels. There are two important factors that cause the small-scale fading effects in addition to the large-scale fading. [57]:

- A small location change (travel) will give rise to the rapid variation on signal magnitude, especially for the case without line-of-sight paths for signal propagation.
- Doppler effect due to mobility and the variation of media physical parameters will form random modulations on the signals.

A linear fading channel can be modeled as a time-varying filter. The relationship between the transmitted signal and the received signal normally is expressed as follows [58]:

- Transmitted signal can be written as:

$$S(t) = \text{Re}\{S_l(t)e^{j2\pi f_c t}\} \quad (1.6)$$

where  $S_l$  is an equivalent low-pass signal and  $f_c$  is the carrier's frequency.

- A multipath fading channel can be characterized by its impulse response with a random magnitude of coefficients  $\alpha_n(t)$  and the random delays  $\tau_n$  as follows:

$$c(\tau, t) = \sum_n \alpha_n(t) e^{j2\pi f_c \tau_n(t)} \delta(\tau - \tau_n) = \alpha(\tau; t) e^{j2\pi f_c \tau} \quad (1.7)$$

where  $\alpha(\tau; t)$  represents the attenuation of the signal components at delay  $\tau$  at the time instant of  $t$ .

- The received signal can be modeled as a convolution of transmitted signal and time-varying channel impulse.

$$x(t) = \text{Re}\left\{\left[\int_{-\infty}^{\infty} c(\tau; t) s_l(t - \tau) d\tau\right] e^{j2\pi f_c t}\right\} \quad (1.8)$$

- The time-variant transfer function of the channel is:

$$C(f, t) = \int_{-\infty}^{\infty} c(\tau; t) e^{-j2\pi f \tau} d\tau \quad (1.9)$$

- Under wide-sense stationary assumption, the autocorrelation function is

$$\phi_c(f_1, f_2; \Delta t) = \frac{1}{2} \mathbf{E}[(C^*(f_1; t)C(f_2; t + \Delta t))] \quad (1.10)$$

and the scattering function of the channel is:

$$S(\tau, \lambda) = \int_{-\infty}^{\infty} \int_{-\infty}^{\infty} \phi_c(\Delta f; \Delta \alpha) e^{-j2\pi\lambda\Delta t} e^{-j2\pi\tau\Delta f} d\Delta t d\Delta f \quad (1.11)$$

where  $\tau$  is a parameter for time delay and  $\lambda$  is a parameter for a Doppler frequency. Both the correlation function and scattering function systematically describe the channel situation. The received signal is a convolution of transmitted signal and the time-varying channel impulse response without considering noise components.

The classification of the multipath channels can be done using different criteria [1]. The channel falls into the category of frequency-selective fading if the multipath delay is comparable or greater to the symbol time, otherwise it is called flat-fading channel.

On the other hand, the channel belongs to the category of slow fading if the channel fading rate is much smaller than the symbol rate, otherwise it is called fast fading channel. Slow fading means the Doppler frequency is low and coherence time is large compared to the symbol time. According to the statistical distribution of the SNR, flat slow fading channel can be classified further as Rayleigh fading channel, Rician fading channel, or other categories. The channel behavior is the critical factor influencing the wireless system performance.

## 1.5 MIMO Channel Characterization

This section presents the mathematical modeling and characterization of MIMO channels relevant to the derivations of the algorithms proposed in this dissertation. In particular, the vector form for the input-output convolution relation is elaborated on. In Section 1.5.1 we review a flat fading channel model, while, in Section 1.5.2, we extend it to the frequency-selective fading channel cases.



### 1.5.1 MIMO Flat-Fading Channel Modeling

MIMO channel modeling is important in predicting channel capacity and system performance, and provides motivating insights into system design and simulation. There is a variety of characterization and modeling methods for the MIMO channels, which can be classified according to different criteria, e.g., (i) the measurement based modeling vs. the scatter based modeling; (ii) the physical models vs. the non-physical models; (iii) the flat fading MIMO channel vs. the frequency-selective fading MIMO channel [59].

In some cases, the MIMO characteristics are not sufficiently described by a small number of physical parameters, such as direction of arrival (DoA), direction of departure (DoD), and time of arrival (ToA). Among the different modeling of MIMO channels, the channel characterization based on distributed scatter models and channel analysis in [60] brought insight into MIMO capacity prediction and system design. The modeling proposed in [9] and [60] classifies the MIMO channel in the following categories:

1. Uncorrelated high rank MIMO channel: the elements in channel matrix  $\mathbf{H}$  in (1.2) are uncorrelated and with independent and identical distribution (i.i.d) of  $\mathcal{CN}(0, 1)$ .
2. Uncorrelated low rank MIMO channel ('pin-hole' or 'key-hole' channel):  $\mathbf{H} = \mathbf{g}_{rx}\mathbf{g}_{tx}^*$  where  $\mathbf{g}_{rx}$  and  $\mathbf{g}_{tx}$  are independent column vectors. The vector  $\mathbf{g}_{rx}$  is of the distribution  $\mathcal{CN}(0, \mathbf{I}_M)$ . The vector  $\mathbf{g}_{tx}$  is of the distribution  $\mathcal{CN}(0, \mathbf{I}_K)$ . Therefore, the channel has a rank of 1, and it loses the multiplexing gain but still achieves certain diversity gain.
3. Correlated low rank MIMO channel:  $\mathbf{H} = g_{rx}g_{tx}^* \mathbf{U}_{rx}\mathbf{U}_{tx}^*$ , where  $g_{rx}$  and  $g_{tx}$  are i.i.d. variables of  $\mathcal{CN}(0, 1)$ , and,  $\mathbf{U}_{rx}$  and  $\mathbf{U}_{tx}^*$  are fixed vectors of unit modulus entries. At this situation, MIMO channel can only offer array gain.

In the transceiver scenario illustrated in Fig. 1.6, a channel model to characterize the statistical behavior of the MIMO channel was proposed as in [9] and [60], which is as

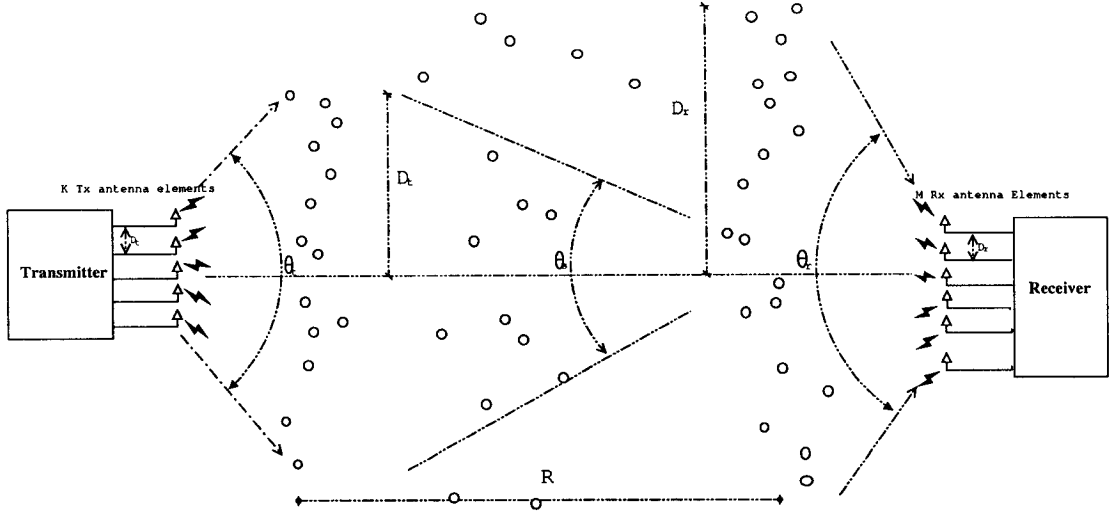


Figure 1.6: Visualization of the MIMO Scatter Modeling.

follows:

$$\mathbf{H} = \frac{1}{\sqrt{S}} \mathbf{R}_{\theta_r, d_r}^{\frac{1}{2}} \mathbf{G}_r \mathbf{R}_{\theta_s, 2D_r/s}^{\frac{1}{2}} \mathbf{G}_t \mathbf{R}_{\theta_t, d_t}^{\frac{1}{2}} \quad (1.12)$$

where  $\mathbf{R}_{\theta_r, d_r}$  is a  $M \times M$  receive correlation matrix. In the case of rich-scattering (rich-multipath), (i) the receive angle spread is large, and (ii) the matrix  $\mathbf{R}_{\theta_r, d_r}$  will converge to identity matrix. The matrix  $\mathbf{R}_{\theta_s, 2D_r/s}$  is an  $S \times S$  correlation matrix determined by scatters of the wave propagation. The matrix  $\mathbf{R}_{\theta_t, d_t}$  is a  $K \times K$  transmit correlation matrix to characterize correlation of the transmit antenna elements. The matrix  $\mathbf{G}_t$  is an  $S \times K$  matrix, whose element is i.i.d. of  $\mathcal{CN}(0, 1)$ . The matrix  $\mathbf{G}_r$  is a  $M \times S$  matrix, whose element is i.i.d. of  $\mathcal{CN}(0, 1)$  as well.

As analyzed in [60] and characterized by (1.12), rich-multipath scattering normally causes wide angle spreads. In this situation, the channel gain matrix can be modeled as a high rank matrix. For outdoor MIMO channels, a formula suggested in [60] to predict a high rank channel situation is:

$$\frac{2D_t}{K-1} \frac{2D_r}{M-1} > \frac{R\lambda}{M} \quad (1.13)$$

where (i)  $D_t, D_r$  stands for the transmit and receive scattering radius, respectively, as illustrated in Fig. 1.6; (ii)  $R$  is the distance between transmitter and receiver; and (iii)  $\lambda$  is

the wavelength. This formula indicates that a large number of scatters (and large antenna spacing), large angle spreading and small range  $R$  will easily build up the high rank MIMO channels, which offer significant spatial multiplexing and diversity gains [14].

The ‘pin-hole’ channel refers to the situation where the MIMO channel is rank deficient, though the antenna elements for both transmit and receive MEA are uncorrelated. The ‘pin-hole’ channel situation occurs when  $\mathbf{R}_{\theta_s, 2D_r/s}^{\frac{1}{2}}$  is rank deficient in the cases of large  $R$  and small  $D_t$  or  $D_r$  or scatter free line-of-sight cases.

Rank-deficiency of MIMO channels occurs when the scatter angle spreads become small. The scatter radii and range  $R$  will determine the rank of the MIMO channel rather than the physical spacing of the antenna elements, unless the spacing is too small to keep the element uncorrelation. Whenever, the scattering is absent, the antenna spacing becomes a determining factor to the channel capacity. Increasing the antenna spacing at this situation will help to achieve a high rank of MIMO channels.

### 1.5.2 MIMO Time-Dispersive Fading Channel Characterization

At the receiver, each element of the antenna array receives a superposition of signals sent by different transmitter antennas. For the unique pair of transmit and receive antenna elements, the signal from the transmit antenna element arrives at the receiving antenna element along many paths with different delays and different signal attenuation. SNRs at the receive antenna elements are also different.

The MIMO channel can be expressed using a tapped delay line model in a matrix format as follows [60]:

$$\mathbf{H}(\tau) = \sum_{l=0}^L \mathcal{H}_l \delta(\tau - \tau_l) \quad (1.14)$$

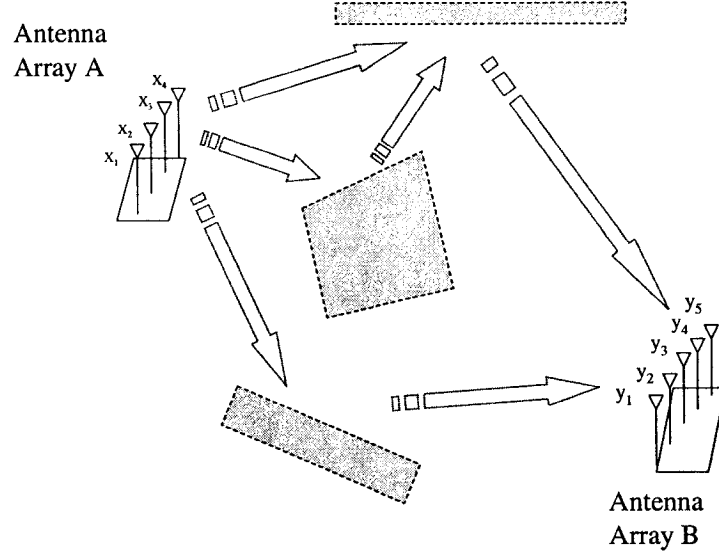


Figure 1.7: Visualization of the Multipath Propagation and Scattering.

where matrices  $\{\mathcal{H}_l, l = 0, 1, 2, \dots, L\}$  are used to capture the channel impulse responses:

$$\mathcal{H}_l = \begin{bmatrix} h_{11}^{[l]} & h_{12}^{[l]} & \cdots & h_{1K}^{[l]} \\ h_{21}^{[l]} & h_{22}^{[l]} & \cdots & h_{2K}^{[l]} \\ \vdots & \vdots & \vdots & \vdots \\ h_{M1}^{[l]} & h_{M2}^{[l]} & \cdots & h_{MK}^{[l]} \end{bmatrix}, \quad l = 0, 1, 2, \dots, L.$$

$l$  is a delay index,  $h_{mk}^{[l]}$  represents the gain from the  $k^{th}$  transmit to the  $m^{th}$  receive antenna.  $\tau_l$  is the delay amount for the  $l$ -th delay. According to the stochastic modeling expressed as (1.12)

$$\mathcal{H}_l = \frac{1}{\sqrt{s}} (\mathbf{R}_{\theta_r, d_r}^{[l]})^{\frac{1}{2}} \mathbf{G}_r^{[l]} (\mathbf{R}_{\theta_s, 2D_r/s}^{[l]})^{\frac{1}{2}} \mathbf{G}_t^{[l]} (\mathbf{R}_{\theta_t, d_t}^{[l]})^{\frac{1}{2}} \quad (1.15)$$

Therefore, the relation for the continuous-time transmitted signal and received signal is:

$$\mathcal{Y}(t) = \int \mathbf{H}(\tau) \mathcal{X}(t - \tau) d\tau \quad (1.16)$$

where  $\mathcal{Y}(t) = \{y_1(t), y_2(t), \dots, y_M(t)\}^T$  and  $\mathcal{X}(t) = \{x_1(t), x_2(t), \dots, x_K(t)\}^T$ .

The equation (1.15) holds under the condition that both the mean DoA at the receiver and mean DoD at the transmitter are zero, see Fig. 1.6. When the directional properties are captured in the stochastic model, the equations (1.12) and (1.15) should be modified as follows:

$$\mathbf{H} = \frac{1}{\sqrt{S}} \mathbf{W}_r(\phi_r) \mathbf{R}_{\theta_r, d_r}^{\frac{1}{2}} \mathbf{G}_r \mathbf{R}_{\theta_s, 2D_r/s}^{\frac{1}{2}} \mathbf{G}_t \mathbf{R}_{\theta_t, d_t}^{\frac{1}{2}} \mathbf{W}_t(\phi_t); \quad (1.17)$$

$$\mathcal{H}_l = \frac{1}{\sqrt{S}} \mathbf{W}_r(\phi_r) (\mathbf{R}_{\theta_r, d_r}^{[l]})^{\frac{1}{2}} \mathbf{G}_r^{[l]} (\mathbf{R}_{\theta_s, 2D_r/s}^{[l]})^{\frac{1}{2}} \mathbf{G}_t^{[l]} (\mathbf{R}_{\theta_t, d_t}^{[l]})^{\frac{1}{2}} \mathbf{W}_t(\phi_t) \quad (1.18)$$

where

$$\mathbf{W}_{M \times M}(\phi_r) = \begin{bmatrix} w_r^{[1]}(\phi_r) & 0 & \dots & 0 \\ 0 & w_r^{[2]}(\phi_r) & & 0 \\ \vdots & & \ddots & \\ 0 & \dots & & w_r^{[M]}(\phi_r) \end{bmatrix}; \quad (1.19)$$

$$\mathbf{W}_{K \times K}(\phi_t) = \begin{bmatrix} w_t^{[1]}(\phi_t) & 0 & \dots & 0 \\ 0 & w_t^{[2]}(\phi_t) & & 0 \\ \vdots & & \ddots & \\ 0 & \dots & & w_t^{[K]}(\phi_t) \end{bmatrix}; \quad (1.20)$$

$w_t^{[i]}$  and  $w_r^{[i]}$  denotes the phase shift relative to the first antenna while the mean DoD is  $\phi_t$  and the mean DoA is  $\phi_r$ . Therefore, the modified version of  $\mathbf{H}$  and  $\mathcal{H}_l$  captures the directional properties.

Provided that the MEAs are the uniform linear antenna array (ULA),

$$w_t^{[i]} = f_t^{[i]}(\phi_t) \exp[-j(m-1)d\lambda^{-1}2\pi \sin \phi_t] \quad (1.21)$$

where  $f_t^{[i]}(\phi_t)$  is the complex radiation pattern of transmit antenna element  $i$ ;

$$w_r^{[i]} = f_r^{[i]}(\phi_r) \exp[-j(m-1)d\lambda^{-1}2\pi \sin \phi_r]; \quad (1.22)$$

where  $f_r^{[i]}(\phi_r)$  is the complex radiation pattern of receive antenna element  $i$  [60].

The discrete-time input-output relation of the MIMO time dispersive channels can be described through the following equation in the  $z$ -domain [28] :

$$Y_m(z) = \sum_{k=1}^K H_{mk}(z) X_k(z), \quad 1 \leq m \leq M \quad (1.23)$$

where  $Y_m(z)$ ,  $H_{mk}(z)$ ,  $X_k(z)$  are polynomials of  $z$ , as illustrated in Fig 1.8. .

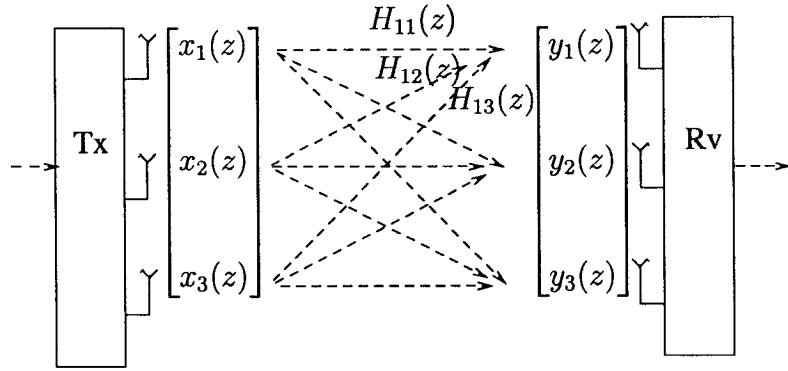


Figure 1.8: MIMO System Input-Output Relations in the  $z$ -domain.

This relationship in a matrix format becomes:

$$\mathbf{Y}(z) = \mathbf{H}(z)\mathbf{X}(z), \quad (1.24)$$

where

$$\mathbf{H}(z) = \begin{bmatrix} H_{11}(z) & H_{12}(z) & \cdots & H_{1K}(z) \\ H_{21}(z) & H_{22}(z) & \cdots & H_{2K}(z) \\ \cdots & \cdots & \cdots & \cdots \\ H_{M1}(z) & H_{M2}(z) & \cdots & H_{MK}(z) \end{bmatrix};$$

$$\mathbf{Y}(z) = \begin{bmatrix} Y_1(z) \\ Y_2(z) \\ \cdots \\ Y_M(z) \end{bmatrix}; \quad \mathbf{X}(z) = \begin{bmatrix} X_1(z) \\ X_2(z) \\ \cdots \\ X_K(z) \end{bmatrix};$$

$H_{mk}(z)$  denotes the transfer function from the  $k^{th}$  input to the  $m^{th}$  output;  $\mathbf{Y}(z)$  stands for the multiple-output (received signals) of the MIMO system; and  $\mathbf{X}(z)$  represents the multiple-input (transmitted signals) to the MIMO system.

In a MIMO system, the interpretation of the  $z$ -transform can be expressed in a matrix form as follows:

$$\mathbf{H}(z) = \sum_{l=0}^L \mathbf{h}(l)z^{-l}$$

where

$$\mathbf{h}(l) = \begin{bmatrix} h_{11}^{[l]} & h_{12}^{[l]} & \cdots & h_{1K}^{[l]} \\ h_{21}^{[l]} & h_{22}^{[l]} & \cdots & h_{2K}^{[l]} \\ \cdots & \cdots & \cdots & \cdots \\ h_{M1}^{[l]} & h_{M2}^{[l]} & \cdots & h_{MK}^{[l]} \end{bmatrix}, \quad l = 0, 1, \dots, L. \quad (1.25)$$

$$\mathbf{X}(z) = \sum_{l=-\infty}^{\infty} \mathbf{x}(l)z^{-l} \text{ where } \mathbf{x}(l) = [x_1(l) \ x_1(l) \cdots x_K(l)]^T$$

$$\mathbf{Y}(z) = \sum_{l=-\infty}^{\infty} \mathbf{y}(l)z^{-l} \text{ where } \mathbf{y}(l) = [y_1(l) \ y_1(l) \cdots y_M(l)]^T$$

In the time domain, the relationship between inputs and outputs of a MIMO system is:

$$\mathbf{y}(l) = \sum_{i=-\infty}^{\infty} \mathbf{h}(i)\mathbf{x}(l-i) = \sum_{i=-\infty}^{\infty} \mathbf{h}(l-i)\mathbf{x}(i) \quad (1.26)$$

The received signal vector sequence  $\mathbf{y}(l)$  is a convolution of the transmitted signal vector sequence  $\mathbf{x}(i)$  and the channel impulse response matrix sequence  $\mathbf{h}(i)$  [28]. In order to cancel the echoes caused by the multipath, a de-convolution of the multichannel signals is required.

Figure 1.9 illustrates the  $z$ -domain and time domain input-output relations in the time-invariant MIMO system for the first and last receive antenna based on (1.23) and (1.26), respectively.

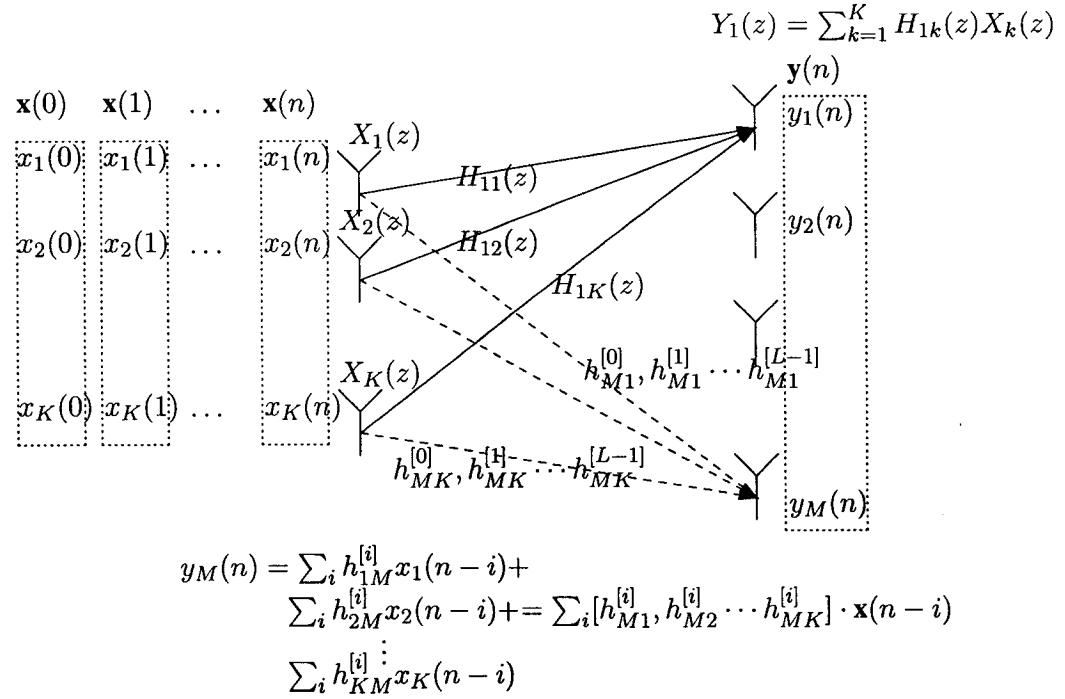


Figure 1.9: Mathematical Modeling of a MIMO System with  $K$  Transmit and  $M$  Receive Antennas.

## 1.6 Channel Identification and Equalization

In this section, a short review of multiple channel identification and equalization methods is presented.

The development in MIMO transmission systems indicates that it is beneficial to exploit the time, frequency, and spatial detail characteristics of the wave propagation. Hence, an active research trend in MIMO transceiver design is to optimally take advantage of these fine details instead of some ad hoc approximation to recover the signal from channel distortions. Developing advanced methods for multiple-channel identification is part of these investigation endeavors, and, channel identification is a prerequisite to some channel equalization approaches which assume the prior knowledge of the CIR.

Among all the approaches, the *blind* identification and equalization algorithms, which only have access to the received signals, have a *self-start (self-recovery)* feature. Blind methods facilitate the transmission efficiency because they do not need training sections



and are preferable in time-varying fading channels.

In the past twenty years, the signal subspace analysis based channel identification methods are among the algorithms which have attracted a lot of research attention, [61]-[65]. Deterministic subspace methodology has a superior performance when the channel order is known. However, its performance will degrade severely when the channel order is over-estimated or under-estimated. When the noise statistics is assumed to be spatially colored, many subspace-methods assuming noise to be both temporally and spatially white are not feasible. There are many other algorithms with various features, different processing complexity and assumptions, such as outer-product methods in [66] based on the prediction error methods for improved performance, joint data and channel estimation methods [67] and a mutually referenced filter method in [68]. Higher order statistic cumulant subspace method [69] became a recent contribution on multiple channel identification.

System performance loss due to channel frequency-selective effects will not be recovered by increasing the transmission power. A variety of channel equalization algorithms serve as a main methodology to recover the signal from frequency-selective channel distortions. These approaches initially were proposed for the SISO transceivers and are generalized to MIMO systems nowadays.

Several examples of the blind or training-aided equalization approaches are as follows [58], [70]: Linear equalization algorithms were constructed according to criterion: Zero-Forcing, ML [58], [71] with FIR filters. With improved performance, the decision-feedback equalization (DFE), [72], [73], [74], has been attracting enormous research efforts in MIMO framework. The performance degradation due to error propagation and the high complexity of the receiver structure in the scenarios with MIMO channels are the limiting factors to this type of schemes. Recursive LS equalization [70], [75] brings adaptivity in the signal reception, but there are major concerns on the convergence rate and complexity. Equalization based on signal property forcing, such as constant modulus algorithm (CMA) [76] offers blind algorithms, but it still has to deal with the convergence issues.

OFDM is a special kind of scheme with high resilience against frequency selective fading channels [77], [78], [79], which distributes the symbols along the frequency axis instead of time axis. As such, it splits a broadband channel into multiple narrow-band channels so that the frequency-selectivity of the channel could be efficiently compensated or mitigated by differential amplitude phase shift keying (DAPSK). Several combined schemes such as CDMA-OFDM, MIMO-OFDM [80], [81], have been shown to possess the superior performance.

Instead of processing signal at a symbol rate, using fractional-sampling to exploit the cyclostationarity, blind identification and equalization based on second-order statistics (SOS) was proposed in [82], [83], which started a new branch of SOS methods. Blind second order deconvolution proposed in [84] offers an improved robustness against the channel order estimation error.

Blind least-squares approach in [67] offers a new insight to the joint estimation of the data and the channel at a cost of high complexity. As a recent development based on this approach, an adaptive solution using deterministic maximum likelihood was presented in [85].

For high-mobility radio systems, channel characteristics vary rapidly, and make the approaches assuming time-invariant channels impractical. For time-varying channels, the basis expansion models and space-time techniques for blind equalization have been presented in [86]. Another algorithm which circumvents the channel identification by the direct signal subspace estimation discussed in [87] is also preferable for high-mobility fading channels.

Two of the schemes proposed in this dissertation are blind channel equalization schemes and one of the schemes falls into the category of direct signal subspace estimation methods. All of them are the deterministic approaches which can operate on a small number of samples, i.e., the signal samples within a short time period when the MIMO channel is assumed to be stationary. Because of this feature of the proposed approaches using quasi-static channel modeling, it is possible to deal with the time-varying channels that is static over the duration of a few frames.

In addition, several modulation and multiple access schemes have less vulnerability to the frequency selective channel impairment, i.e., Frequency-Hopping-CDMA-SS and Direct-Sequence-CDMA-SS inherently have the interference suppression property. Therefore, ISI can be mitigated to some extent by employing such robust modulation/access methods. Combination of coding and modulation such as TCM, multiple TCM also are effective tools in improving the signal quality.

## Chapter 2

# Frequency Domain Equalization for MIMO Space-Time Transmissions with Single Carrier Signaling

**T**HIS chapter presents a space-time MIMO transceiver scheme for reliable transmissions over frequency selective fading channels using conventional single-carrier M-ary PSK or QAM modulations. The main feature of this scheme is to exploit the induced signal circulant structure at the receiver to mitigate the ISI effect in the context of MIMO channel. Through a large number of Monte-Carlo simulations, it is demonstrated that the performance of this scheme over time-dispersive channels is comparable to that of MIMO-OFDM. Because the OFDM scheme has high peak-to-average power ratio (PAPR), and as a result, it demands the use of highly linear power amplifiers (PA), the proposed scheme is an excellent alternative as it offers the advantage of reduced constraints on the PA linearity. In general, it is difficult to implement the high-power PA at the transmitter to meet both constraints of linearity and power efficiency.

The chapter consists of six sections: Section 2.1 briefly describes the background of the research in this chapter. Section 2.2 details the signaling proposed in the scheme. Section 2.3 derives the receiver algorithm for SIMO channel cases, which has a single antenna

at the transmitter and multiple antennas at the receiver side. Section 2.4 generalizes the SIMO cases to the MIMO channel scenario, where the multiple antennas are assumed to be employed at both sides of the transmission link. Section 2.5 demonstrates the systems performance via simulation results and related analysis. The final section summarizes this chapter.

## 2.1 Motivations

The ever-increasing transmission rate of wireless applications places demands on the equalization algorithms to be even more efficient in terms of convergence, complexity and adaptability. For high-rate wideband communications, the channel time-spreading could be very large compared to a symbol time slot. Conventional time-domain decision-feedback equalizers (DFE) have to have a large number of taps to equalize such kind of channels. For the case of MIMO spatial multiplexing, in which multiple data streams are simultaneously transmitted within the same frequency band exploiting spatial signatures in a rich-scattering environment [5], [9], [15], [60], [88], the computation of the optimal coefficients of MIMO-DFE for long time-spreading channels is very demanding and costly [72]- [74]. Moreover, the feedback data error propagation problem always degrades the performance of MIMO-DFE.

In the last ten years, owing to its unique signaling structure to facilitate efficient channel equalization, OFDM became one of the most prominent schemes in time-dispersive channels [77], [79], [81], [78]. However, the OFDM advantages in channels impaired by ISI are offset by its high PAPR. Nonlinear distortions of the channel or transceiver cause dramatic OFDM performance degradation as they give rise to severe inter-carrier-interference (ICI) [89].

The single carrier frequency domain equalization (SCFDE) scheme [90] employs the M-ary PSK or QAM single-carrier signaling and has comparable performance over time-dispersive fading channels as OFDM. This chapter extends the SCFDE from SISO to the

MIMO cases. The proposed scheme has a favorable tradeoff between the channel equalization performance and the processing complexity. This scheme has the advantage that it does not face the high PAPR problem as MIMO-OFDM, and has a same overall transceiver complexity as that of MIMO-OFDM. It is practical and capable of fully removing ISI via efficient processing in the frequency domain. Its signaling frames possess a circular suffix segment and the receiver exploits the signal structure of circulant matrix. It is this special signaling frame structure that facilitates the ISI mitigation at the receiver.

## 2.2 Transmission Signaling

In the SCFDE,  $N$  information-bearing  $M$ -ary PSK or QAM symbols  $s_j^{[k]}$ ,  $j = 1, \dots, N$  are assumed to be carried in the  $k$ -th frame time slot  $\mathbf{S}^{[k]} = [s_1^{[k]}, s_2^{[k]}, s_3^{[k]}, \dots, s_N^{[k]}]$ . The transmission procedure is illustrated in Fig. 2.1. Rather than transmitting the data vector  $\mathbf{S}^{[k]}$ ,  $G$  circular-shift-suffix symbols (or fixed symbol sequence) are appended following the data symbols in the guard time interval  $T_G$ . Appending a fixed symbol sequence is favorable for the purposes of semiblind channel estimation, tracking, and synchronization [91]. Without losing generality, we assume a circular-shift-suffix is transmitted here. Hence, what enters the channel is the frame defined as:

$\mathbf{F}^{[k]} = \overbrace{[s_1^{[k]}, s_2^{[k]}, s_3^{[k]}, s_4^{[k]}, s_5^{[k]}, \dots, s_N^{[k]}, s_1^{[k]}, s_2^{[k]}, \dots, s_G^{[k]}]}^W$  where  $W = N + G$  is the frame length;  $G = \frac{T_G}{T_s} \geq L$ ; and  $L + 1$  is the maximum length of the multiple channels. The transmitted signal in the  $k^{th}$  frame from a transmit antenna is modulated with a single carrier as expressed in the following equation:

$$s(t) = \Re\left\{\sum_{w=1}^W g(t - (w-1)T_s - (k-1)T_f) \times \mathbf{F}_{(w)}^{[k]} e^{j2\pi f_c(t - (w-1)T_s - (k-1)T_f)}\right\} \quad (2.1)$$

where  $g(t)$  is a shaping pulse,  $f_c, T_f, T_s$  are the carrier's frequency, the time interval for a frame and the time slot for a symbol, respectively.

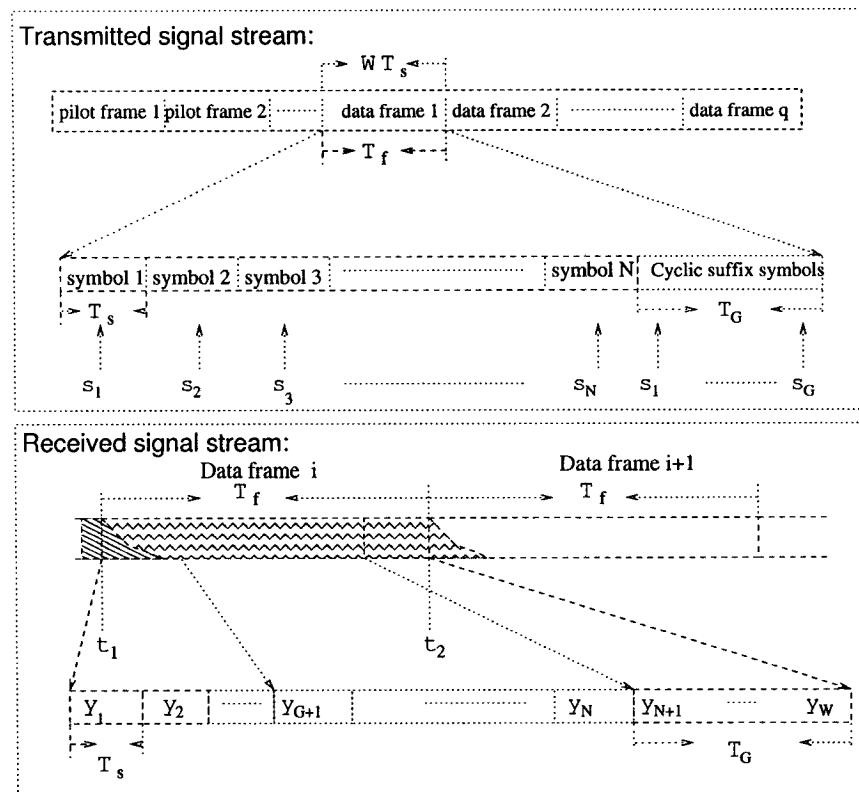


Figure 2.1: The Timing of the Transmitted and Received Signal Streams.

## 2.3 Receiver Algorithm for SIMO Cases

In this section,  $M$  antennas are assumed to be employed at the receiver and transmitter only has a single antenna. For a quasi-static discrete-time modeling of single input and multiple output (SIMO) channels as demonstrated in Fig. 2.2, in the time domain, a matrix  $\mathbf{H}$  is used to capture the impulse responses of the multiple channels [57]:

$$\begin{aligned} \mathbf{H}_{M \times (L+1)} &= \begin{bmatrix} h_1^{[0]} & h_1^{[1]} & \dots & h_1^{[L]} \\ h_2^{[0]} & h_2^{[1]} & \dots & h_2^{[L]} \\ \vdots & \vdots & \vdots & \vdots \\ h_M^{[0]} & h_M^{[1]} & \dots & h_M^{[L]} \end{bmatrix} \\ &= [\mathbf{h}(0) \quad \mathbf{h}(1) \quad \dots \quad \mathbf{h}(L)] \end{aligned} \quad (2.2)$$

where  $h_q^{[i]}$  represents the gain from the transmit antenna to the  $q^{th}$  receive antenna, and  $i$  is a delay index. The vector  $\mathbf{h}(i)$  is the  $i^{th}$  column of the matrix  $\mathbf{H}_{M \times (L+1)}$ .

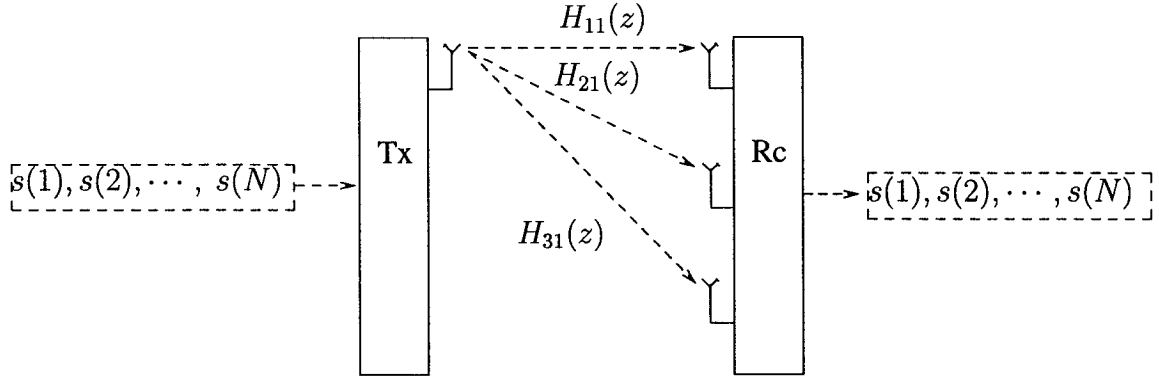


Figure 2.2: Single-Input Multiple-Output System.

In the proposed scheme, the received signals, after down-converting and base-band filtering, are sampled at the symbol rate and arranged in a matrix  $\mathcal{Y}^{[k]}$  within the  $k^{th}$  frame interval between  $t_1$  to  $t_2$  as illustrated in Fig. 2.1, where samples from the same receive antenna are in one row. Without noise, the sampled data matrix  $\mathcal{Y}^{[k]}$  is a convolution of



discrete-time channel impulse response with the transmitted signals. In a matrix format, this relationship could be expressed as follows:

$$\mathcal{Y}_{M \times W}^{[k]} = \mathbf{H}_{M \times (L+1)} \mathcal{X}_{(L+1) \times W}^{[k]} + \mathcal{N}_{M \times W} \quad (2.3)$$

where  $\mathcal{N}$  stands for the noise component matrix, and  $\mathcal{Y}^{[k]}$  and  $\mathcal{X}^{[k]}$  are the matrices as follows.

$$\mathcal{Y}_{M \times W}^{[k]} = \begin{bmatrix} y_{(1,1)}^{[k]} & y_{(1,2)}^{[k]} & \cdots & \cdots & y_{(1,W)}^{[k]} \\ y_{(2,1)}^{[k]} & y_{(2,2)}^{[k]} & \cdots & \cdots & y_{(2,W)}^{[k]} \\ \vdots & \vdots & \vdots & \vdots & \vdots \\ y_{(M,1)}^{[k]} & y_{(M,2)}^{[k]} & \cdots & \cdots & y_{(M,W)}^{[k]} \end{bmatrix}$$

$$\mathcal{X}_{(L+1) \times W}^{[k]} = \begin{bmatrix} \mathbf{F}_{(1)}^{[k]} & \mathbf{F}_{(2)}^{[k]} & \cdots & \cdots & \cdots & \mathbf{F}_{(W)}^{[k]} \\ \mathbf{F}_{(W)}^{[k-1]} & \mathbf{F}_{(1)}^{[k]} & \cdots & \cdots & \cdots & \mathbf{F}_{(W-1)}^{[k]} \\ \vdots & \vdots & \vdots & \vdots & \vdots & \vdots \\ \mathbf{F}_{(W-L+1)}^{[k-1]} & \cdots & \mathbf{F}_{(W)}^{[k-1]} & \mathbf{F}_{(1)}^{[k]} & \cdots & \mathbf{F}_{(W-L)}^{[k]} \end{bmatrix}$$

The first processing of proposed receiver is to remove the first  $G$  columns from the received data matrix  $\mathcal{Y}^{[k]}$  so that a shorter data matrix  $\mathbb{Y}^{[k]}$  is obtained:

$$\mathbb{Y}_{M \times N}^{[k]} = \begin{bmatrix} y_{(1,G+1)}^{[k]} & y_{(1,G+2)}^{[k]} & \cdots & \cdots & y_{(1,W)}^{[k]} \\ y_{(2,G+1)}^{[k]} & y_{(2,G+2)}^{[k]} & \cdots & \cdots & y_{(2,W)}^{[k]} \\ \vdots & \vdots & \vdots & \vdots & \vdots \\ y_{(M,G+1)}^{[k]} & y_{(M,G+2)}^{[k]} & \cdots & \cdots & y_{(M,W)}^{[k]} \end{bmatrix}$$

such that

$$\mathbb{Y}_{M \times N}^{[k]} = \mathbf{H}_{M \times (L+1)} \mathbb{X}_{(L+1) \times N}^{[k]} + \mathbb{N}_{M \times N} \quad (2.4)$$

and

$$\mathbb{X}_{(L+1) \times N}^{[k]} = \begin{bmatrix} \mathbf{F}_{(G+1)}^{[k]} & \mathbf{F}_{(G+2)}^{[k]} & \cdots & \cdots & \mathbf{F}_{(W)}^{[k]} \\ \mathbf{F}_{(G)}^{[k]} & \mathbf{F}_{(G+1)}^{[k]} & \cdots & \cdots & \mathbf{F}_{(W-1)}^{[k]} \\ \vdots & \vdots & \vdots & \vdots & \vdots \\ \mathbf{F}_{(G-L+1)}^{[k]} & \mathbf{F}_{(G-L+2)}^{[k]} & \cdots & \cdots & \mathbf{F}_{(W-L)}^{[k]} \end{bmatrix} \quad (2.5)$$

Furthermore, from (2.2) and (2.4),  $\mathbb{Y}_{M \times N}^{[k]}$  is expressed as follows:

$$\mathbb{Y}_{M \times N}^{[k]} = \sum_{i=1}^{L+1} \mathbf{h}_{M \times 1}(i-1) \mathbb{X}_{(i,:)}^{[k]} + \mathbb{N}_{M \times N} \quad (2.6)$$

where  $\mathbb{X}_{(i,:)}$ , the  $i^{th}$  row of  $\mathbb{X}$ , is a circularly shifted version of  $\mathbf{S}^{[k]}$ . This fact can be observed from matrix (2.5) and the definition of  $\mathbf{F}^{[k]}$ . Hence,

$$\mathbb{Y}_{M \times N}^{[k]} = \sum_{i=1}^{L+1} \mathbf{h}_{M \times 1}(i-1) \mathcal{S}_{(G-i+1)}^{[k]} + \mathbb{N}_{M \times N} \quad (2.7)$$

where  $\mathcal{S}_{(i)}^{[k]}$  stands for  $\mathbf{S}^{[k]}((n+i))_N$ , a left circularly shifted version of  $\mathbf{S}^{[k]}$ . The following properties and theorem about the Discrete Fourier Transform (DFT) and the Inverse Discrete Fourier Transform (IDFT) are useful for further analysis of the signal structure and the derivation of the receiver algorithm. If  $\mathbf{x} = [x(1), x(2), x(3), \dots, x(N)]$  and  $\mathbf{X} = [X(1), X(2), X(3), \dots, X(N)]$  are the DFT pair:  $\mathbf{x}_N \xrightarrow[N]{DFT} \mathbf{X}_N$ . The DFT relation can be written in a matrix format as follows:

$$\text{DFT: } \mathbf{X}_N = \mathbf{x}_N \mathbf{V}, \quad \text{IDFT: } \mathbf{x}_N = \frac{1}{N} \mathbf{X}_N \mathbf{V}^H \quad (2.8)$$

$$\mathbf{V}_{N \times N} = \begin{bmatrix} 1 & 1 & 1 & \dots & 1 \\ 1 & v & v^2 & \dots & v^{N-1} \\ 1 & v^2 & v^4 & \dots & v^{2(N-1)} \\ \vdots & \vdots & \vdots & \vdots & \vdots \\ 1 & v^{N-1} & v^{2(N-1)} & \dots & v^{(N-1)(N-1)} \end{bmatrix} \quad (2.9)$$

$\mathbf{V}_{N \times N}$  is a Vandermonde matrix with  $v = e^{-j2\pi/N}$  [58]. In this case,  $\mathbf{V}$  is also a Fourier transform matrix.

**Theorem 2** [92] If  $x(n) \xrightarrow[N]{DFT} X(k)$ ,

$$x((n-l))_N \xrightarrow[N]{DFT} X(k) e^{-j2\pi kl/N} \quad (2.10)$$

From Theorem 2, it could be concluded that:

$$\mathcal{S}_{(i)}^{[k]} = IDFT((\mathbf{Q}(i) \odot DFT(\mathbf{S}^{[K]}))) \quad (2.11)$$

where  $\odot$  stands for element by element product and

$$\mathbf{Q}(i) = [e^{j2\pi i/N}, e^{j2\pi 2i/N}, e^{j2\pi 3i/N}, \dots, e^{j2\pi Ni/N}] \quad (2.12)$$

Hence,

$$\mathcal{S}_{(G-i+1)}^{[k]} = \mathbf{Q}(G-i+1)\mathbf{S}^{[k]} \quad (2.13)$$

where

$$\mathbf{S}^{[k]} = \frac{1}{N} \begin{bmatrix} \gamma_1^{[k]} & 0 & \dots & 0 \\ 0 & \gamma_2^{[k]} & \dots & 0 \\ \vdots & \vdots & \vdots & \vdots \\ 0 & 0 & \dots & \gamma_N^{[k]} \end{bmatrix} \mathbf{V}^H \quad (2.14)$$

and  $[\gamma_1^{[k]}, \gamma_2^{[k]}, \gamma_3^{[k]}, \dots, \gamma_N^{[k]}] = [s_1^{[k]}, s_2^{[k]}, s_3^{[k]}, \dots, s_N^{[k]}]\mathbf{V}$ .

From (2.7) and (2.13),

$$\mathbb{Y}_{M \times N}^{[k]} = \sum_{i=1}^{L+1} \mathbf{h}_{M \times 1}(i-1) \mathbf{Q}(G-i+1) \mathbf{S}^{[k]} + \mathbf{N}$$

and this relation in matrix form is:

$$\mathbb{Y}_{M \times N}^{[k]} = \mathbf{C} \mathbf{S}^{[k]} + \mathbf{N} \quad (2.15)$$

where

$$\mathbf{C} = \sum_{i=1}^{L+1} \mathbf{h}_{M \times 1}(i-1) \mathbf{Q}(G-i+1) = \mathbf{H} \mathbf{Q},$$

and

$$\mathbf{Q} = [\mathbf{Q}(G)^T, \mathbf{Q}(G-1)^T, \mathbf{Q}(G-2)^T, \dots, \mathbf{Q}(G-L)^T]^T.$$

The signaling structure described by (2.11) and (2.15) facilitates direct and efficient processing to be conducted in frequency domain to achieve channel equalization and the symbol detection. The parameter matrix  $\mathbf{C}$  can be expressed as:

$$\mathbf{C} = \begin{bmatrix} c_{11} & c_{12} & \cdots & c_{1N} \\ c_{21} & c_{22} & \cdots & c_{2N} \\ \vdots & \vdots & \vdots & \vdots \\ c_{M1} & c_{M2} & \cdots & c_{MN} \end{bmatrix} \quad (2.16)$$

$$= [\mathbf{C}(:, 1), \mathbf{C}(:, 2), \dots, \mathbf{C}(:, N)]$$

where  $\mathbf{C}(:, i)$  is the column vector of  $\mathbf{C}$ . From (2.15), it is concluded that:

$$\mathbb{Y}_{M \times N}^{[k]} \mathbf{V} = [\gamma_1^{[k]} \mathbf{C}(:, 1), \gamma_2^{[k]} \mathbf{C}(:, 2), \dots, \gamma_N^{[k]} \mathbf{C}(:, N)] + \mathbf{N} \mathbf{V} \quad (2.17)$$

Therefore, the estimation of  $\gamma_i^{[k]}$  via maximum ratio combining method can be expressed as follows:

$$\hat{\gamma}_i^{[k]} = \mathbf{C}(:, i)^H [\mathbb{Y}_{M \times N}^{[k]} \mathbf{V}]_{(:, i)} / (\mathbf{C}(:, i)^H \mathbf{C}(:, i)) \quad (2.18)$$

Eventually, once  $\hat{\gamma}_i^{[k]}$  is calculated, the original symbols in the time domain are obtained via IDFT:

$$\begin{aligned} \hat{\mathbf{S}}^{[k]} &= [\hat{s}_1^{[k]}, \hat{s}_2^{[k]}, \dots, \dots, \hat{s}_N^{[k]}] \\ &= \mathcal{E}(\text{IDFT}\{[\hat{\gamma}_1^{[k]}, \hat{\gamma}_2^{[k]}, \hat{\gamma}_3^{[k]}, \dots, \hat{\gamma}_N^{[k]}]\}) \end{aligned} \quad (2.19)$$

where  $\mathcal{E}$  stands for the detection of the symbol. The proposed detector for SIMO cases requires calculation of  $\hat{\gamma}_i^{[k]}$  as in (2.18), and the original symbols are obtained using (2.19).

## 2.4 MIMO: Spatial Multiplexing Cases

This section extends the SIMO signal reception scheme from Section 2.3 to the case of MIMO spatial multiplexing, in which  $K$  transmit antennas and  $M$  receive antennas are employed, and each of the transmit antennas independently sends a data stream within the

same frequency band. This scheme is demonstrated in Fig. 2.3 where ‘DF’ stands for ‘Data Frame’.

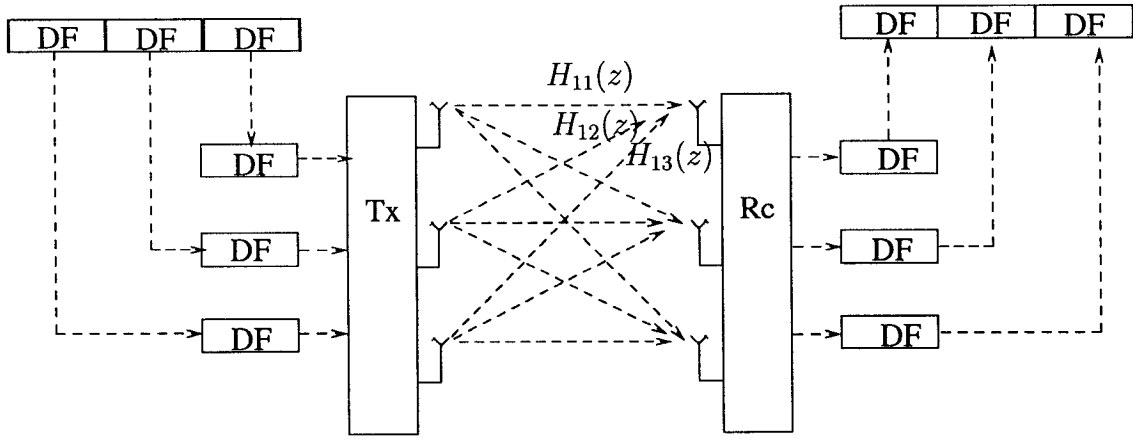


Figure 2.3: Spatial Multiplexing Transceiver.

The received signals at the receiver antenna array are the superposition of all the signals from different transmit antennas. Hence, based on (2.17), the following equation holds for the cases of spatial multiplexing with multiple transmit and receive antennas:

$$\mathbb{Y}_{M \times N}^{[k]} \mathbf{V} = \left[ \sum_{i=1}^K \gamma_1^{[i,k]} \mathbf{C}_i(:, 1), \sum_{i=1}^K \gamma_2^{[i,k]} \mathbf{C}_i(:, 2), \dots, \sum_{i=1}^K \gamma_N^{[i,k]} \mathbf{C}_i(:, N) \right] + \mathbf{N}_{M \times N} \mathbf{V} \quad (2.20)$$

where superscript  $[i, k]$  denotes the signal components of the  $k^{th}$  frame from the  $i^{th}$  transmit antenna.  $\mathbf{C}_i$ ,  $i = 1, 2, \dots, K$  plays the same role as  $\mathbf{C}$  in equation 2.16, and it corresponds to  $i^{th}$  transmit antenna. In matrix format, (2.20) becomes:

$$\mathbb{Y}_{M \times N}^{[k]} \mathbf{V} = [\mathbf{C}_1 \Gamma_1^{[k]}, \mathbf{C}_2 \Gamma_2^{[k]}, \dots, \mathbf{C}_N \Gamma_N^{[k]}] + \mathbf{N}_{M \times N} \mathbf{V} \quad (2.21)$$

where,

$$\mathbf{C}_j = [\mathbf{C}_1(:, j), \mathbf{C}_2(:, j), \dots, \mathbf{C}_K(:, j)],$$

and

$$\Gamma_j^{[k]} = [\gamma_j^{[1,k]}, \gamma_j^{[2,k]}, \gamma_j^{[3,k]}, \dots, \gamma_j^{[K,k]}]^T, \quad j = 1, 2, \dots, N.$$

As a sub-optimal solution, to reduce the receiver complexity, each  $\Gamma_j^{[k]}, j = 1, 2, \dots, N$ , is estimated separately. Hence, the block-wise maximum likelihood (ML) estimator for  $\Gamma_i^{[k]}$  is:

$$\hat{\Gamma}_j^{[k]} = (\mathbf{C}_j^T \mathbf{R}_j^{-1} \mathbf{C}_j)^{-1} \mathbf{C}_j^T \mathbf{R}_j^{-1} (\mathbf{Y}_{n \times N}^{[k]} \mathbf{V})_{(:,j)} \quad (2.22)$$

where  $\{\mathbf{N}_{M \times N} \mathbf{V}\}_{(:,j)}$  is assumed of Gaussian distribution  $\mathcal{CN}[0, \mathbf{R}_j], j = 1, 2, \dots, N$ . Similarly, the least squares (LS) estimator for each  $\Gamma_i^{[k]}$  is:

$$\hat{\Gamma}_j^{[k]} = (\mathbf{C}_j^T \mathbf{C}_j)^{-1} \mathbf{C}_j^T (\mathbf{Y}_{n \times N}^{[k]} \mathbf{V})_{(:,j)} \quad (2.23)$$

From the relationship in (2.19),  $\hat{\mathbf{S}}$  can be obtained from  $\hat{\Gamma}$  for each data stream through the IDFT.

However, as mentioned in [5], [7], the layered processing by signal nulling and canceling outperforms the processing via only nulling. The optimal ordering of detection and canceling is conducted according to the SNR of each data stream from a single transmit antenna. A larger subchannel gain for a data stream results in a greater SNR. The channel gain is parameterized as  $\|\mathbf{H}_p\|, p = 1, 2, \dots, K$ , for each data stream, which is proportional to  $\|\mathbf{C}_p\|, p = 1, 2, \dots, K$ .

We propose the following procedure for symbol detection in the MIMO-SCFDE scheme.

1. Calculate and sort  $\{g_p = \|\mathbf{C}_p\|, p = 1, 2, \dots, K\}$  decreasingly to obtain the optimal ordering  $\{O_p, p = 1, 2, \dots, K\}$  for detection and cancellation;
2. Detect the  $O_p$ th data stream and cancel it from the received signals, the finite alphabet (FA) property of the transmitted signaling is exploited implicitly here. Mathematically, it can be formulated as follows:

(a) MLE (block-wise):

$$\tilde{\gamma}_j^{[O_p, k]} = ((\mathbf{C}_j^T \mathbf{R}_j^{-1} \mathbf{C}_j)^{-1} \mathbf{C}_j^T \mathbf{R}_j^{-1})_{(O_p, :)} \mathfrak{Y}_{(:,j)}^{[k]},$$

or LSE (block-wise):

$$\tilde{\gamma}_j^{[O_p, k]} = ((\mathbf{C}_j^T \mathbf{C}_j)^{-1} \mathbf{C}_j^T)_{(O_p, :)} \mathfrak{Y}_{(:,j)}^{[k]},$$

where  $\mathfrak{Y}^{[k]} = \mathbf{Y}_{n \times N}^{[k]} \mathbf{V}, j = 1, 2, \dots, N$ ;

- (b)  $\tilde{\mathbf{S}}^{[O_p, k]} = [\tilde{s}_1^{[O_p, k]}, \tilde{s}_2^{[O_p, k]}, \dots, \tilde{s}_N^{[O_p, k]}]$   
 $= IDFT\{\tilde{\gamma}_1^{[O_p, k]}, \tilde{\gamma}_2^{[O_p, k]}, \tilde{\gamma}_3^{[O_p, k]}, \dots, \tilde{\gamma}_N^{[O_p, k]}\};$
- (c)  $\hat{\mathbf{S}}^{[O_p, k]} = \mathcal{E}\{\tilde{\mathbf{S}}^{[O_p, k]}\};$
- (d)  $[\hat{\gamma}_1^{[O_p, k]}, \hat{\gamma}_2^{[O_p, k]}, \hat{\gamma}_3^{[O_p, k]}, \dots, \hat{\gamma}_N^{[O_p, k]}] = DFT\{\hat{s}_1^{[O_p, k]}, \hat{s}_2^{[O_p, k]}, \dots, \hat{s}_N^{[O_p, k]}\};$
- (e)  $\{\mathfrak{Y}^{[k]} - [\mathbb{C}_1(:, O_p)\hat{\gamma}_1^{[O_p, k]}, \mathbb{C}_2(:, O_p)\hat{\gamma}_2^{[O_p, k]}, \dots, \mathbb{C}_N(:, O_p)\hat{\gamma}_N^{[O_p, k]}]\} \Rightarrow \mathfrak{Y}^{[k]};$
- (f) Column vector  $\mathbb{C}_j(:, O_p)$  is removed from  $\mathbb{C}_j$  for  $j = 1, 2, \dots, N$ .

3. Continue on procedure 2 according the ordering of  $\{O_p, p = 1, 2, \dots, K\}$  until all the data streams are detected;
4. Decode the detected symbol sequence if an encoding scheme is employed. The interleaving and coding will bring substantial performance enhancement against the time-selective magnitude fading effects of the wireless channels.

There are numbers of methods to estimate the channel via blind or semiblind methods as well as their adaptive versions for time-varying channels. Full discussion on how to apply these methods in the proposed scheme is beyond the scope of this chapter. Owing to the nature of the SCFDE scheme, there is an efficient method to estimate the channel impulse response (CIR) of MIMO channels. A procedure for estimating CIR with block-wise linear minimum mean-squared estimation after [93] is:

1.  $\mathbb{C}_j = \mathbf{R}_{(\mathfrak{Y}_{(:,j)}, \Gamma_j)} \mathbf{R}_{(\Gamma_j, \Gamma_j)}^{-1}, j = 1, 2, \dots, N.$
2.  $\mathbb{C}_j, \{j = 1, 2, \dots, N.\} \implies \mathbf{C}_i, i = 1, 2, \dots, K.$   
 according to their definitions.
3.  $\mathbf{H}_i = \mathbf{C}_i \mathbf{Q}^H (\mathbf{Q} \mathbf{Q}^H)^{-1}, i = 1, 2, \dots, K.$

It is feasible to make use of detected signal frame in updating the estimation of  $\mathbf{R}_{(\Gamma_j, \Gamma_j)}$  and  $\mathbf{R}_{(\mathfrak{Y}_{(:,j)}, \Gamma_j)}$  so that the channel variance could be tracked continuously.  $\mathbf{H}_i$  is the CIR matrix corresponding to the  $i^{th}$  transmit antenna.

## 2.5 Performance Simulations

In order to verify the performance of the proposed MIMO-SCFDE scheme in multipath fading environments, extensive simulations were conducted to obtain the Bit Error Rate (BER) as a function of Signal-to-Noise Ratio (SNR). The SNR values in the figures of the simulation results throughout this dissertation is SNR per bit per receive antenna defined as:  $SNR = 10 \log_{10}(\frac{\mathcal{E}_b}{N_0})$ , where  $\mathcal{E}_b$  is the signal energy per bit obtained from a single receive antenna, and  $N_0$  is the one-sided power spectral density of the white noise. The channel model in the simulations is a Rayleigh fading FIR channel. The typical BER results and the symbol constellations before and after equalization are illustrated in Figs. 2.4, 2.6, 2.5 and 2.7. In the simulations, the maximum number of symbols contributing to the ISI given by the parameter  $L$  was assumed as indicated in the figures. Parameters  $M = 4, 5, 6$ , and  $K = 4, 6$  were assumed for different simulations as denoted. The modulation schemes applied are QPSK and 16-ary QAM, respectively. The simulation results were statistically averaged over all the cases of random multipath delays, random channel states, random bit streams and random additive Gaussian noise components.

The performances of SIMO cases were also simulated and the typical results for BER as a function of SNR are illustrated in Fig. 2.8 and Fig. 2.9 for QPSK and 16-ary QAM signaling, respectively. Symbol constellations before and after channel equalization are in Fig. 2.10 with certain typical SNR values.

For comparison purposes, the performances of QPSK-OFDM and 16QAM-OFDM were simulated as well with the same transceiver antenna setup and time-dispersive fading channels. The results are reported in Fig. 2.4 and Fig. 2.6 with curves being labeled as OFDM. It can be observed the MIMO-SCFDE achieved a robust performance for MIMO fading channels which is comparable to the performance of OFDM schemes with the same transmission rates, provided that the number of receiver antennas is greater than that of the transmitter antennas.

From the symbol constellation diagrams for the signals before and after the equalization in Figs. 2.5, 2.7 and 2.10, it can be observed that (i) before the equalization, the



constellations of the transmitted symbols were drastically distorted by the ISI caused by the time-dispersive channels; (ii) after the equalization, the noise instead of ISI becomes the dominant limiting factor resulting in the detection errors.

From the performance curves in Figs. 2.4 and 2.6, it is evident that, with the same transceiver antenna setups, the BER of the proposed scheme drops as fast as that of the corresponding MIMO-OFDM scheme does when the SNR increases, provided that the receive antenna number is larger than the transmit antenna number. When the transmit antenna number and the receive antenna number equal, the BER performance of the proposed scheme is inferior to that of the corresponding MIMO-OFDM systems. This situation does not exist in SIMO cases where the receive antenna number is always no less than the transmit antenna number.

By increasing the receive antenna number, the power savings could be obtained to a certain extent depending on the BER operating point of the transceivers, signal constellation employed, and the numbers of the transmit and receive antennas. In Figs. 2.4 and 2.6, the increase of  $M = 5$  to  $M = 6$  brought 3.5 dB and 4 dB power savings for the QPSK and 16QAM constellations at the BER operating point of  $10^{-3}$ , respectively. With the same transceiver antenna setups, at the BER of  $10^{-4}$ , the power savings are 4.5 dB and 4.8 dB for the schemes with the QPSK and 16 QAM constellations, respectively.

It also can be observed that the power savings contributed by the increase of receive antenna number conforms to the law of diminishing returns. The smaller the receive antenna number is, with the same signaling, the greater power savings could be obtained by the same increase of  $M$ .

Through the comparison of the Figs. 2.4 and 2.6, it is observed as well that, at the same BER operating point, the scheme with the QPSK constellation requires a smaller SNR than the scheme with the 16-QAM constellation. For example, at the BER operating point of  $10^{-3}$  with  $k = 4$  and  $M = 5$ , the scheme with the QPSK constellation requires SNR to be 8.5 dB while the scheme with the 16-QAM constellation needs SNR to be 13 dB.

This is similar to the cases of the conventional SISO transceivers with the QPSK and 16-QAM constellations. However, the bandwidth utilization is higher with 16-QAM. When the symbol transmission rate is same, the bit rate of the schemes with 16-QAM is a double of that with QPSK.

There is a variety of other configurations for the proposed MIMO-SCFDE schemes in terms of different number of receiver antennas, modulation levels, frame lengths and guard time intervals. These parameters should be properly chosen by taking into account channel length, SNR and time-varying characteristics of the channel.

## 2.6 Summary

This chapter proposed an efficient sub-optimal transceiver framework for MIMO transmissions over time-dispersive fading channels. This scheme achieves a comparable performance to that of MIMO-OFDM when the number of the receive antennas is greater than that of the transmitter antennas. Because the scheme is based on the conventional modulations as PSK and QAM, it does not require a highly linear PA as in the case of MIMO-OFDM. With a proper choice of parameters  $W$ ,  $N$ ,  $T_s$  and the guard time  $T_G$ , the proposed MIMO-SCFDE scheme is able to fully mitigate the multipath time-dispersive impairments. The simulations demonstrate (i) the MIMO-SCFDE's robust performance over the multi-path fading channels and (ii) the scheme insensitivity to the different channel lengths provided the  $T_G > LT_s$ .

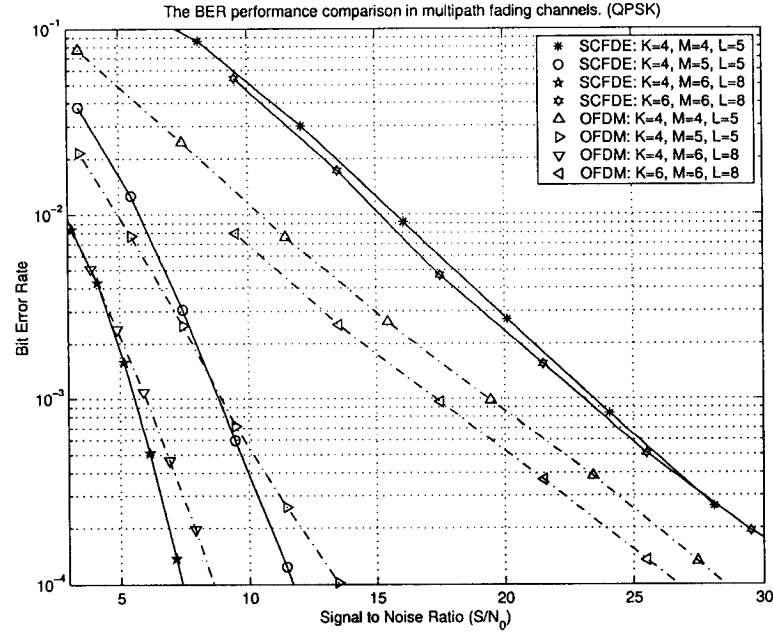


Figure 2.4: The BER Performance over Multipath Fading Channel (MIMO cases: QPSK-SCFDE, QPSK-OFDM).

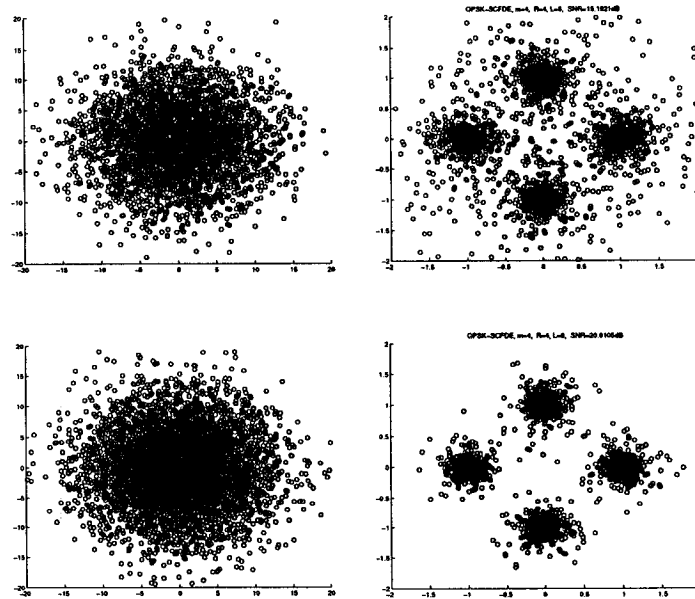


Figure 2.5: Symbol Constellations Before and After Equalization (MIMO cases: QPSK-SCFDE,  $M=4$ ,  $K=4$ ,  $\text{SNR}=15.2$  dB for upper figures,  $\text{SNR}=20$  dB for lower figures).

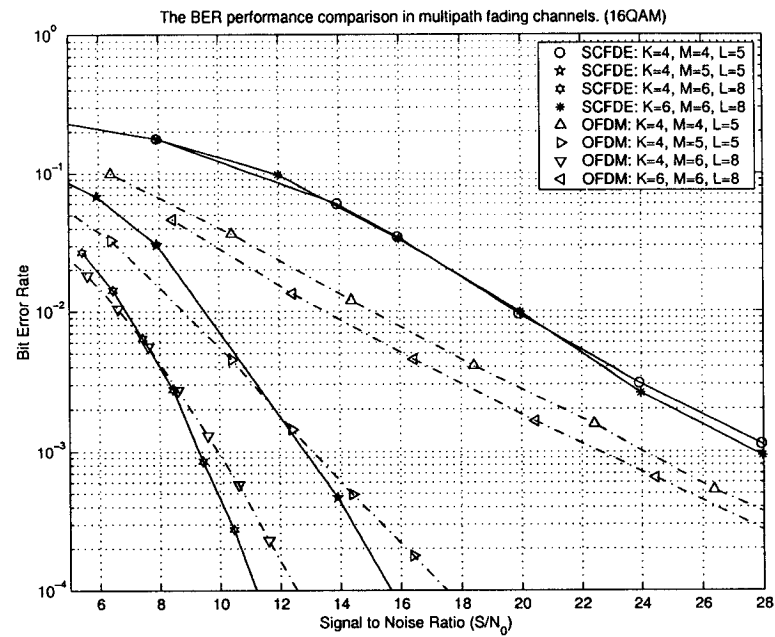


Figure 2.6: The BER Performance over Multipath Fading Channel (MIMO cases: 16QAM-SCFDE, 16QAM-OFDM).

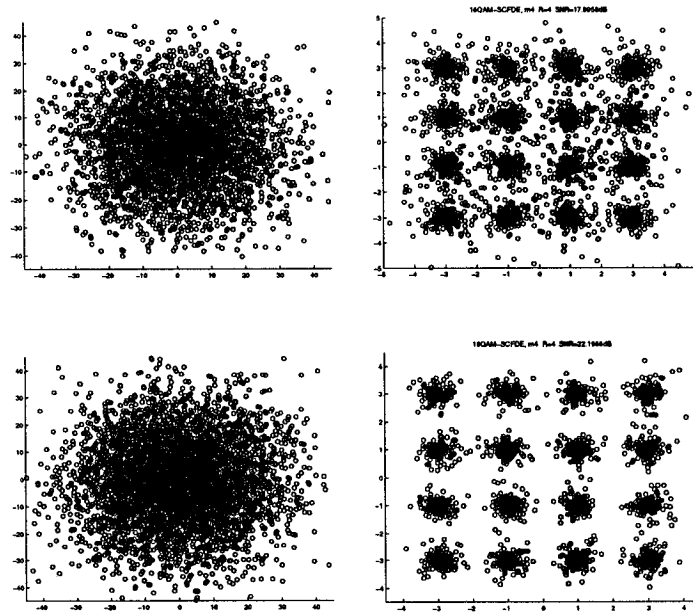


Figure 2.7: Symbol Constellations Before and After Equalization (MIMO cases: 16-ary QAM SCFDE,  $M=4$ ,  $K=4$ ,  $\text{SNR}=18$  dB for Upper Figures,  $\text{SNR}=22.2$  dB for Lower Figures).

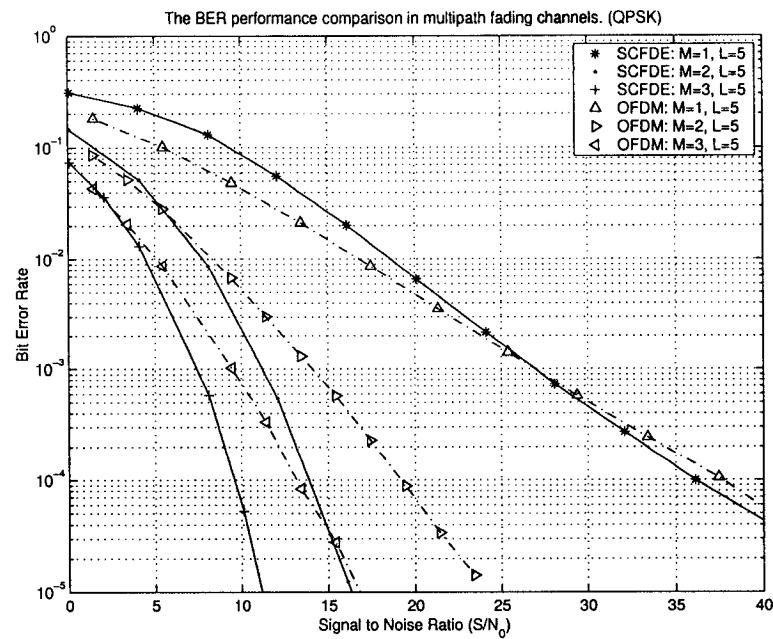


Figure 2.8: The BER Performance over Multipath Fading Channel (SIMO Cases: QPSK-SCFDE, QPSK-OFDM).

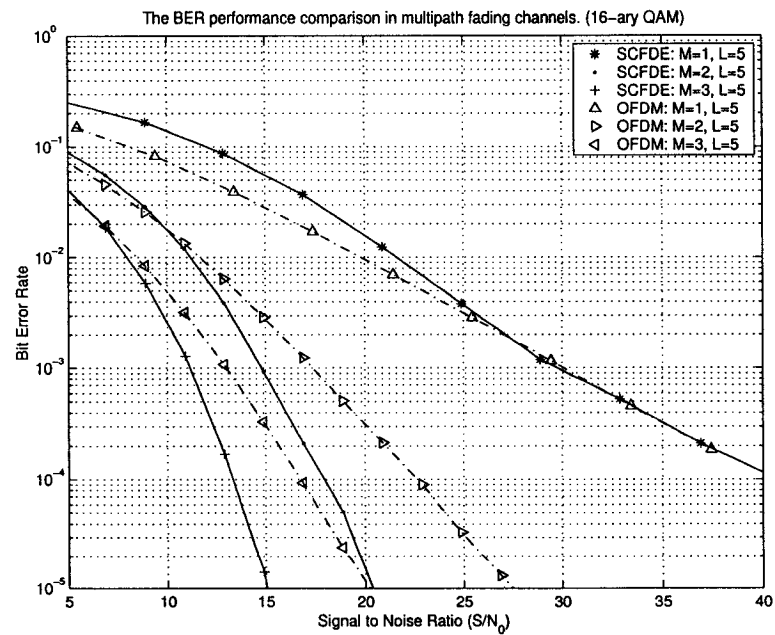


Figure 2.9: The BER Performance over Multipath Fading Channel (SIMO Cases: 16QAM-SCFDE, 16QAM-OFDM).

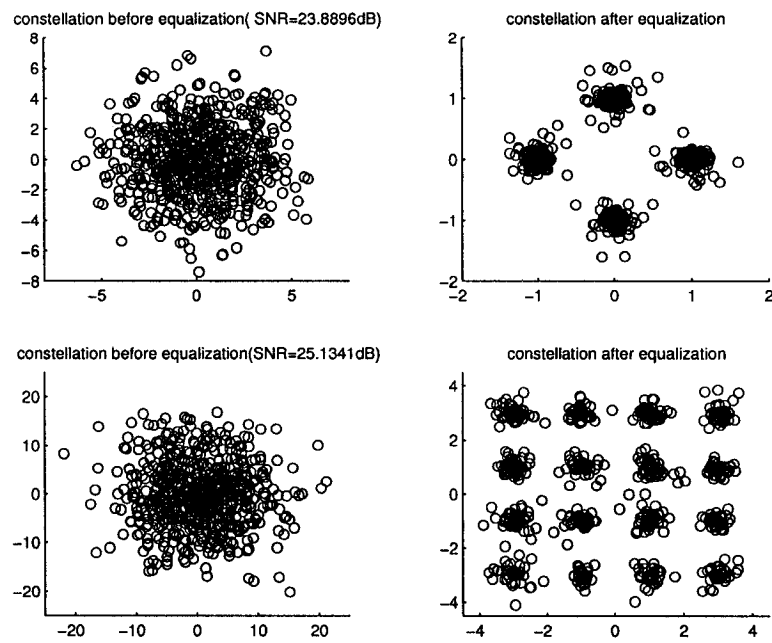


Figure 2.10: Symbol Constellation Before and After Channel Equalization (SIMO Cases: QPSK-SCFDE, 16QAM-SCFDE).

## Chapter 3

# Blind Channel Equalization for DSTM Signaling Transmissions over Rich-Multipath Channels

“For broadband transmissions, equalization is indispensable for mitigating inter-symbol interference. STC makes equalization more challenging because it generates multiple correlated signals that are transmitted simultaneously at equal power.” [41]

**W**ITH sophisticated signal and information processing algorithms, air-interface with space-time (ST) coding and multiple antennas improves the reliability and the capacity of wireless links. This chapter proposes a new receiver algorithm with ST processing for differential ST coded transmissions over FIR rich-multipath fading channels. The symbol detection introduced in this chapter is a deterministic subspace-based approach in a MIMO system framework. The receiver (i) assumes non-coherent reception; (ii) operates in a blind fashion without estimating the channel or its inverse; and (iii) recovers the data directly from the received signals. The scheme proposed in this chapter employs a multiple element antenna (MEA) at both sides of the transceiver and exploits both the antenna diversity and the multiple-constant-modulus characteristics of the received signals.

The proposed receiver is able to blindly mitigate the ISI in a rich-multipath propagation environment, and this is verified through the extensive Monte-Carlo simulations.

This chapter has five sections: Section 3.1 briefly presents the motivations and characteristics of the receiver algorithms in this chapter; Section 3.2 reviews the unitary differential space-time modulation; In Section 3.3, derivations about the new receiver algorithm is provided; Section 3.4 presents the performance simulation results; Section 3.5 summarizes this chapter.

### 3.1 Introduction

Among a variety of ST coding schemes [45] [46], differential space-time modulation (DSTM) and differential space-code modulation (DSCM) are ones of the most promising schemes for wireless fading channels [48, 51, 53, 55, 56]. Of particular interest to this chapter is differential unitary group codes introduced in [48], [51], and [53]. These differential schemes can work whether the channel state information (CSI) is available or not, and this is what makes them very attractive. When an accurate estimation of the CSI is difficult or costly, the differential space-time modulation schemes are obviously preferable than the other schemes which assume full knowledge of the CSI. The precision of the CSI estimation will substantially affect the performance of the equalizer that is based on the CSI knowledge. Small estimation biases or errors will cause a severe degradation in the equalization process. In the cases of mobile wireless channels, the channel CSI changes quickly. A frequent training for the CSI estimation will degrade the transmission efficiency. Therefore, in this chapter, we assume that no CSI is available either at the transmitter or receiver.

Both schemes, DSTM and DSCM, were designed to maximize the diversity advantage of code pairs while maintaining a receiver implementation to be as simple as possible. However, a flat fading channel model was assumed in the design and analysis of their receivers in [48] and [51]. In this chapter, we consider reception of the DSTM signals under



more realistic channel conditions in a rich multipath environment. Multipath scattering and reflection effects characterize most of wireless channels. They cause both time and angle spreads. As a result, most wireless channels are selective in time, space, and frequency, this is a reason why this chapter addresses multipath scattering impairments in the design of the ST receiver.

In this chapter, for transmissions over multipath frequency selective channels, a new transceiver scheme exploiting DSTM signaling properties is proposed, which consists of (i) a DSTM transmitter, (ii) an equalization algorithm based on direct input signal subspace estimation, and (iii) a non-coherent detection. In general, the proposed receiver mitigates the multipath time-spread impairments without CSI estimation. The approach used to recover the data relies on the modified version of subspace based method introduced in [87]. The novelty of this chapter stems from integrating (i) subspace based signal de-convolution and (ii) the exploitation of constant modulus property to facilitate the non-coherent detection of DSTM signaling in rich-multipath environment.

## 3.2 Review of the Differential Space-Time Modulation

In this section, the differential space-time modulation and unitary group codes presented in [51] are briefly described. A transmitter equipped with  $K$  antennas and a receiver equipped with  $M$  antennas are assumed to constitute the transceiver system. The unitary space-time codeword matrix  $\mathbf{C}_{(m)i}$  of size  $K \times K$  is transmitted in the  $i$ -th time slot  $T_i$  of duration  $T_c = K \cdot T_s$ , where  $\frac{1}{T_s}$  is the symbol rate. Each code matrix  $\mathbf{C}_{(m)}$  is of the form  $\mathbf{C}_{(m)} = \mathbf{D}\mathbf{G}_{(m)}$  where (i)  $\mathbf{G}_{(m)} \in \mathcal{G} = \{\mathbf{G}_{(m)} | \mathbf{G}_{(m)}\mathbf{G}_{(m)}^H = \mathbf{I}\}$  represents user data; (ii)  $\mathbf{D}$  is called the initial matrix, and (iii)  $m$  is a codeword index ( $m = 1, 2, \dots, \mathcal{M}$ ). The code has the property:

$$\mathbf{C}_{(m)}\mathbf{C}_{(m)}^H = K\mathbf{I}_{K \times K} \quad (3.1)$$

It was proved in [53] that  $\mathbf{D}\mathbf{D}^H = K\mathbf{I}_{K \times K}$  if  $\mathbf{D}\mathbf{G}$  is an optimal  $K \times K$  space-time group code. Moreover, full-rank unitary group codes with  $\mathcal{M} = 2^n$  codewords are equivalent

to either cyclic group codes or dicyclic group codes. Assuming the unknown flat fading channel being characterized by  $\mathbf{H} \in \mathcal{C}_{M \times K}$ , the received data of a differential ST coded signal at a multi-element antenna (MEA) is given as [51]:

$$\mathbf{Y}_j = \mathbf{H}\mathbf{X}_j + \mathbf{N}_j. \quad (3.2)$$

where (i) the coded signal  $\mathbf{X}_j = \mathbf{X}_{j-1}\mathbf{G}_j$ ,  $j = 0, 1, 2, 3, \dots, J-1$ ; (ii)  $J$  is a frame length in codewords; and (iii)  $\mathbf{N}_j$  stands for the matrix version of AWGN. In such a flat fading channel model, the channel state  $\mathbf{H}$  and the noise term  $\mathbf{N}_j$  are independent. When the CSI is not available,  $\mathbf{G}_{(m)}$  can be estimated by observing the last two received data blocks  $\bar{\mathbf{Y}}_j = [\mathbf{Y}_{j-1}, \mathbf{Y}_j]$ . With this modeling and a flat fading channel, a maximum likelihood (ML) decoder derived in [51] is:

$$\hat{\mathbf{G}}_{(m)} = \arg \max_{\mathbf{G}_{(m)}} \Re\{\text{Trace}\{\mathbf{G}_{(m)} \mathbf{Y}_j^H \mathbf{Y}_{j-1}\}\} \quad (3.3)$$

### 3.3 New Receiver Algorithm for Transmission over FIR Rich-Multipath Fading Channels

#### 3.3.1 Basis Representations of the Transmitted Signals

In what follows, after a frame-based transmitter is proposed, the discussion will focus on an algorithm for the equalization based on direct input signal subspace estimation.

Our transmission scenario proposed in this chapter for MIMO rich-multipath channel is a frame-by-frame transmit/receive scheme illustrated in Fig. 1.2 and Fig. 3.1, where  $T_c$  is a time slot for a codeword, and  $T_G = LT_s$  is a frame guard interval to avoid the inter-frame interference ( $L$  is the maximum channel length).

Initially, the continuous time received signal vector  $\mathbf{Y}(t)$  is sampled at the symbol rate ( $1/T_s$ ) after down-converting and receive filtering. For a period of each signal frame ( $T_F$ ),

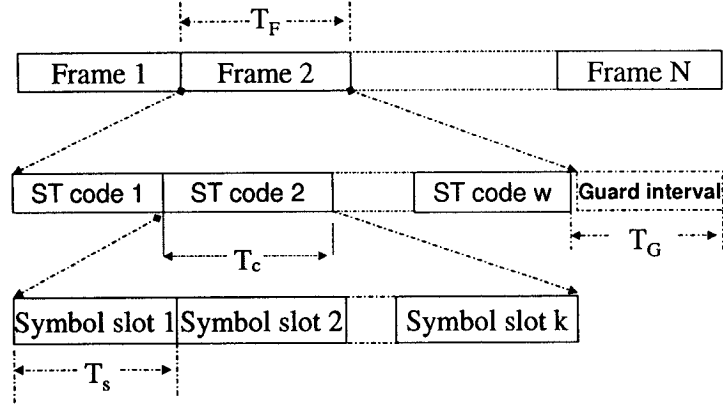


Figure 3.1: Transmitted Signal Frame Structure and Timing.

the sampled data sequence of  $Y(t)$  at a receiver is arranged in a matrix form as follows:

$$\mathbf{Y}_{M \times (N+L-1)} = [\mathbf{y}_0, \mathbf{y}_1, \dots, \mathbf{y}_{N+L-1}] = \begin{bmatrix} y_1(0) & y_1(1) & \dots & y_1(N+L-1) \\ y_2(0) & y_2(1) & \dots & y_2(N+L-1) \\ \dots & \dots & \dots & \dots \\ y_M(0) & y_M(1) & \dots & y_M(N+L-1) \end{bmatrix}$$

where (i)  $N$  is a transmitted frame length in symbols; (ii)  $L$  is the maximum channel length of the multi-channels; and (iii)  $\mathbf{y}_i$  is a column vector of sampled data at the receiver MEA. We assume the quasi-static channel, i.e., over the duration of one frame, the MIMO channel is time-invariant.

In this section, motivated by the direct input signal subspace basis estimation in [87], we develop a modified input (transmitted) signal estimation algorithm for the deconvolution of the ST multichannel signals, which facilitates the detection of the unitary differentially encoded signals over frequency-selective fading channels.

For MIMO channels of maximum length  $L$ , to capture the channel states, a matrix sequence  $\{\mathbf{h}(i), i = 0, 1, \dots, L\}$  is used as in (1.25). From equation (1.26), if the noise

effects are temporarily disregarded and with the proper arrangement of data, we get the following input-output relation in a matrix format for the  $k^{th}$  frame:

$$\mathbf{Y}_{M \times (N+L)}^{[q]} = \mathbf{H}_{M \times K(L+1)} \mathcal{X}_{K(L+1) \times (N+L)}^{[q]} \quad (3.4)$$

where

$$\mathbf{H}_{M \times K(L+1)} = [\mathbf{h}(0), \mathbf{h}(1), \dots, \mathbf{h}(L)];$$

$$\mathcal{X}_{K(L+1) \times (N+L)}^{[k]} = \begin{bmatrix} \mathbf{x}(0) & \mathbf{x}(1) & \dots & \mathbf{x}(N-1) & 0 & \dots & 0 \\ 0 & \mathbf{x}(0) & \dots & \mathbf{x}(N-2) & \mathbf{x}(N-1) & \dots & 0 \\ \dots & \dots & \dots & \dots & \dots & \dots & \dots \\ 0 & \dots & 0 & \mathbf{x}(0) & \mathbf{x}(1) & \dots & \mathbf{x}(N-1) \end{bmatrix};$$

the  $\mathbf{x}(i)$  is a column vector  $\mathbf{x}(i) = [x_1(i), x_2(i), \dots, x_K(i)]^T$ .

In order to retrieve input (transmitted) signals from the observation of the convoluted (received) signals, first, an auxiliary matrix sequence  $\{\mathfrak{Y}^{(k)} | k = 0, 1, 2, \dots, L\}$  is formed such that

$$\mathfrak{Y}^{(k)} = [\mathbf{y}_k, \mathbf{y}_{k+1}, \dots, \mathbf{y}_{k+N-1}]; \quad k = 0, 1, 2, \dots, L. \quad (3.5)$$

$\mathfrak{Y}^{(k)}, k = 0, 1, \dots, L$ , can be viewed as the vector sequences of  $[\mathbf{y}_0, \mathbf{y}_1, \dots, \mathbf{y}_{N+L-1}]$  within a sliding window of width  $N$  corresponding to the shift  $k = 0, 1, \dots, L$ .

For every  $\mathfrak{Y}^{(k)}$ , we calculate a matrix  $\Xi^{(k)}$  which consists of the spanning row vector set for  $\mathfrak{Y}^{(k)}$ , i.e., the rows of  $\Xi^{(k)}$  are the orthonormal basis for the subspace spanned by the rows of  $\mathfrak{Y}^{(k)}$ . The matrix  $\Xi^{(k)}$  can be obtained by singular value decomposition (SVD) or some other efficient estimation methods. This processing is denoted in this chapter by:

$$\mathfrak{Y}^{(k)} \Rightarrow \Xi^{(k)}, \quad k = 0, 1, 2, \dots, L. \quad (3.6)$$

**Proposition 1** Let row vector subspace of  $\mathbf{X}_{K \times N} = [\mathbf{x}(0) \ \mathbf{x}(1) \ \dots \ \mathbf{x}(N-1)]$  be denoted by  $\mathcal{S}_X$ . In absence of the noise, the intersection of the row vector subspaces of  $\Xi^{(k)}, k = 0, 1, \dots, L$ , is equivalent to  $\mathcal{S}_X$  with a probability of 1 for transmissions employing unitary ST group codes, provided  $\mathbf{H}$  is of a full column rank and the signal frame length  $N$  is sufficiently large for matrix  $\mathbf{X}$  to have full row rank.

Proof:

Let  $\mathcal{S}_{\mathcal{Y}^{(k)}}$  denote the row span of  $\Xi^{(k)}$ ,  $k = 0, 1, 2, \dots, L$ . If  $\mathbf{H}$  is of a full column rank, from (3.4), it could be concluded that:

- $k=0$ ,

$$\mathcal{S}_{\mathcal{Y}^{(0)}} = \text{row\_span} \left\{ \begin{bmatrix} \mathbf{x}(0) & \mathbf{x}(1) & \mathbf{x}(2) & \mathbf{x}(3) & \dots & \dots & \mathbf{x}(N-1) \\ 0 & \mathbf{x}(0) & \mathbf{x}(1) & \mathbf{x}(2) & \dots & \dots & \mathbf{x}(N-2) \\ \dots & \dots & \dots & \dots & \dots & \dots & \dots \\ 0 & \dots & 0 & \mathbf{x}(0) & \mathbf{x}(1) & \dots & \mathbf{x}(N-L) \end{bmatrix} \right\}; \quad (3.7)$$

- $k=1$ ,

$$\mathcal{S}_{\mathcal{Y}^{(1)}} = \text{row\_span} \left\{ \begin{bmatrix} \mathbf{x}(1) & \mathbf{x}(2) & \dots & \dots & \mathbf{x}(N-1) & 0 \\ \mathbf{x}(0) & \mathbf{x}(1) & \dots & \dots & \dots & \mathbf{x}(N-1) \\ \dots & \dots & \dots & \dots & \dots & \dots \\ 0 & \dots & \mathbf{x}(0) & \mathbf{x}(1) & \dots & \mathbf{x}(N-L+1) \end{bmatrix} \right\}; \quad (3.8)$$

- $k = i$

$\vdots$

$\vdots$

$\vdots$

- $k = L$ ,

$$\mathcal{S}_{\mathcal{Y}^{(L)}} = \text{row\_span} \left\{ \begin{bmatrix} \mathbf{x}(L) & \mathbf{x}(L+1) & \cdot & \mathbf{x}(N-1) & 0 & 0 \\ \mathbf{x}(L-1) & \mathbf{x}(L) & \cdot & \cdot & \mathbf{x}(N-1) & 0 \\ \cdot & \cdot & \cdot & \cdot & \cdot & \cdot \\ \mathbf{x}(0) & \mathbf{x}(1) & \mathbf{x}(2) & \cdot & \cdot & \mathbf{x}(N-1) \end{bmatrix} \right\}$$

By observing the above relationship, it is evident that:

$$\mathcal{S}_X \subset \mathcal{S}_{\mathcal{Y}^{(i)}} \text{ respectively for } i = 0, 1, 2, \dots, L. \quad (3.9)$$

Therefore, according to set theory,

$$\mathcal{S}_X \subset \left\{ \bigcap_{i=0}^L \mathcal{S}_{\mathcal{Y}^{(i)}} \right\} \quad (3.10)$$

Consider  $\mathcal{S}_{\mathfrak{Y}^{(1)}} \cap \mathcal{S}_{\mathfrak{Y}^{(2)}}$ , which is equivalent to the intersection of row-subspaces of :

$$\begin{bmatrix} \mathbf{x}(0) & \mathbf{x}(1) & \mathbf{x}(2) & \cdots & \cdots & \cdots & \cdots & \mathbf{x}(N-1) \\ 0 & \mathbf{x}(0) & \mathbf{x}(1) & \mathbf{x}(2) & \cdots & \cdots & \cdots & \mathbf{x}(N-2) \\ \cdots & \cdots & \cdots & \cdots & \cdots & \cdots & \cdots & \cdots \\ 0 & \cdots & \cdots & \mathbf{x}(0) & \mathbf{x}(1) & \cdots & \cdots & \mathbf{x}(N-L) \end{bmatrix}$$

and

$$\begin{bmatrix} \mathbf{x}(1) & \mathbf{x}(2) & \cdots & \cdots & \mathbf{x}(N-1) & 0 \\ \mathbf{x}(0) & \mathbf{x}(1) & \mathbf{x}(2) & \cdots & \cdots & \mathbf{x}(N-1) \\ \cdots & \cdots & \cdots & \cdots & \cdots & \cdots \\ 0 & \cdots & \mathbf{x}(0) & \mathbf{x}(1) & \cdots & \mathbf{x}(N-L+1) \end{bmatrix}$$

If frame length  $N$  is sufficiently large, the rows in  $\mathcal{X}^{[k]}$  are independent with probability of 1. Observing a block Toeplitz structure of above matrices, the rank of the intersection is  $(K(L+1) - K)$ . Therefore, the number of basis vectors of  $\mathcal{S}_{\mathfrak{Y}^{(1)}} \cap \mathcal{S}_{\mathfrak{Y}^{(2)}}$  is also  $(K(L+1) - K)$ .

Following the similar verification procedure, it could be observed that the number of basis vectors of  $\mathcal{S}_{\mathfrak{Y}^{(1)}} \cap \mathcal{S}_{\mathfrak{Y}^{(2)}} \cap \mathcal{S}_{\mathfrak{Y}^{(3)}}$  is  $(K(L+1) - 2K)$ .

Moreover, the number of basis vectors of  $\left\{ \bigcap_{i=0}^L \mathcal{S}_{\mathfrak{Y}^{(i)}} \right\}$  is  $K$ , which is equal to the number of basis vectors for  $\mathcal{S}_X$ . Hence, from (3.10), it is concluded that:

$$\mathcal{S}_X = \left\{ \bigcap_{i=0}^L \mathcal{S}_{\mathfrak{Y}^{(i)}} \right\} \quad (3.11)$$

□

Defining a new matrix  $\Xi$  whose row vectors span  $\bigcap_{i=0}^L \mathcal{S}_{\mathfrak{Y}^{(i)}}$ , from Proposition 1, we have that the rows of  $\Xi$  also span subspace  $\mathcal{S}_X$  with probability 1. Therefore,

$$\mathbf{X}_{K \times N} = \mathbf{W}_{K \times K} \Xi_{K \times N} \quad (3.12)$$

holds with probability 1, where  $\mathbf{W}_{K \times K}$  is a weight matrix. Hence, with a proper  $\mathbf{W}$ , the transmitted signals could be recovered completely from  $\mathfrak{Y}^{(k)}$  by finding the spanning vector

set in the light of Proposition 1. In the other words, the transmitted data could be recovered from  $\mathfrak{Y}^{(k)}$  within the ambiguity of a transformation  $\mathbf{W}$ .

The above observation is a fundamental point in this chapter for the direct input signal subspace estimation. The estimation of  $\mathbf{W}$  will be discussed later in Section 3.3.3.2.

The full column rank assumption of  $\mathbf{H}$  could be met with probability of 1 if it is a matrix with a row number larger than the column number. Evidently, if channel length increases, accordingly, the number of receive antennas should be increased. The improved methods to meet this assumption is discussed in Section 3.3.2. This assumption is a sufficient condition for the algorithm we proposed in Section 3.3.3.1, however, it is not a necessary condition to apply the algorithm.

As a matter of fact, for the proposed algorithm, it is only assumed that some matrices among  $\mathbf{h}(i), i = 0, 1, \dots, L$ , individually have a full column rank. This normally is true with probability of 1 for rich-multipath environment and the number of the receive antennas being larger than that of the transmit antennas. This assumption could be relaxed by the data stacking discussed in Section 3.3.2.

### 3.3.2 Column Rank Assumption of Channel Matrices and Oversampling

Regarding the assumption for the column rank of  $\mathbf{h}(i)$ , the following discussion is in order. As discussed in paper [60], rich-multipath scattering normally causes wide angle spreads. For MIMO flat fading channels, the criterion (1.13) could be applied to predict a high-rank channel situation where channel gain matrix can be modeled as a high-rank matrix.

For MIMO frequency-selective channels, the prediction method (1.13) can be adopted to predict the high-rank property of those channel matrices among  $\mathbf{h}(i), i = 0, 1, \dots, L$ , that do not have zero columns. Therefore, it still brings insight to investigation of the MIMO frequency-selective channels and the scheme discussed in this paper.

It is possible to arrange the received sample data for each frame by stacking the data  $v$  times as follows, to facilitate using minimum receiver antenna number to meet the channel

matrix full column rank requirements:

$$\mathbb{Y}_{Mv \times (N+L+v-1)}^{[q]} = \mathbb{H}_{Mv \times K(L+v)} \mathbb{X}_{K(L+v) \times (N+L+v-1)}^{[q]}, \quad (3.13)$$

$$\mathbb{Y}^{[q]} = \begin{bmatrix} \mathbf{y}_0^{[q]} & \mathbf{y}_1^{[q]} & \cdots & \cdots & \mathbf{y}_{N+L-1}^{[q]} & 0 & 0 \\ 0 & \mathbf{y}_0^{[q]} & \mathbf{y}_1^{[q]} & \cdots & \mathbf{y}_{N+L-2}^{[q]} & \cdots & 0 \\ \cdots & \cdots & \cdots & \cdots & \cdots & \cdots & \cdots \\ 0 & 0 & 0 & \mathbf{y}_0^{[q]} & \cdots & \cdots & \mathbf{y}_{N+L-1}^{[q]} \end{bmatrix}$$

$$\mathbb{H} = \begin{bmatrix} \mathbf{h}(0) & \mathbf{h}(1) & \cdots & \cdots & \mathbf{h}(L) & 0 & 0 \\ 0 & \mathbf{h}(0) & \mathbf{h}(1) & \cdots & \mathbf{h}(L-1) & \cdots & 0 \\ \cdots & \cdots & \cdots & \cdots & \cdots & \cdots & \cdots \\ 0 & 0 & 0 & \mathbf{h}(0) & \cdots & \cdots & \mathbf{h}(L) \end{bmatrix} \quad (3.14)$$

$$\mathbb{X}^{[q]} = \begin{bmatrix} \mathbf{x}^{[q]}(0) & \mathbf{x}^{[q]}(1) & \cdots & \cdots & \mathbf{x}^{[q]}(N-1) & 0 & 0 \\ 0 & \mathbf{x}^{[q]}(0) & \mathbf{x}^{[q]}(1) & \cdots & \mathbf{x}^{[q]}(N-2) & \cdots & 0 \\ \cdots & \cdots & \cdots & \cdots & \cdots & \cdots & \cdots \\ 0 & 0 & 0 & \mathbf{x}^{[q]}(0) & \cdots & \cdots & \mathbf{x}^{[q]}(N-1) \end{bmatrix} \quad (3.15)$$

The arrangement of received data in the matrix above is different from that of [87] for improving signal detection at the first and last  $L$  symbols in each transmitted frame.

If a large receive antenna number is not feasible, oversampling and larger reception bandwidth could be considered as an alternative approach to meet the necessary channel matrix full-rank condition. If the over-sampling rate is  $P$ ,  $P-1$  times more data can be obtained and arranged as follows:

$$[\bar{\mathbf{y}}_0, \bar{\mathbf{y}}_1 \cdots \bar{\mathbf{y}}_{N+L-1}] = \begin{bmatrix} \mathbf{y}(0) & \mathbf{y}(1) & \cdots & \mathbf{y}(N+L-1) \\ \mathbf{y}(\frac{1}{P}) & \mathbf{y}(1+\frac{1}{P}) & \cdots & \mathbf{y}(N+L-1+\frac{1}{P}) \\ \cdots & \cdots & \cdots & \cdots \\ \mathbf{y}(\frac{P-1}{P}) & \mathbf{y}(1+\frac{P-1}{P}) & \cdots & \mathbf{y}(N+L-1+\frac{P-1}{P}) \end{bmatrix}$$



where the index  $i + \frac{j}{P}$  stands for the  $j$ th sample in the  $i$ th symbol. Therefore, with a MIMO channel characterized by:

$$[\bar{\mathbf{h}}(0), \bar{\mathbf{h}}(1) \cdots \bar{\mathbf{h}}(L)] = \begin{bmatrix} \mathbf{h}(0) & \mathbf{h}(1) & \cdots & \mathbf{h}(L) \\ \mathbf{h}(\frac{1}{P}) & \mathbf{h}(1 + \frac{1}{P}) & \cdots & \mathbf{h}(L + \frac{1}{P}) \\ \cdots & \cdots & \cdots & \cdots \\ \mathbf{h}(\frac{P-1}{P}) & \mathbf{h}(1 + \frac{P-1}{P}) & \cdots & \mathbf{h}(L + \frac{P-1}{P}) \end{bmatrix}$$

and the effects of transmit shaping filtering and receive filtering being encompassed into the channel  $[\bar{\mathbf{h}}(0), \bar{\mathbf{h}}(1) \cdots \bar{\mathbf{h}}(L)]$ , the input-output relation in the over-sampling case becomes:

$$\bar{\mathbf{Y}}_{PMv \times (N+L+v-1)} = \bar{\mathbf{H}}_{PMv \times K(L+v)} \mathbf{X}_{K(L+v) \times (N+L+v-1)} \quad (3.16)$$

where

$$\bar{\mathbf{Y}} = \begin{bmatrix} \bar{\mathbf{y}}_0^{[q]} & \bar{\mathbf{y}}_1^{[q]} & \cdots & \cdots & \bar{\mathbf{y}}_{N+L-1}^{[q]} & 0 & 0 \\ 0 & \bar{\mathbf{y}}_0^{[q]} & \bar{\mathbf{y}}_1^{[q]} & \cdots & \bar{\mathbf{y}}_{N+L-2}^{[q]} & \cdots & 0 \\ \cdots & \cdots & \cdots & \cdots & \cdots & \cdots & \cdots \\ 0 & 0 & 0 & \bar{\mathbf{y}}_0^{[q]} & \cdots & \cdots & \bar{\mathbf{y}}_{N+L-1}^{[q]} \end{bmatrix}, \quad (3.17)$$

$$\bar{\mathbf{H}} = \begin{bmatrix} \bar{\mathbf{h}}(0) & \bar{\mathbf{h}}(1) & \cdots & \cdots & \bar{\mathbf{h}}(L) & 0 & 0 \\ 0 & \bar{\mathbf{h}}(0) & \bar{\mathbf{h}}(1) & \cdots & \bar{\mathbf{h}}(L-1) & \cdots & 0 \\ \cdots & \cdots & \cdots & \cdots & \cdots & \cdots & \cdots \\ 0 & 0 & 0 & \bar{\mathbf{h}}(0) & \cdots & \cdots & \bar{\mathbf{h}}(L) \end{bmatrix}$$

and  $\mathbf{X}_{K(L+v) \times (N+L+v-1)}$  is as in (3.15).

In the over-sampling case, it is possible to meet the full-rank requirement with a receiver antenna number smaller than that of transmitter antenna at the cost of oversampling complexity and wider reception bandwidth. The latter factor also causes degradation in SNR.

### 3.3.3 Estimation of the Multiple Transmitted Signals from Received Data in Presence of Noise and Rich Multipath Channels

The sub-channels of the ST channel are normally of different lengths and the multipath signals are contaminated by the noise. In the presence of noise,  $\mathcal{S}_X$  may not necessarily be the subspace intersection of  $\Xi^{(k)}$ . However, we can still try to search orthogonal vectors whose linear combinations can approximate row vectors in  $\mathcal{S}_X$  based on derivations in the previous section. The following sub-optimum algorithm is proposed for determining a spanning vector set from the received signals to approximate the transmitted signal vectors. This scheme is verified later through simulations to provide a robust performance.

#### 3.3.3.1 The Basis Estimation and Approximation of Transmitted Signals

In the description of the receiver algorithm, the following notation is adopted:

- $[A; B]$  stands for the a matrix formed by a stacking of matrices A and B;
- $L$  is the maximum length of the ST multiple sub-channels and is assumed to be known to the receiver;
- $[n_\eta, \mathbf{q}] = \mathbb{M}_{i=1}^{i_{max}} \{\Xi^{(i)}\}_{|\eta}$  denotes the following computation procedure:
  1. Calculate singular value decomposition:
 
$$\mathbf{U}\Sigma\mathbf{Q} = \mathcal{SVD}([\Xi^{(1)}; \Xi^{(2)}; \dots; \Xi^{(i_{max})}])$$
  2.  $\mathbf{q} = \mathbf{Q}_{[1:n_\eta, :]}$ , where  $n_\eta$  is the number of singular vectors whose corresponding singular values  $\geq \eta$ .  $\mathbf{Q}_{[a:b, :]}$  denotes a matrix consisting of the rows from  $a^{th}$  to  $b^{th}$  of matrix  $\mathbf{Q}$ .

The proposed algorithm to estimate  $\mathcal{S}_X$  proceeds in three steps as follows:

*Algorithm Procedure:*

- (Step a)

1.  $i_{max} = L + v, \quad r = 0;$

2. Calculate  $[n_\eta, \mathbf{q}] = \mathbb{M}_{i=1}^{i_{max}} \{\Xi^{(i)}\}|_{\eta=0.96(\lambda_{max}-1)}$  where  $\lambda_{max}$  is the current largest singular value;

3.  $\mathbf{V}^{(r)} = \mathbf{q}; r + 1 \Rightarrow r;$

If  $n_\eta < K$ , go to (b);

else go to (c);

• (Step b)

If  $i_{max} > 1$ ,

1.  $i_{max} = i_{max} - 1;$

2. calculate  $[n_\eta, \mathbf{q}] = \mathbb{M}_{i=1}^{i_{max}} \{\Xi^{(i)}\}|_{\eta=0.96(\lambda_{max}-1)}$  where  $\lambda_{max}$  is the current largest singular value;

3.  $\mathbf{V}^{(r)} = \mathbf{q}; r + 1 \Rightarrow r;$

4. if  $n_\eta < K$ , repeat (b), else go to (c);

Else go to (c).

• (Step c)

1. Calculate  $[n_\eta, \mathbf{q}] = \mathbb{M}_{i=1}^r \{\mathbf{V}^{(i)}\}|_{\eta=0.95};$

2.  $\hat{\Xi} = \mathbf{q}.$

In the above algorithm, if there is not noise and the  $\mathbf{H}$  is of full column rank,  $\lambda_{max}$  is equal to  $\sqrt{i_{max}}$ . However, for the cases that there is noise and  $\mathbf{H}$  is column-rank deficient, this relation does not hold. This is the reason for calculating  $\lambda_{max}$  at each step, which is important and is one of the major features of this algorithm.

Once the matrix  $\hat{\Xi}$  is obtained, the transmitted signal matrix  $\mathbf{X}_{K \times N}$  can be extracted by exploiting the constant modulus property of multiple signals. Similarly as in (3.12), the relation between  $\hat{\mathbf{X}}_{K \times N}$  and  $\hat{\Xi}_{S \times N}$  can be expressed as follows:

$$\hat{\mathbf{X}}_{K \times N} = \hat{\mathbf{W}}_{K \times S} \hat{\Xi}_{S \times N}, \quad S \geq K \quad (3.18)$$

where (i)  $\widehat{\Xi}$  stands for a matrix whose row vectors are the estimated basis, and (ii)  $\widehat{\mathbf{X}}$  represents the estimate of signal frame after deconvolution. The number of row vectors in  $\widehat{\Xi}$  may be equal or greater than the number of the transmit signal subspace basis in the above procedure due to the noise effects. As a result, the matrix  $\widehat{\mathbf{W}}$  is not necessarily a square matrix as  $\mathbf{W}$  in (3.12).

The weight matrix  $\widehat{\mathbf{W}}$  can be calculated using the alternating projection iterations algorithm presented in the next subsection.

### 3.3.3.2 Multiple Signal Composite Property Projection

DSTM employs PSK signaling so that transmitted signals have multiple constant modulus characteristics. Therefore, the alternating projections procedure from [94] is adopted here to calculate  $\widehat{\mathbf{W}}$  in the following way:

*Algorithm Procedure:*

For  $j = 0, 1, \dots, n$ :

1.  $\widehat{\mathbf{X}}_{K \times N}^{(j)} = \widehat{\mathbf{W}}_{K \times S}^{(j)} \widehat{\Xi}_{S \times N}$
2.  $\widetilde{\mathbf{X}}_{K \times N}^{(j)} = \text{Proc\_G\_S}\{\widehat{\mathbf{X}}^{(j)}\}$
3.  $\bar{\mathbf{X}}^{(j)} = \lambda^{(j)} \widehat{\mathbf{X}}^{(j)} + (\mathbf{I} - \lambda^{(j)}) \widetilde{\mathbf{X}}^{(j)}$
4.  $\bar{\mathbf{X}}^{(j+1)} = \bar{\mathbf{X}}^{(j)} ./ |\bar{\mathbf{X}}^{(j)}|$
5.  $\widehat{\mathbf{W}}_{K \times S}^{(j+1)} = \bar{\mathbf{X}}_{K \times N}^{(j+1)} \widehat{\Xi}_{S \times N}^\dagger$

where *Proc\_G\_S* means the Gram-Schmidt orthogonalization procedure, and  $\lambda^{(j)}$  is a diagonal relaxation matrix. The initial matrix  $\widehat{\mathbf{W}}^{(0)}$  could be either determined using pilot signals or choosing randomly a high-rank matrix. As mentioned in [94], the Gram-Schmidt orthogonalization procedure is applied here to prevent the algorithm from being biased to

certain signals of strong power. The iteration stops when  $\widehat{\mathbf{W}}^{(j)}$  reaches a stable state, i.e.,  $\text{norm}(\widehat{\mathbf{W}}^{(j+1)} - \widehat{\mathbf{W}}^{(j)}) \leq \varepsilon$  where  $\varepsilon$  is an arbitrarily chosen small constant.

### 3.3.3.3 Signal Detection

In the presence of noise, the transmitted signal could be approximated as in (3.18). The relation between the original coded signal frame  $\mathbf{X} = [\mathbf{x}_1, \mathbf{x}_2, \mathbf{x}_3 \cdots, \mathbf{x}_c]$  and the estimate  $\widehat{\mathbf{X}} = [\widehat{\mathbf{x}}_1, \widehat{\mathbf{x}}_2, \widehat{\mathbf{x}}_3 \cdots, \widehat{\mathbf{x}}_c]$  can be modeled as:

$$\widehat{\mathbf{X}} = \mathbf{A}\mathbf{X} + \mathbf{N}, \quad (3.19)$$

$$\widehat{\mathbf{x}}_i = \mathbf{A}\mathbf{x}_i + \mathbf{n}_i, \quad i = 1, 2, \cdots, c. \quad (3.20)$$

where  $\mathbf{A}$  is an admissible matrix and  $\mathbf{x}_i$  is a ST group code matrix.

**definition 1** [94] If  $\alpha_k \in \{\alpha \mid |\alpha_k| = 1, k = 1, \cdots, d\} \subset \mathcal{C}$  and  $\mathbf{P}$  is a permutation matrix, the matrix  $\mathbf{W} = (\text{diag}(\alpha_1, \alpha_2, \cdots, \alpha_d)\mathbf{P})$ , is an admissible transformation matrix.

Noise elements are assumed to have i.i.d. circularly symmetric complex Gaussian distribution  $\mathcal{CN}(0, \delta^2)$  with zero mean.

The ambiguity represented by  $\mathbf{A}$  between  $\widehat{\mathbf{x}}_i$  and  $\mathbf{x}_i$  can be removed by the differential signaling and differential detection. This processing is formulated as follows:

$$\widehat{\mathbf{x}}_i = \mathbf{A}\mathbf{x}_i + \mathbf{n}_i; \quad \widehat{\mathbf{x}}_{i+1} = \mathbf{A}\mathbf{x}_{i+1} + \mathbf{n}_{i+1}; \quad \mathbf{x}_{i+1} = \mathbf{x}_i \mathbf{G}_{[m]};$$

Therefore

$$\widehat{\mathbf{x}}_{i+1} = \widehat{\mathbf{x}}_i \mathbf{G}_{[m]} + \ddot{\mathbf{n}}_{i+1} \quad \text{where} \quad \ddot{\mathbf{n}}_{i+1} = \mathbf{n}_{i+1} - \mathbf{n}_i \mathbf{G}_{[m]}$$

The dependence between  $\widehat{\mathbf{x}}_{k+1}$  and  $\widehat{\mathbf{x}}_k$  indicates a differential relation with the multiplicative matrix  $\mathbf{G}_{[m]}$ . Hence, the detection of  $\mathbf{G}^{[k]}$  can be carried out using a least square error detector:

$$\widehat{\mathbf{G}}^{[k+1]} = \arg \min_{\mathbf{G}_{[r]}} \|\widehat{\mathbf{x}}_{k+1} - \widehat{\mathbf{x}}_k \mathbf{G}_{[r]}\| \quad (3.21)$$

where, for the  $\mathbf{G}$  matrices, the matrix subscript is a ST code-word alphabet index, and the superscript is a time index of the ST code-word.

From (3.21), we get:

$$\begin{aligned}
\hat{\mathbf{G}}^{[k+1]} &= \arg \min_{\mathbf{G}_{[r]}} \text{Trace}\{(\hat{\mathbf{x}}_{k+1} - \hat{\mathbf{x}}_k \mathbf{G}_{[r]})^H (\hat{\mathbf{x}}_{k+1} - \hat{\mathbf{x}}_k \mathbf{G}_{[r]})\} \\
&= \arg \min_{\mathbf{G}_{[r]}} \text{Trace}\{\hat{\mathbf{x}}_{k+1}^H (\hat{\mathbf{x}}_{k+1}) - (\hat{\mathbf{x}}_k \mathbf{G}_{[r]})^H \hat{\mathbf{x}}_{k+1} - (\hat{\mathbf{x}}_{k+1})^H (\hat{\mathbf{x}}_k \mathbf{G}_{[r]}) \\
&\quad + (\hat{\mathbf{x}}_k \mathbf{G}_{[r]})^H (\hat{\mathbf{x}}_k \mathbf{G}_{[r]})\}
\end{aligned}$$

Because  $\text{Trace}\{(\hat{\mathbf{x}}_k \mathbf{G}_{[r]})^H (\hat{\mathbf{x}}_k \mathbf{G}_{[r]})\}$  is a constant for different  $\mathbf{G}_{[r]}$ , a non-coherent detector for DSTM's differential signaling is:

$$\hat{\mathbf{G}}^{[k+1]} = \arg \max_{\mathbf{G}_{[r]}} \Re\{\text{Trace}\{(\hat{\mathbf{x}}_k \mathbf{G}_{[r]})^H (\hat{\mathbf{x}}_{k+1})\}\} \quad (3.22)$$

### 3.3.3.4 Summary of the Receiver Algorithm

The complete receiver algorithm for DSTM signaling over the FIR rich-multipath channels can be summarized into the following four steps:

1. *Estimate direct input signal subspace basis and signal approximations according to 3.3.3.1;*
2. *Calculate  $\hat{\mathbf{W}}$  by iterating the alternating projections exploiting 'Multiple Constant Modulus' using the algorithm presented in 3.3.3.2;*
3. *Determine  $\tilde{\mathbf{X}} = \hat{\mathbf{W}}\hat{\mathbf{\Xi}}$ ;*
4. *Perform signal detection according to (3.22) as described in 3.3.3.3.*

Exploiting the block Toeplitz structure and the constant modulus property of the signals, the above processing procedures detailed in Sections 3.3.3.1, 3.3.3.2 and 3.3.3.3 can accomplish the data recovery from the received signal over the time-dispersive channels in a rich multipath environment without channel estimation. The procedures in Sections 3.3.3.1 and 3.3.3.2 mitigate frequency-selective effects, and the differential detection of symbols described in Section 3.3.3.3 removes the ambiguity of an admissible transform  $\mathbf{A}$  in (3.19).

### 3.4 Performance Simulations

Simulations of the new receiver algorithm were conducted to verify the BER performance in the presence of AWGN and Rayleigh FIR fading channels. Figs. 3.2–3.7 illustrate the signal constellation of the signals before and that after the equalization for different values of SNR per antenna. From Figs. 3.3, 3.5 and 3.7, it is evident that enforcing the constant modulus property in our algorithm causes the constellation of signals after equalization to have the appearance of a circular gathering shape.

The representative simulation results with the parameters  $\{K = 4, M = 5, 6, N = 256, P = 1\}$  are illustrated in Fig. 3.8, Fig. 3.9 and Fig. 3.10 for the maximum channel lengths of the sub-channels  $L = 3, 5, 7$ , respectively. The multiple channels were simulated to be the time-dispersive Rayleigh fading channels.

In the simulations, the parameter  $N$  was chosen to be 256. At the circumstances of the  $L = 3, 5, 7$ , and  $K = 4$ , this choice of the parameter  $N$  met the requirement that  $N$  should be sufficiently large so that matrix  $\mathbf{X}$  had a full row rank with a probability of 1.

The simulations were carried out by employing a  $(\mathcal{M}; k_1, \dots, k_4) = (4, 1, 1, 1, 1)$  cyclic group code [53] and Q-PSK signaling. The results were statistically averaged over all possible cases of random path delays, random ST channel states, random bit streams and random additive noise components. The SNR values in Fig. 3.8, Fig. 3.9 and Fig. 3.10 are the spatially and temporally averaged SNR per antenna for all data acquired from different receive antennas.

For comparison purposes, the performance of DSTM signaling with the previous receiver's algorithm were simulated with time-dispersive channels. From the figures, it is evident that the schemes (without equalization) derived under the assumption of the flat fading channels fail in the frequency selective fading channels considered in the simulations (curves are labeled as 'without equalization' in the figures). On the other hand, the proposed algorithm (with equalization) maintains a robust performance in rich-multipath time-dispersive fading channels.

When the channel length is increased, it is more difficult to remove the ISI effects: this

is evident by comparing the performance curves in Figs. 3.8, 3.9, and 3.10 where the length of the channel is  $L = 3, 5$ , and  $7$  respectively. From these figures, we can observe that in order to obtain the same performance of BER of  $10^{-3}$  using the same transceiver setup, the SNR has to be increased from 4 dB to 7dB and 15 dB, respectively.

When comparing the curves in the Figs. 3.8, 3.9 and 3.10 individually, it can be observed that the increase of the receive antenna number from 5 to 6 results in approximately 1dB to 2dB improvements at the BER of  $10^{-3}$ . The power savings by increasing the receiver antenna number depends on the BER operating point of the system .

Similarly, for different  $N = 64, 128, 192$ , the simulation results with the parameters  $\{K = 4, M = 5, 6, P = 1\}$  are illustrated in Fig. 3.11, Fig. 3.12 and Fig. 3.13 for the maximum lengths of the sub-channels  $L = 5, 6, 7$ , respectively. From these figures, we could observe the different choices of  $N$  with a large value difference have an evident influence on the system performance. Generally, for the short channel length cases, within a certain range, a relatively larger  $N$  facilitates the higher performance. But, for the cases of long channel length, this trend does not exist.

### 3.5 Summary

This chapter proposes a blind space-time receiver algorithm for DSTM transmissions over quasi-static time-dispersive fading channels. The algorithm derived is suitable for different number of antennas. Simulation results demonstrate the new receiver algorithm's robust performance with unknown rich-multipath time-dispersive fading channels. With a proper design of the transceiver parameters in the new scheme, the symbol detection error drops significantly when SNR passes certain thresholds despite the delay spread of the multipath channels.

The proposed receiver is not subjected to the effects of the channel state changes provided the channel states are invariant within one frame time slot. This is because the new detection algorithm does not rely on the CSI knowledge. In contrast to the methods based



on the statistics of the signals, it is capable to operate with short sample data of the signals.

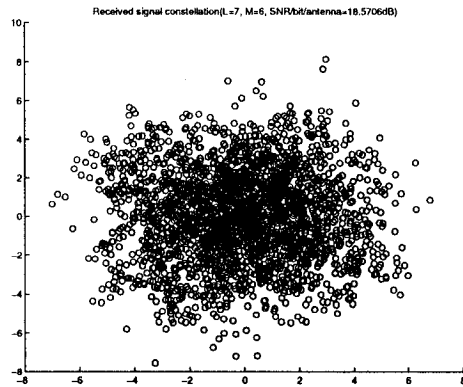


Figure 3.2: Received Signal Constellation Diagram  $\{L=7, M=6, K=4, P=1, \text{SNR} = 18.5 \text{ dB}\}$

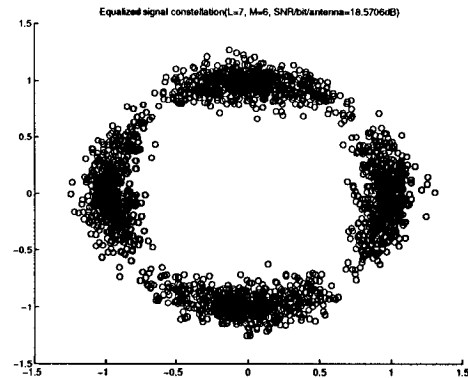


Figure 3.3: Signal Constellation Diagram After Equalization  $\{L=7, M=6, K=4, P=1, \text{SNR}= 18.5 \text{ dB}\}$

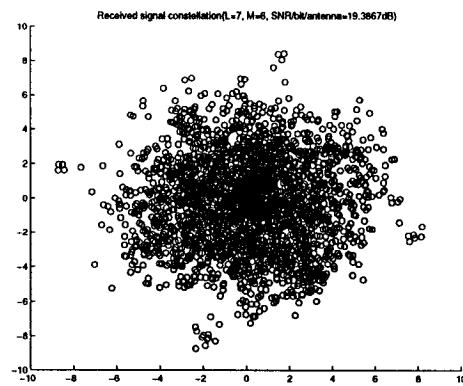


Figure 3.4: Received Signal Constellation Diagram  $\{L=7, M=6, K=4, P=1, \text{SNR} = 19.3 \text{ dB}\}$

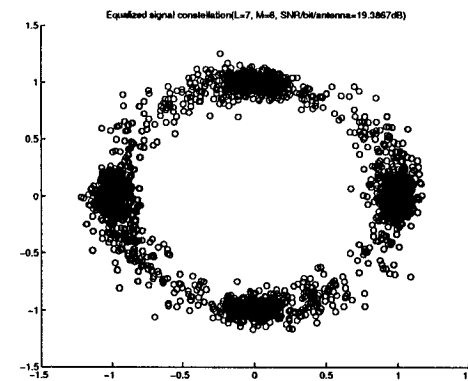


Figure 3.5: Signal Constellation Diagram After Equalization  $\{L=7, M=6, K=4, P=1, \text{SNR}= 19.3 \text{ dB}\}$

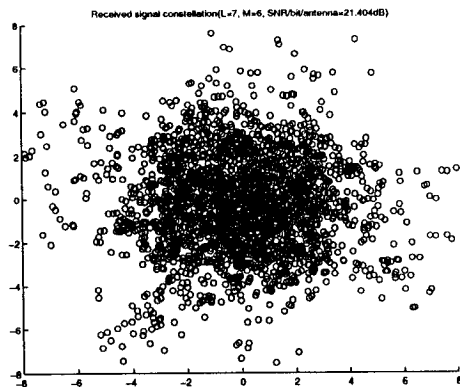


Figure 3.6: Received Signal Constellation Diagram  $\{L=7, M=6, K=4, P=1, \text{SNR} = 21.4 \text{ dB}\}$

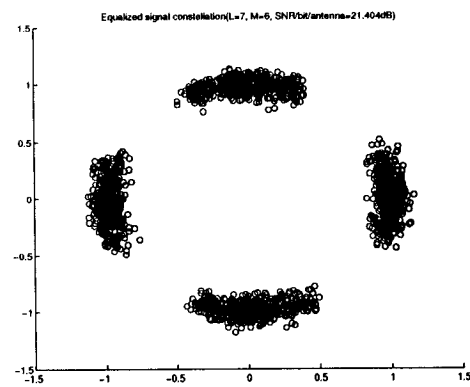


Figure 3.7: Signal Constellation Diagram After Equalization  $\{L=7, M=6, K=4, P=1, \text{SNR} = 21.4 \text{ dB}\}$

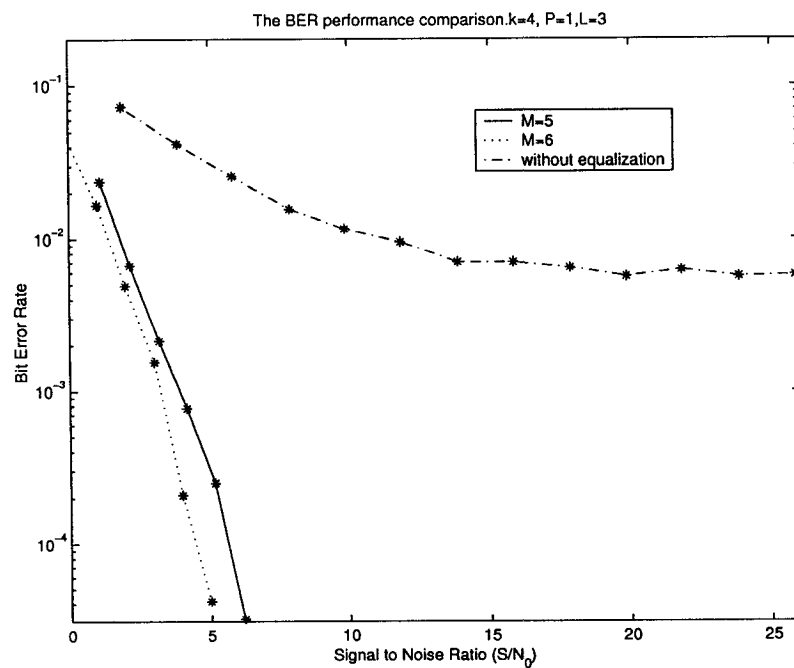


Figure 3.8: System BER Performance in Time-Dispersive Fading Channel ( $L=3, K=4, P=1$ ).

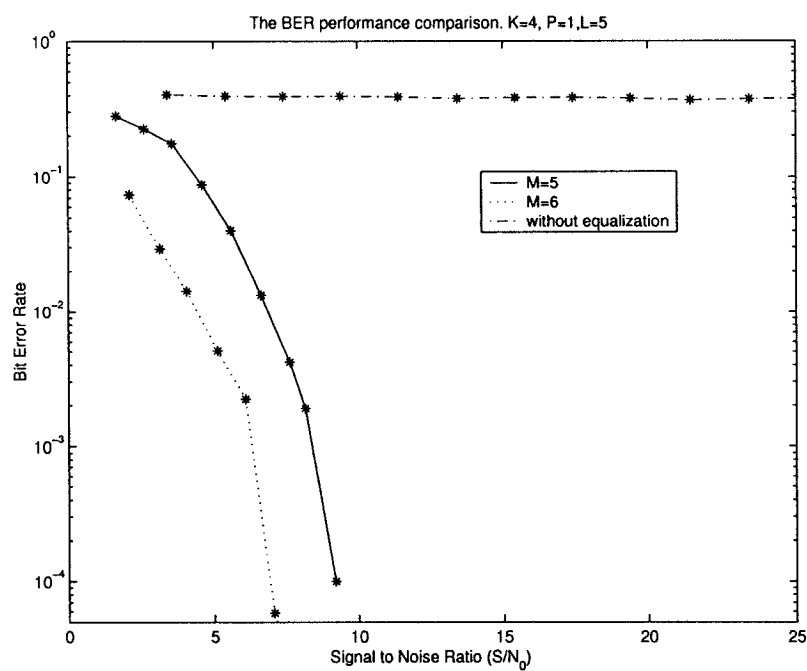


Figure 3.9: System BER Performance in Time-Dispersive Fading Channel ( $L=5, K=4, P=1$ ).

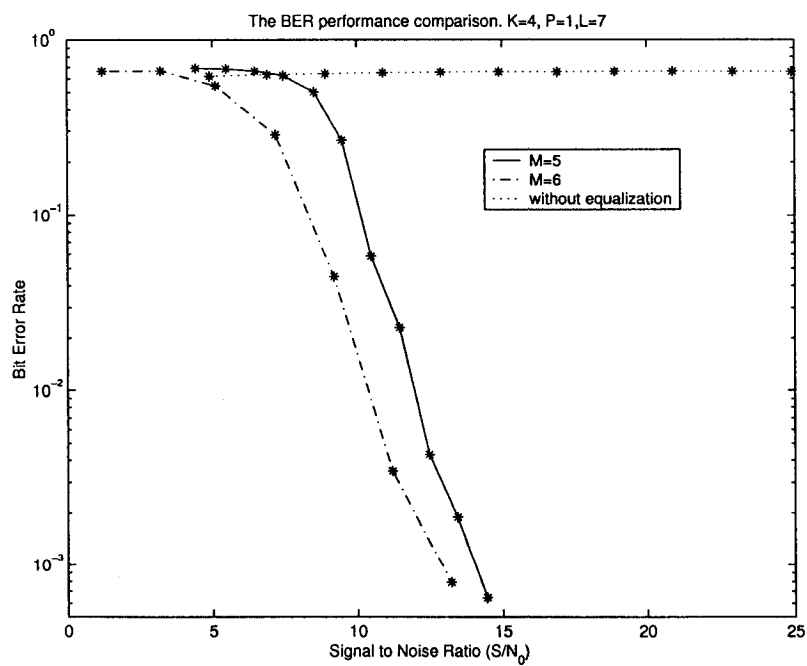


Figure 3.10: System BER Performance in Time-Dispersive Fading Channel ( $L=7, K=4, P=1$ ).

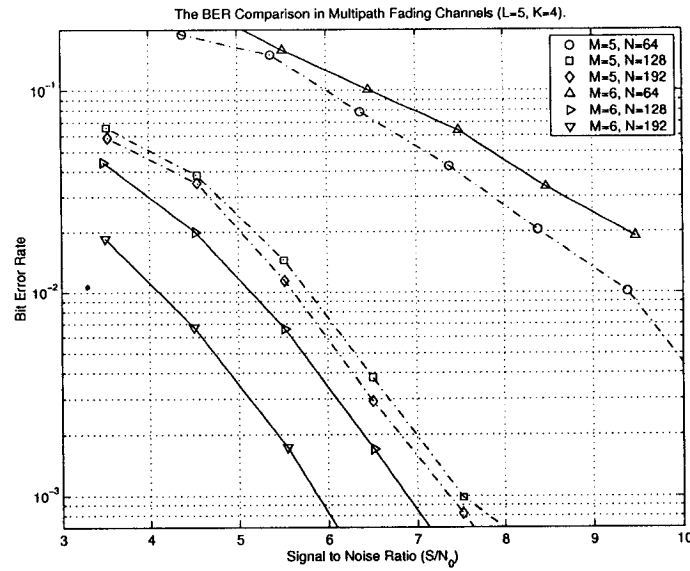


Figure 3.11: System Bit Error Rate Performance in Time-Dispersive Fading Channel ( $L=5$ ,  $K=4$ ,  $M=5, 6$ ,  $P=1$ ).

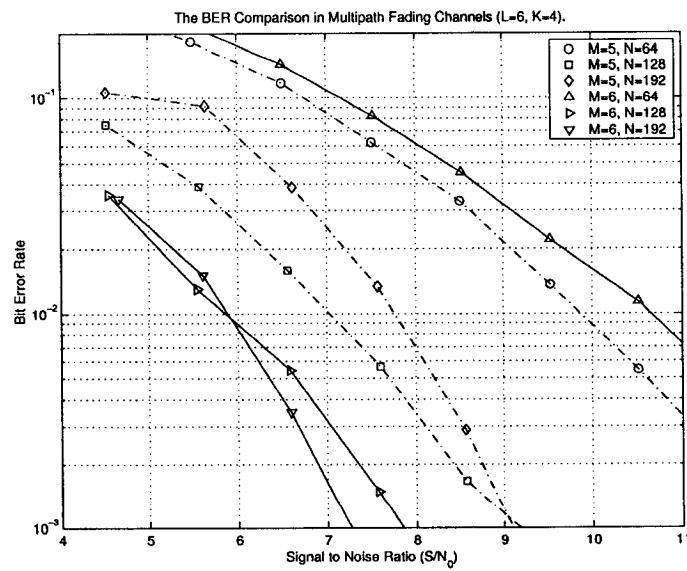


Figure 3.12: System Bit Error Rate Performance in Time-Dispersive Fading Channel ( $L=6$ ,  $K=4$ ,  $M=5, 6$ ,  $P=1$ ).

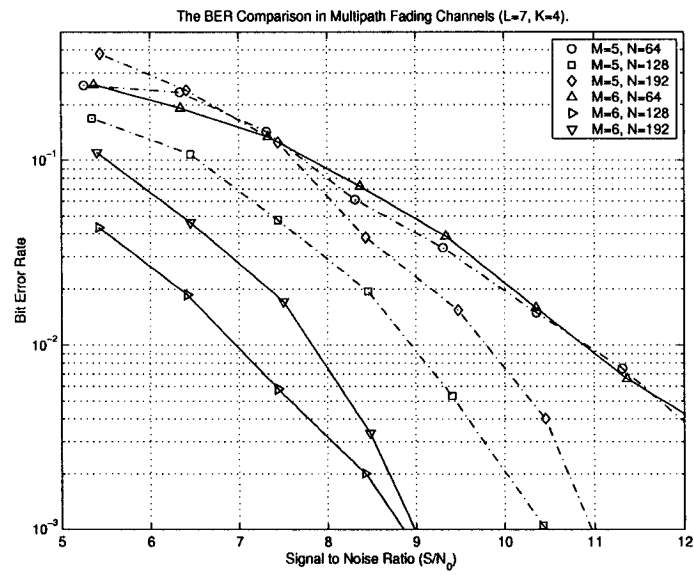


Figure 3.13: System Bit Error Rate Performance in Time-Dispersive Fading Channel ( $L=7$ ,  $K=4$ ,  $M=5, 6$ ,  $P=1$ ).

## Chapter 4

# Differential Space-Time Modulation for Transmissions Over Unknown Time-Dispersive Channels

**T**HIS chapter presents a new differential space-time transceiver over multiple-input multiple-out (MIMO) time-dispersive channels. The underlying idea is to transform the block Toeplitz signal structure caused by the finite impulse response (FIR) multipath channels into a block circulant matrix structure through the special signaling transmitted through multiple antennas, and then to exploit this signal structure by using the efficient space-time processing at the receiver to mitigate the channel multipath effects. The new, low complexity, transceiver is based on cyclic group codes, and a differential ST modulation and demodulation. The proposed scheme falls into the category of the deterministic approaches that are able to operate on short sample data of the signals without the convergence issue. Due to the nature of the scheme, it is capable to accommodate the quasi-static channels with proper parameter setting.

This chapter has five sections: Section 4.1 describes the background information and methodology for the development of the scheme in this chapter; Section 4.2 details about

the transmitted signal frame structure and its modulation; Section 4.3 considers the reception algorithm for this type of signaling; Section 4.4 presents the simulation results for the performance evaluation; The final section, Section 4.5, summarizes this chapter.

## 4.1 Motivation and Methodology

The ST coded transmission and ST signal processing are the most effective techniques in improving fading resistance. However, the computational complexity of channel equalization for such type of systems is fairly high for the existing ST transceivers, which demand much higher processing capacity on the receiver than those of conventional SISO cases. Therefore, the real-time processing for high-data-rate schemes is challenging.

Most current ST encoding schemes were designed with a flat fading modeling. This modeling assumes no ISI in the received signals. The DSTM schemes reviewed in Section 3.2 are regarded as a natural generalization of the standard differential phase-shift keying (DPSK). In this scheme, the receiver can decode the data in flat fading environments without knowing the MIMO channel gain matrix as long as the channel remains constant over the duration of two consecutive data frames.

However, a severe system performance degradation of DSTM will take place when channel is time-dispersive. To solve this problem, the DSTM can be combined with OFDM in the same way that Alamouti's ST coding was combined with OFDM in a scheme proposed in paper [95]. In this solution, it is only possible to apply the original detection algorithm at the receiver if each ST code is sent by different antenna but with the same tone. Namely, if each ST code is transmitted through same frequency subchannel from different transmit antennas of OFDM system, we could still utilize the low-complexity detection algorithm, originally designed for flat fading channels, for the DSTM signaling reception over the frequency-selective fading channels. However, transmitting with the same tone has two major drawbacks: (i) in a case of the spatial subchannels having a common deep null at the frequency of a tone, severe detection errors occur; (ii) in case of the interference

with a relatively strong component within a narrow band at the frequency of a tone, even the average SNR in the whole bandwidth is still high, the transmit diversity gain is offset drastically by the interferences.

This chapter presents a new differential space-time transceiver (DSTT) scheme which not only has the merit of the full transmit diversity but also is able to mitigate the ISI impairments of channels. This scheme has a reduced processing complexity at the receiver for channel equalization. Therefore, the proposed scheme is preferable for the forward-link transmission from the communication base-station to mobile devices.

In order to take into account the time-variability of the channel and to improve the transmission efficiency, the research described in this chapter focuses on exploiting the signal structure without relying on the CIR knowledge. The proposed transceiver is a differential ST modulation approach. This new solution is with a scenario of frame-by-frame transmitting and processing.

## 4.2 DSTT's Signal Frame and Modulation

This section describes the DSTT's encoding procedure which maps the information bits into the signaling frames. It is assumed again that the transmitter is equipped with  $K$  antennas and the receiver is equipped with  $M$  antennas.

### 4.2.1 Encoding the Information Bits to the ST Frames

First, the information bits are encoded using *Cyclic Group Codes* [53]. A cyclic group code set with parameters  $(\mathcal{M}, k_1, k_2, \dots, k_K)$  is:  $\mathfrak{g} = \{\mathbf{I}, \mathbf{g}_0, \mathbf{g}_0^2, \dots, \mathbf{g}_0^{\mathcal{M}-1}\}$  where

$$\mathbf{g}_0 = \begin{bmatrix} e^{2\pi j k_1 / \mathcal{M}} & 0 & \dots & 0 \\ 0 & e^{2\pi j k_2 / \mathcal{M}} & \dots & 0 \\ \vdots & \vdots & \vdots & \vdots \\ 0 & 0 & \dots & e^{2\pi j k_K / \mathcal{M}} \end{bmatrix}$$



In the proposed DSTT scheme, each batch of  $J$  such ST codes will be accommodated and sent within a frame. An auxiliary matrix  $\mathbf{G}^{[q]}$  is constructed for the  $q^{th}$  frame as follows:

$$\mathbf{G}_{N \times N}^{[q]} = \begin{bmatrix} \mathbf{g}_{(1)}^{[q]} & \mathbf{0} & \cdots & \mathbf{0} \\ \mathbf{0} & \mathbf{g}_{(2)}^{[q]} & \cdots & \mathbf{0} \\ \vdots & \vdots & \ddots & \vdots \\ \mathbf{0} & \mathbf{0} & \cdots & \mathbf{g}_{(J)}^{[q]} \end{bmatrix} \quad (4.1)$$

where  $\mathbf{g}_{(i)}^{[q]}$  is the  $i^{th}$  ST code in the  $q^{th}$  frame and  $N = JK$ . In order to facilitate blind detection of signals, each frame  $\mathbf{F}^{[q]}$  is differentially encoded with its previous frame according to:

$$\mathbf{F}^{[q+1]} = \frac{1}{N} \mathbf{F}^{[q]} \mathbf{Q}^{[q+1]} \quad (4.2)$$

$$\mathbf{Q}^{[q+1]} = \mathbf{V} \mathbf{G}^{[q+1]} \mathbf{V}^H \quad (4.3)$$

where  $q = 0, 1, \dots, P$  and  $\mathbf{V}_{N \times N}$  is a Vandermonde matrix as in equation (2.9). The initial frame  $\mathbf{F}^{[0]}$  is:

$$\mathbf{F}^{[0]} = \mathbf{Z} \mathbf{Q}^{[0]} \quad (4.4)$$

where

$$\mathbf{Z}_{K \times N} = \begin{bmatrix} 1 & 0 & \cdots & 0 & 0 & \cdots & \cdots & 0 & \cdots & 0 \\ 0 & 0 & \cdots & 0 & 1 & \cdots & 0 & \cdots & \cdots & 0 \\ 0 & \cdots & \cdots & \cdots & \cdots & \cdots & \cdots & \cdots & \cdots & 0 \\ 0 & 0 & \cdots & 0 & 0 & \cdots & 0 & 1 & \cdots & 0 \end{bmatrix} \quad (4.5)$$

Matrix  $\mathbf{Z}$  is a simple selection matrix, which only has non-zero element at the coordinates of  $(i, (i-1)J+1)$  where  $\{i = 1, 2, 3, \dots, K\}$ .

$$\mathbf{G}^{[0]} = \mathbf{I}_{N \times N}, \quad \mathbf{Q}^{[0]} = N \mathbf{I}_{N \times N}$$

The matrices of interest have the following, unitary-like, properties:

$$\mathbf{Q}^{[q]} (\mathbf{Q}^{[q]})^H = N^2 \mathbf{I}_{N \times N} \quad (4.6)$$

$$\mathbf{F}^{[q]} ((\mathbf{F})^{[q]})^H = JN^2 \mathbf{I}_{K \times K} \quad (4.7)$$

### 4.2.2 Extending the ST Frame Circularly and Modulating the Symbols

Rather than transmitting  $\mathbf{F}^{[q]}$  directly, what enters the channel is  $\mathbf{X}^{[q]}$  which is an extended frame of  $\mathbf{F}^{[q]}$  by appending it at the tail with the head segment according to the following mathematical expression:

$$\mathbf{X}_{[:,w]}^{[q]} = \begin{cases} \mathbf{F}_{(:,w)}^{[q]} & \text{if } w \leq N \\ \mathbf{F}_{(:,w-N)}^{[q]} & \text{if } w > N \end{cases} \quad (4.8)$$

where  $w = 1, 2, \dots, W$ ,  $W$  is the frame length; Without losing generality, let  $W = (N + L)$ ; and  $L$  is the maximum length of the multiple channels. The transmitted signal from the  $j^{th}$  antenna in the  $q^{th}$  ST frame is:

$$s_j(t) = \Re\left\{\sum_{w=1}^W g(t - (w-1)T_s - (q-1)T_f) \times \mathbf{X}_{(j,w)}^{[q]} e^{j2\pi f_c(t - (w-1)T_s - (q-1)T_f)}\right\} \quad (4.9)$$

where  $g(t)$  is a shaping pulse,  $f_c, T_f, T_s$  are respectively the carrier's frequency, the time interval for a frame and the time slot for a symbol. The frame structure is illustrated in Fig. 4.1.

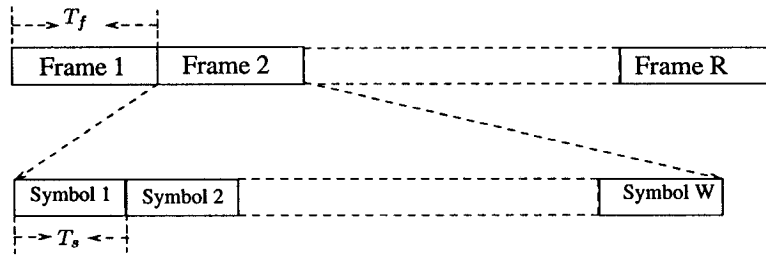


Figure 4.1: The Timing of the Symbol Stream in the Transmitted Frame.

## 4.3 The Receiver Algorithm

### 4.3.1 The Received Signal Structure

In the proposed DSTT, the received signals, after down-converting and base-band filtering, are sampled at the symbol rate and arranged in a matrix  $\mathbb{Y}^{[q]}$  so that data from the same receive antenna are in one row. For MIMO channels of maximum length  $L$ , to capture the channel states, a matrix set as the one in equation (1.25),  $\{\mathbf{h}(i), i = 0, 1, 2, \dots, L\}$  is used, where

$$\mathbf{h}(i) = \begin{bmatrix} h_{11}^{[i]} & h_{12}^{[i]} & \cdots & h_{1K}^{[i]} \\ h_{21}^{[i]} & h_{22}^{[i]} & \cdots & h_{2K}^{[i]} \\ \vdots & \vdots & \vdots & \vdots \\ h_{M1}^{[i]} & h_{M2}^{[i]} & \cdots & h_{MK}^{[i]} \end{bmatrix}, \quad i = 0, 1, 2, \dots, L,$$

and  $i$  is a delay index,  $h_{pr}^{[i]}$  represents the gain from the  $r^{th}$  transmit to the  $p^{th}$  receive antenna. The input-output relation between the sampled data matrix  $\mathbb{Y}^{[q]}$  (within the  $q^{th}$  frame interval) and the transmitted frames  $\mathbf{X}^{[q]}$  is:

$$\mathbb{Y}_{M \times W}^{[q]} = \mathbb{H}_{M \times (L+1)K} \mathbb{X}_{(L+1)K \times W}^{[q]} + \mathbb{N}_{M \times W}^{[q]} \quad (4.10)$$

where  $\mathbb{N}$  stands for the noise component matrix,

$\mathbb{H}_{M \times (L+1)K} = [\mathbf{h}(0), \mathbf{h}(1), \dots, \mathbf{h}(L)]$  and

$$\mathbb{X}_{(L+1)K \times W}^{[q]} = \begin{pmatrix} \mathbf{X}_{(:,1)}^{[q]} & \mathbf{X}_{(:,2)}^{[q]} & \cdots & \cdots & \cdots & \mathbf{X}_{(:,W)}^{[q]} \\ \mathbf{X}_{(:,W)}^{[q-1]} & \mathbf{X}_{(:,1)}^{[q]} & \cdots & \cdots & \cdots & \mathbf{X}_{(:,W-1)}^{[q]} \\ \vdots & \vdots & \vdots & \vdots & \vdots & \vdots \\ \mathbf{X}_{(:,W-L+1)}^{[q-1]} & \cdots & \mathbf{X}_{(:,W)}^{[q-1]} & \mathbf{X}_{(:,1)}^{[q]} & \cdots & \mathbf{X}_{(:,W-L)}^{[q]} \end{pmatrix}$$

The Toeplitz structure of  $\mathbb{X}_{(L+1)K \times W}^{[q]}$  is generated by the FIR channel. The following theorem is useful for further analysis of the signal structure and the derivation of the receiver algorithm.

**Theorem 3** [96] For a matrix  $\Lambda = \text{diag}\{\lambda_1, \lambda_2, \dots, \lambda_N\}$ , if  $\mathbf{C}_{N \times N} = \mathbf{V}\Lambda\mathbf{V}^H$ , where  $\mathbf{V}$  is the Vandermonde matrix as in (2.9),  $\mathbf{C}_{N \times N}$  is a circulant matrix defined by the row  $[c_1, c_2, \dots, c_N]$  and  $\lambda_i = \sum_{k=0}^{N-1} c_k e^{-j2\pi i k/N}$ .

Theorem 3 describes a DFT relation between the row elements of a circulant matrix  $\mathbf{C}_{N \times N}$  and the elements of a diagonal matrix  $\Lambda$ . From (4.3), it is evident that  $\mathbf{Q}^{[q]}$  has a circulant structure.

The data matrix  $\mathbb{Y}^{[q]}$  is processed by removing the first  $L$  columns so that a shorter data matrix  $\mathbb{Y}_{M \times N}^{[q]}$  is obtained and from (4.10):

$$\mathbb{Y}_{M \times N}^{[q]} = \mathbb{H}_{M \times (L+1)K} \tilde{\mathbf{X}}_{(L+1)K \times N}^{[q]} + \tilde{\mathbf{N}} \quad (4.11)$$

where

$$\tilde{\mathbf{X}}_{(L+1)K \times N}^{[q]} = \begin{pmatrix} \mathbf{X}_{(:,L+1)}^{[q]} & \mathbf{X}_{(:,L+2)}^{[q]} & \cdots & \cdots & \mathbf{X}_{(:,W)}^{[q]} \\ \mathbf{X}_{(:,L)}^{[q]} & \mathbf{X}_{(:,L+1)}^{[q]} & \cdots & \cdots & \mathbf{X}_{(:,W-1)}^{[q]} \\ \vdots & \vdots & \vdots & \vdots & \vdots \\ \mathbf{X}_{(:,1)}^{[q]} & \mathbf{X}_{(:,2)}^{[q]} & \mathbf{X}_{(:,3)}^{[q]} & \cdots & \mathbf{X}_{(:,W-L)}^{[q]} \end{pmatrix} \quad (4.12)$$

As a matter of fact, matrix  $\tilde{\mathbf{X}}_{(L+1)K \times N}^{[q]}$  is a block circulant matrix because of the transmitted signaling structure. Furthermore, with proper arrangement in (4.11),  $\mathbb{Y}_{M \times N}^{[q]}$  is expressed as follows:

$$\mathbb{Y}_{M \times N}^{[q]} = \sum_{i=1}^{L+1} \mathbf{h}(i-1)_{M \times K} \tilde{\mathbf{F}}_{(i)}^{[q]} + \tilde{\mathbf{N}}_{M \times N} \quad (4.13)$$

where  $\{\tilde{\mathbf{F}}_{(i)}^{[q]} = \tilde{\mathbf{X}}_{((i-1)K+1:iK,:)}^{[q]}, i = 1, 2, \dots, L+1\}$  are circularly shifted versions of  $\mathbf{F}^{[q]}$ . The latter observation results from (4.8), (4.12) and the definition of  $\tilde{\mathbf{X}}_{(i)}^{[q]}$ .

From (4.2), it can be observed that :

$$\tilde{\mathbf{F}}_{(i)}^{[q]} = \frac{1}{N} \mathbf{F}^{[q-1]} \tilde{\mathbf{Q}}_{(i)}^{[q]}, \quad q = 1, 2, \dots, P. \quad (4.14)$$

where  $\tilde{\mathbf{Q}}_{(i)}^{[q]}$  is a circularly shifted version of  $\mathbf{Q}^{[q]}$ , with the same shift as when obtaining  $\tilde{\mathbf{F}}_{(i)}^{[q]}$  from  $\mathbf{F}^{[q]}$ .

A circulant matrix remains circulant after a specific circular shift operation on each row. Hence,  $\tilde{\mathbf{Q}}_{(i)}^{[q]}$  is still circulant. From (4.1), (4.3) and theorem 2 and 3, it could be concluded that

$$\tilde{\mathbf{Q}}_{(i)}^{[q]} = \mathbf{V}\mathbf{G}^{[q]}\text{diag}\{e^{-j\xi_i}\}\mathbf{V}^H, i = 1, 2, \dots, L. \quad (4.15)$$

$$\text{where } \text{diag}\{e^{-j\xi_i}\} = \begin{bmatrix} e^{-j\xi_i} & 0 & \dots & 0 \\ 0 & e^{-j2\xi_i} & \dots & 0 \\ \vdots & \vdots & \ddots & \vdots \\ 0 & 0 & \dots & e^{-jN\xi_i} \end{bmatrix} \quad (4.16)$$

and  $\xi_i$  is a factor caused by different circular shifts. Thus,

$$\tilde{\mathbf{F}}_{(i)}^{[q]} = \frac{1}{N}\mathbf{F}^{[q-1]}\mathbf{V}\mathbf{G}^{[q]}\text{diag}\{e^{-j\xi_i}\}\mathbf{V}^H \quad (4.17)$$

Because  $\mathbf{G}^{[q]}$  is a diagonal matrix,

$$\tilde{\mathbf{F}}_{(i)}^{[q]} = \frac{1}{N}\mathbf{F}^{[q-1]}\mathbf{V}\text{diag}\{e^{-j\xi_i}\}\mathbf{G}^{[q]}\mathbf{V}^H \quad (4.18)$$

From (4.13) and (4.18) and the fact that  $\mathbf{V}^H\mathbf{V} = N\mathbf{I}$ ,

$$\mathbb{Y}_{M \times N}^{[q]} = \frac{1}{N} \sum_{i=1}^{L+1} \mathbf{h}_{M \times K}(i-1)\mathbf{F}^{[q-1]}\mathbf{V}\text{diag}\{e^{-j\xi_i}\}\mathbf{G}^{[q]}\mathbf{V}^H + \tilde{\mathbf{N}}$$

Therefore, provided the channel remains invariant within two frame intervals and temporarily dropping the noise term, with the help of (4.2), (4.3) and Theorem 3,  $\mathbb{Y}_{L \times N}^{[q+1]}$  is expressed as follows:

$$\mathbb{Y}_{M \times N}^{[q+1]} = \frac{1}{N}\mathbb{Y}_{M \times N}^{[q]}\mathbf{Q}^{[q+1]} \quad (4.19)$$

### 4.3.2 Signal Detection

Even though  $\mathbf{X}^{[q]}$  is transmitted over the time-dispersive MIMO channels, the dependence between  $\mathbb{Y}_{M \times N}^{[q+1]}$  and  $\mathbf{Q}^{[q+1]}$  in (4.19) indicates such a relation as if data of the matrix  $\mathbb{Y}_{M \times N}^{[q+1]}$  are received from MIMO flat fading channels. This results from: (i) the DFT relation between rows of  $\mathbf{Q}^{[q]}$  and the diagonal structure of  $\mathbf{G}^{[q]}$ ; (ii) processing in (4.8) and (4.11);

and (iii) the differential encoding of  $\mathbf{F}^{[q]}$  as in (4.2). Hence, the detection of  $\mathbf{Q}^{[q]}$  can be carried out using a least square error detector:

$$\hat{\mathbf{Q}}^{[q+1]} = \arg \min_{\mathbf{Q}_{[r]}} \left\| \mathbf{Y}^{[q+1]} - \frac{1}{N} \mathbf{Y}^{[q]} \mathbf{Q}_{[r]} \right\| \quad (4.20)$$

where the matrix subscript in  $[\ ]$  is a code-word alphabet index and the superscript is a time index. From (4.20),

$$\begin{aligned} \hat{\mathbf{Q}}^{[q+1]} &= \arg \min_{\mathbf{Q}_{[r]}} \text{Trace} \left\{ \left( \mathbf{Y}^{[q+1]} - \frac{1}{N} \mathbf{Y}^{[q]} \mathbf{Q}_{[r]} \right) \times \left( \mathbf{Y}^{[q+1]} - \frac{1}{N} \mathbf{Y}^{[q]} \mathbf{Q}_{[r]} \right)^H \right\} \\ &= \arg \min_{\mathbf{Q}_{[r]}} \text{Trace} \left\{ \mathbf{Y}^{[q+1]} (\mathbf{Y}^{[q+1]})^H - \frac{1}{N} \mathbf{Y}^{[q+1]} (\mathbf{Y}^{[q]} \mathbf{Q}_{[r]})^H \right. \\ &\quad \left. - \frac{1}{N} (\mathbf{Y}^{[q]} \mathbf{Q}_{[r]}) (\mathbf{Y}^{[q+1]})^H + \frac{1}{N^2} \mathbf{Y}^{[q]} \mathbf{Q}_{[r]} (\mathbf{Y}^{[q]} \mathbf{Q}_{[r]})^H \right\} \end{aligned}$$

Because

$$\text{Trace} \{ \mathbf{Y}^{[q]} \mathbf{Q}_{[r]} (\mathbf{Y}^{[q]} \mathbf{Q}_{[r]})^H \} = N^2 \text{Trace} \{ \mathbf{Y}^{[q]} (\mathbf{Y}^{[q]})^H \}$$

is a constant for different  $\mathbf{Q}_{[r]}$ , a least-square-error detector for DSTT's differential frame signaling can be obtained as:

$$\hat{\mathbf{Q}}^{[q+1]} = \arg \max_{\mathbf{Q}_{[r]}} \Re \{ \text{Trace} \{ \mathbf{Y}^{[q]} \mathbf{Q}_{[r]} (\mathbf{Y}^{[q+1]})^H \} \} \quad (4.21)$$

According to the definition equation (4.3), the following equation holds.

$$\hat{\mathbf{Q}}^{[q+1]} = \arg \max_{\mathbf{Q}_{[r]}} \Re \{ \text{Trace} \{ \mathbf{Y}^{[q]} \mathbf{V} \mathbf{G}_{[r]} (\mathbf{Y}^{[q+1]} \mathbf{V})^H \} \} \quad (4.22)$$

Furthermore, the above detection criteria is equivalent to what follows:

$$\hat{\mathbf{g}}_{(i)}^{[q+1]} = \arg \max_{\mathbf{g}_{[r]}} \Re \{ \text{Trace} \{ \mathfrak{Y}_{(i)}^{[q]} \mathbf{g}_{[r]} (\mathfrak{Y}_{(i)}^{[q+1]})^H \} \} \quad (4.23)$$

where

$$\mathfrak{Y}_{(i)}^{[q]} = (\mathbf{Y}^{[q]} \mathbf{V})_{(1:M, 1+(i-1)K:iK)}, \quad i = 1, 2, 3, \dots, J.$$

Provided that the maximum delay spread is less than  $(W - N)T_s$ , the special signaling structure of  $\mathbf{X}^{[q]}$  enables the efficient algebraic data recovery without channel estimation.

This feature is very desirable for transmission over quasi-static frequency-selective channels.

Additionally, DSTT can have a different version as discussed in the following. It can be observed that, instead of using the single carrier modulation described in (4.9), if the  $\mathbf{X}^{[q]}$  is treated as a special type of ST signaling being directly sent to D/A converter for transmissions as same as an OFDM system does, this version of DSTT system becomes a system very similar to ST-OFDM system. However, it transmits each ST symbol through multiple tones and multiple antennas. Hence, in case of common deep fading of the spatial subchannels at the frequency subband of one tone, it still remains strong fading resistance via the access of the spatial subchannels at the other subbands. In case of narrow-band interference or noise at the subband of a certain tone, for this system, it is also possible to suppress such type of subband interference by filtering prior to detection without severe system degradation. An additional advantage is that it only needs the sample data of the last two ST symbols for receiver processing whereas a DSTM-OFDM combining scheme, mentioned in Section 4.1, has to keep much more sample data of the OFDM symbols for receiver processing.

## 4.4 Performance Simulations

The proposed scheme DSTT also has been examined by the computer simulations. The typical results with parameters  $\{\mathcal{M}, k_1, k_2, k_3\} = \{8, 1, 1, 3\}$ ,  $\{K, M, J\} = \{4, 1, 12\}$  and  $\{K, M, J\} = \{4, 2, 12\}$  are illustrated in Fig. 4.2 and Fig. 4.3. Besides, Figs. 4.5 and 4.7 demonstrate the simulation results with  $\{\mathcal{M}, k_1, k_2, k_3, k_4\} = \{4, 1, 1, 1, 1\}$ , where  $\{K, M, J\} = \{4, 1, 4\}$  and  $\{K, M, J\} = \{4, 2, 4\}$  were respectively assumed.

The maximum lengths of the multiple-channels were chosen in the simulations as a parameter. The typical  $L$  is assumed to be  $L = 3$  and  $L = 5$  times of a symbol interval with the performance curves labeled accordingly in the figures presented. The simulation results were statistically averaged over all the cases of random length of the spatial subchannels,

random channel CIR, random bit streams and random additive noise components.

For comparison purposes, the performance of the DSTM systems [51] with the same transceiver antenna setups but in flat fading channels was simulated as well. These simulations were conducted by employing the optimal cyclic code:  $\{\mathcal{M}, k_1, k_2, k_3\} = \{8, 1, 1, 3\}$ ,  $R = 1 \text{ bit/s/Hz}$  and  $\{\mathcal{M}, k_1, k_2, k_3, k_4\} = \{4, 1, 1, 1, 1\}$ ,  $R = 0.5 \text{ bit/s/Hz}$ . The results are reported in Figs. 4.2, 4.3, 4.5 and Fig. 4.7 with curves being labeled as DSTM.

It can be observed that, over the MIMO time-dispersive fading channels of different channel lengths, the DSTT achieves the same performance as a DSTM scheme does over flat fading channels, provided the channel lengths are smaller than  $(W - N)T_s$ . Namely, over frequency selective fading channel, the proposed scheme can offer the same transmit diversity gain and coding gain as same as the DSTM does in the flat fading channels.

For different communication scenarios, the proposed DSTT scheme may have different setups in terms of the numbers of transmitter and receiver antennas, bandwidth utilization and ST frame lengths. These parameters should be properly chosen by taking into account channel length, SNR and time-varying characteristics of the channel.

To examine the time-dispersive channel effects on the DSTM systems with the same antenna setups, Figs. 4.4 and 4.6 demonstrate that DSTM transceiver fails when it is applied directly in the frequency-selective fading propagation environment. DSTM scheme was designed based on the flat fading channel modeling. Because of the existence of strong ISI, its BER remains above a certain lower bound regardless of the SNR increase. In contrast, Figs. 4.5 and 4.7 demonstrate the BER of DSTT systems drops rapidly when SNR increases. This shows DSST's superior capacity in removing ISI caused by the frequency-selective fading channels.

From the simulation results, one can also observe that the different configuration of antenna numbers of the transmitter and the receiver have a distinct influence on the system BER performance with respect to SNR. The difference between the transceiver antenna setups in Figs. 4.5 and 4.7 is that  $M = 1$  is increased to  $M = 2$ . From these figures, one can observe that at the BER operating point of  $10^{-2}$ , the SNR is required to be 8 dB and 4



dB for  $M = 1$  and  $M = 2$ , respectively. This indicates a 4 dB performance improvement by increasing the number of receive antenna by one.

From the performance curves, we can observe that the improvements by increasing antenna numbers depend on the operating point of the modulation scheme. It has the trend that, at the lower BER operating points, the higher power savings could be achieved by the same antenna number increase. Besides, the smaller the antenna number is, the higher power saving could be obtained by an antenna number increase.

## 4.5 Summary

Through the derivation and discussion of the DSTT, this chapter demonstrated how the induced block circulant matrix structure of the ST signal can be taken advantage of efficiently in an algebraic methodology for transmit diversity system design over frequency-selective channels. The strategy exercised in the design is to jointly develop the ST transmission signaling and the ST receiver algorithm to mitigate the multipath effects. It provides a favorable trade-off between the complexity and the performance. In a fashion of deterministic signal processing, the new transceiver can blindly operate with a small number of the signal samples over the frequency-selective channels. Therefore, it is suitable for quasi-static time-varying channels, and does not have the convergence problems.

The design of DSTT is aimed at the gaining of high system resistance to both ISI and signal fading in unknown MIMO-FIR channels. The simulations verify (i) the high performance of the scheme over the multi-path fading channels and (ii) the insensitivity to the different channel lengths if the  $L < (W - N)$ .

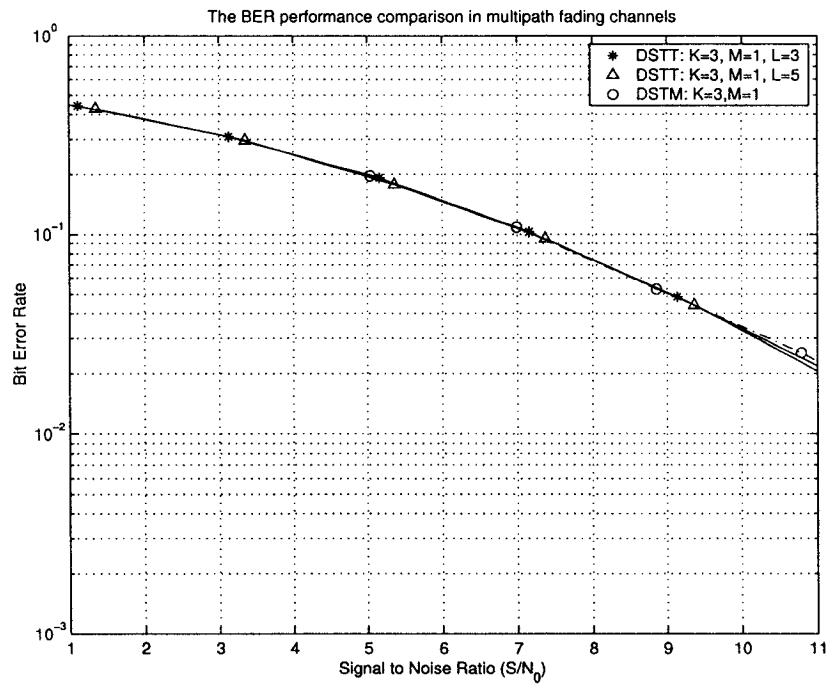


Figure 4.2: The DSTT BER Performance ( $\mathcal{M} = 8, K = 3, M = 1, J = 12$ ).

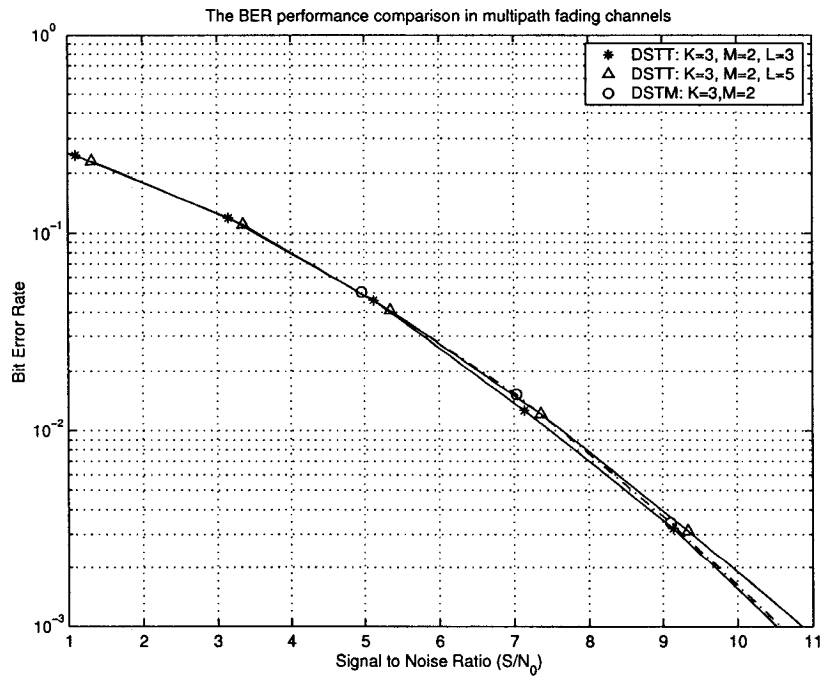


Figure 4.3: The DSTT BER Performance ( $\mathcal{M} = 8, K = 3, M = 2, J = 12$ ).

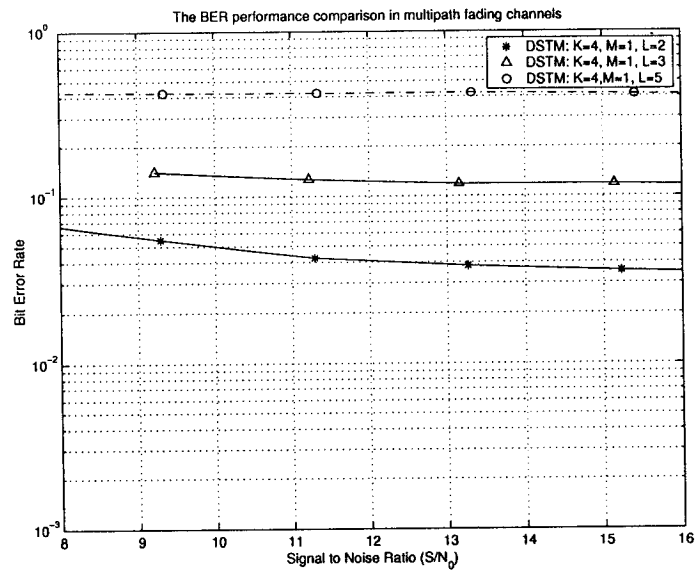


Figure 4.4: The DSTM BER Performance in Frequency-Selective Fading Channels ( $\mathcal{M} = 4$ ,  $K = 4$ ,  $M = 1$ ).

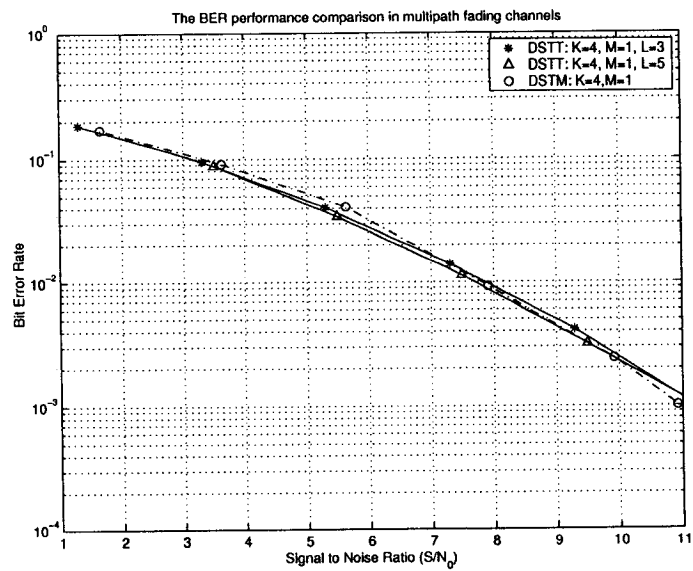


Figure 4.5: The DSTT BER Performance ( $\mathcal{M} = 4$ ,  $K = 4$ ,  $M = 1$ ,  $J = 4$ ).

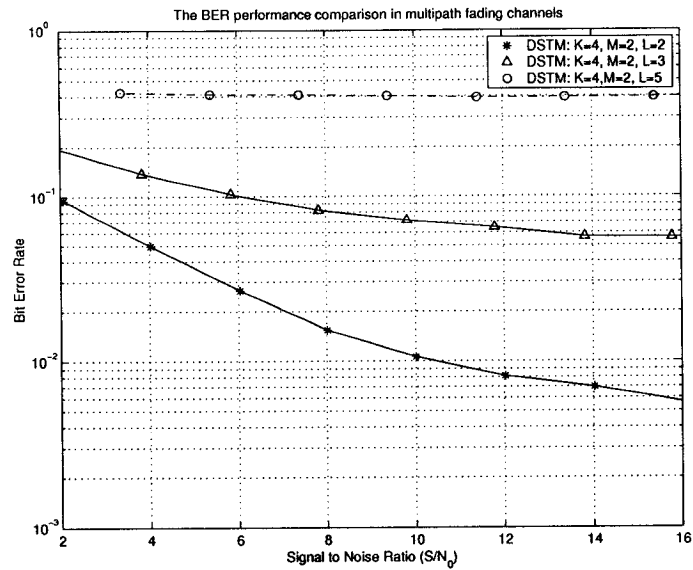


Figure 4.6: The DSTM BER Performance in Frequency-Selective Fading Channels ( $\mathcal{M} = 4, K = 4, M = 2$ ).

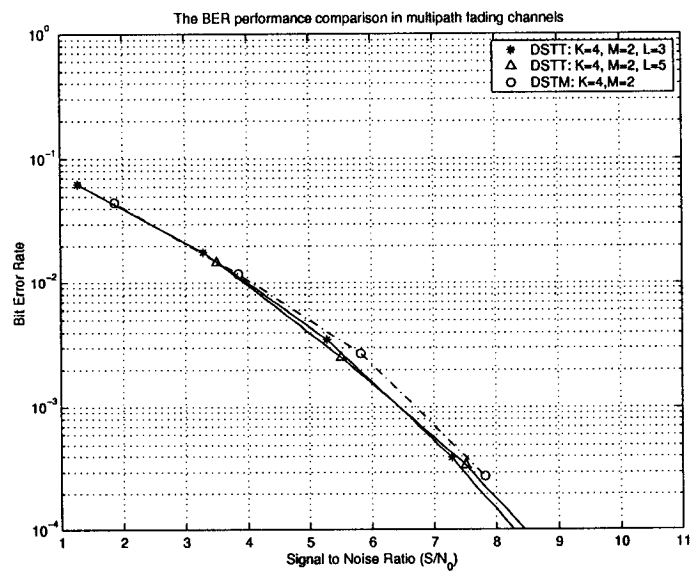


Figure 4.7: The DSTT BER Performance ( $\mathcal{M} = 4, K = 4, M = 2, J = 4$ ).

# Chapter 5

## Conclusions

**I**NTER-SYMBOL interference caused by time-dispersive radio channels where the symbol rate exceeds the coherence bandwidth, is a limiting factor to any high-speed radio communications, including MIMO systems. Removal of the ISI effects has a decisive impact on the performance of the entire wireless system. In the congested spectrum environment where bandwidth is at a premium, computationally efficient algorithms for MIMO channel equalization are fundamental in the deployment of future wireless networks to meet the performance requirements far exceeding those achievable by SISO transceivers. This was the motivation for the work in this dissertation.

In MIMO spatial multiplexing systems, there are multiple correlated signals transmitted within the same frequency bandwidth from multiple antennas placed in different locations. The channel equalization in this case has to facilitate the source separation from the spatially multiplexed signals in a similar fashion as multi-user detection. This problem adds substantial complexity to the MIMO channel equalization, as compared to the SIMO and SISO equalization scenarios.

The overall goal of this dissertation was to utilize deterministic algorithms to mitigate the channel ISI on the received signals in the context of spatial multiplexing or space-time coded communications. The derivation and analysis of the algorithms are from the digital signal processing perspective, exploits signal structure and properties. The schemes

proposed are able to fully mitigate the time-dispersive effects to facilitate the detection of the spatial-multiplexed symbols or space-time block codes. In a radio communication link, the signal radio-interface constitutes an essential factor to the performance of the entire wireless networks. Hence, the research contributed on channel equalization has a crucial impact on the detection error rates and throughput of wireless networks.

## 5.1 Dissertation Summary

This section summarizes the results in this dissertation, chapter by chapter.

Specifically, in Chapter 2, this dissertation proposed a frequency-domain equalization approach for spatial multiplexing transceivers employing single carrier signaling. The new scheme offers the advantage of reduced constraints on the PA linearity and signal frequency synchronization when compared to MIMO-OFDM schemes. The simulation demonstrated that, in general, it had a comparable BER to SNR performance to that of MIMO-OFDM systems with the same overall transceiver complexity. In the simulation results illustrated in Chapter 2, a common phenomenon observed is that the BER of the proposed SCFDE scheme drops relatively faster than that of OFDM schemes when the SNR passes certain thresholds, which are dependent on the transceiver configuration. For both OFDM and SCFDE systems, the increase of the receive antenna number provides a diminishing return. Therefore, the trade-off between diversity gain offered by receiver antennas and the processing complexity is one of the main concerns in the system design.

In Chapter 3, the dissertation presented a blind receiver algorithm for unitary differential space-time modulated signaling. The new receiver algorithm exploits the block Toeplitz signal structure and the signal's constant modulus property to directly estimate the signal frame without channel CIR knowledge. This algebraic approach is especially suitable for the communications over time-varying quasi-static channels where the channel estimation is then ineffective or has prohibitive complexity. The proposed scheme circumvents the

channel estimation by applying the direct signal subspace estimation. In this receiver design, the main computational complexity comes from the intersection basis estimation of the subspaces. An improved computation method with reduced complexity for such basis estimation other than the SVD approach described in this dissertation is of great interest for future research.

The final part of this dissertation introduces a new space-time modulation method to combat the time-dispersive effect of unknown channels. One of the important features is that the receiver burden due to the channel estimation and equalization can be removed or alleviated in this approach. Therefore, this scheme is an advantageous candidate for forward-link transmissions where the receiver structures of the mobile devices need to be of a low complexity and a low power dissipation. From the simulation results, it can be observed that its BER to SNR performance remains robust over the different channel lengths as long as the channel length is less than  $(W - N)T_s$ .

In general, this dissertation proved again that by incorporating a number of antennas in the radio-interface of a wireless communication link, the performance of the system could be significantly improved for the communications over the time-dispersive fading channels. The space-time algorithms based on the digital signal processing, and the space-time channel coding and modulation, can achieve a high diversity gain and coding gain that other methods could not offer. This actually becomes a trend in the transceiver design for future-generation wireless networks. For the high data rate radio transmissions, the deterministic space-time channel equalization approaches proposed in this dissertation provide the efficient candidate systems of high resistance to ISI and signal fading for several typical communication scenarios.

## 5.2 Future Directions

This dissertation has presented the mathematical derivations, discussed the features, and also demonstrated the superior performance of the proposed MIMO equalization schemes.

However, there are still some issues to be explored. What follows are the topics that we believe are worth pursuing for future investigations:

First of all, in the simulations, the samples from the different antennas are assumed to be statistically independent. Rich scattering of the signal wave propagation and large antenna separations result in independent fading across space. Normally, the spatial subchannel gains are assumed stationary random processes which are independent of each other if the transceiver is in rich scattering environments and separation of the antennas is larger than the carrier wavelength. This is a realistic assumption in this dissertation. Further studies should be conducted to examine the influence of correlation of the samples from the different antennas (spatial non-whiteness) on the systems performance and choices of system parameters.

Second, the simulation and derivation were made using the reasonable assumption of white additive complex Gaussian noise. The analysis and simulations with other modeling of the noise with different statistical distributions could be further investigated.

Third, the CIR modeling in this dissertation is based on quasi-static FIR filters with equal-space sampling. For some special wireless channels having a power profile of echo groups with long delays, the variant-space sampling FIR or infinite impulse response (IIR) modeling of the MIMO time-dispersive channels should be established and applied in the analysis and simulation of the proposed schemes.

Additionally, the application-specific system implementation that facilitates the algorithmic computation of the proposed schemes in real-time is yet another aspect for future research.



# Appendix

## Definition of Channel Capacity:

The capacity  $C$  of a noisy channel should be the maximum possible rate of transmission, i.e., the rate when the source is properly matched to the channel. We therefore define the channel capacity by  $C = \text{Max}(H(x) - H_y(x))$  where  $H(x)$  is the entropy of the source and  $H_y$  is a conditional entropy of  $x$  [20].

## Complex Gaussian Random Variables and Vectors:

The random variable  $x = u + jv$  is a scalar complex random variable. The complex Gaussian probability density function (PDF) assumes  $u$  and  $v$  are independent of each other and they respectively have the normal distribution of  $\mathcal{N}(\mu_u, \frac{\sigma^2}{2})$  and  $\mathcal{N}(\mu_v, \frac{\sigma^2}{2})$ . The PDF of a scalar complex random Gaussian variable  $x$  is :

$$p(x) = \frac{1}{\pi\sigma^2} \exp\left[-\frac{1}{\sigma^2}|x - \mu|^2\right]$$

where  $\mu = E(x) = \mu_u + j\mu_v$  and  $E$  stands for the *mean* of the random variable [97]. Usually, the complex Gaussian PDF for a scalar complex random variable is denoted as  $\mathcal{CN}(\mu, \sigma^2)$ .

A complex random vector  $\mathbf{x} = \mathbf{u} + j\mathbf{v}$  has  $n$  complex variables and both of  $\mathbf{u}$  and  $\mathbf{v}$  are

$n \times 1$  real vectors. Random Vector  $\mathbf{x}$  has the PDF:

$$\begin{bmatrix} \mathbf{u} \\ \mathbf{v} \end{bmatrix} \sim \mathcal{N} \left( \begin{bmatrix} \mu_{\mathbf{u}} \\ \mu_{\mathbf{v}} \end{bmatrix}, \begin{bmatrix} C_{\mathbf{uu}} & C_{\mathbf{uv}} \\ C_{\mathbf{vu}} & C_{\mathbf{vv}} \end{bmatrix} \right)$$

and

$$\begin{aligned} C_{\mathbf{uu}} &= C_{\mathbf{vv}}; \\ C_{\mathbf{uv}} &= -C_{\mathbf{vu}}. \end{aligned}$$

then, random vector  $\mathbf{x}$  has the complex multivariate Gaussian PDF [97] , which is denoted as  $\mathbf{x} \sim \mathcal{CN}(\boldsymbol{\mu}, C_{\mathbf{x}})$  where

$$\begin{aligned} \boldsymbol{\mu} &= \mu_{\mathbf{u}} + j\mu_{\mathbf{v}}; \\ C_{\mathbf{x}} &= 2(C_{\mathbf{uu}} + jC_{\mathbf{vu}}); \end{aligned}$$

$C_{\mathbf{vu}} \doteq E((\mathbf{v} - E(\mathbf{v}))(\mathbf{u} - E(\mathbf{u}))^H)$ ,  $C_{\mathbf{uu}} \doteq E((\mathbf{u} - E(\mathbf{u}))(\mathbf{u} - E(\mathbf{u}))^H)$  , and the PDF is:

$$p(\mathbf{x}) = \frac{1}{\pi^n \det(C_{\mathbf{x}})} \exp[-(\mathbf{x} - \boldsymbol{\mu})^H C_{\mathbf{x}}^{-1} (\mathbf{x} - \boldsymbol{\mu})]$$

where ‘*det*’ stands for *determinant*.

## Singular Value Decomposition (SVD):

A general matrix  $\mathbf{A} \in \mathbb{C}^{m \times n}$  can be decomposed as

$$\mathbf{A} = \mathbf{U} \mathbf{D} \mathbf{V}^H$$

where both  $\mathbf{U} \in \mathbb{C}^{m \times m}$  and  $\mathbf{V} \in \mathbb{C}^{n \times n}$  are unitary matrices, and  $\mathbf{D} \in \mathbb{C}^{m \times n}$  is a diagonal matrix in the form of  $\mathbf{D} = \text{diagonal}(\delta_1, \delta_2, \dots, \delta_p)$ , and  $p = \min(m, n)$ . Usually, the SVD algorithm order  $\delta_i$  in the order of  $\{\delta_1 > \delta_2 > \dots > \delta_p > 0\}$  [98]. Hence, matrix  $\mathbf{A}$  could be expressed as a summation of several decomposed matrices as follows:

$$\mathbf{A} = \sum_{i=1}^p \delta_i \mathbf{u}_i \mathbf{v}_i^H$$

where  $\mathbf{U} = [\mathbf{u}_1, \mathbf{u}_2, \dots, \mathbf{u}_m]$  and  $\mathbf{V} = [\mathbf{v}_1, \mathbf{v}_2, \dots, \mathbf{v}_n]$ , and also the Frobenius norm of  $\mathbf{A}$  can be expressed as a summation:

$$\|\mathbf{A}\|_{Frob}^2 = \sum_{i=1}^p \delta_i^2$$

# Bibliography

- [1] B. Sklar, "Rayleigh fading channels in mobile digital communication systems. i. characterization," *IEEE Commun. Mag.*, vol. 35, no. 9, pp. 136–146, Sept. 1997.
- [2] R. S. Kennedy, "Fading dispersive communication channels," *John Wiley Sons, Inc.*, 1969.
- [3] T. S. Rappaport, "Wireless communications: principles and practice," *Prentice Hall PTR*, July 1999.
- [4] G. D. Durgin, *Space-time wireless channels*. Pearson Education, Inc, 2003.
- [5] G. J. Foschini, "Layered space-time architecture for wireless communication in a fading environment when using multi-element antennas," *Bell Labs Tech. Journal*, vol. 1, no. 2, pp. 41–59, Aug 1996.
- [6] M. J. Gans, N. Amitay, Y. S. Yeh, H. Xu, R. A. Valenzuela, T. Sizer, R. Storz, D. Taylor, W. M. MacDonald, C. Tran, A. Adamiecki, "BLAST system capacity measurements at 2.44 ghz in suburban outdoor environment," *VTC 2001 Spring. IEEE VTS 53rd*, vol. 1, pp. 288–292, 2001.
- [7] P. W. Wolniansky, G. J. Foschini, G. D. Golden, R. A. Valenzuela, "V-BLAST: an architecture for realizing very high data rates over the rich-scattering wireless channel," *Signals, Systems, and Electronics, URSI International Symposium on*, vol. 1998, pp. 295–300, 1998.
- [8] H. Balcskei and A. J. Paulraj, *The Communications Handbook, 2nd edition*. CRC Press, 2002.
- [9] D. Gesbert, H. Bolcskei, D. Gore, A. Paulraj, "MIMO wireless channels: capacity and performance prediction," *Global Telecommunications Conference, 2000. GLOBECOM'00. IEEE*, vol. 2, pp. 1083–1088, 2000.
- [10] D. Gesbert, J. Akhtar, "Breaking the barriers of Shannon's capacity: An overview of MIMO wireless systems," *Telenor's Journal: Telekomnikk*, May 2002. [Online]. Available: [www.ifi.uio.no/~gesbert/papers/TelekomnikkMIMO.pdf](http://www.ifi.uio.no/~gesbert/papers/TelekomnikkMIMO.pdf)

- [11] E. Telatar, "Capacity of multi-antenna Gaussian channels," *European Trans. on Telecommun.*, vol. 10, no. 6, pp. 585–595, Nov./Dec. 1999.
- [12] A. J. Paulraj, C. B. Papadidas, "Space-time processing for wireless communications," *IEEE Signal Processing Mag.*, vol. 14, no. 6, pp. 49–83, Nov. 1997.
- [13] A. J. Paulraj, D. Gesbert, C. B. Papadidas, *Smart antenna for mobile communications*. Encyclopedia for electrical engineering, John Wiley publishing Co., 2000.
- [14] C. Schlegel and Z. Bagley, "Efficient processing for high-capacity MIMO channels," Sept. 2002. [Online]. Available: <http://www.ee.ualberta.ca/~schlegel/publications/SchBag02.pdf>
- [15] D. Gesbert, M. Shafi, D. S. Shiu, P. J. Smith, A. Naguib, "From theory to practice: an overview of MIMO space-time coded wireless systems," *IEEE J. Select. Areas Commun.*, vol. 21, no. 3, pp. 281–302, April 2003.
- [16] J. Talvitie, V. Hovinen, M. Hamalainen, I. Oppermann, "Wideband channel measurement and characterization for wireless local loops," *Personal, Indoor and Mobile Radio Communications, 1996. PIMRC'96., Seventh IEEE International Symposium on*, vol. 1, pp. 5–9, Oct. 1996.
- [17] G. Dolmans, M. Collados, "Broadband measurement analysis of indoor space-time channels," *Proc. of URSI General Assembly 2002, Maastricht*, Aug. 2002.
- [18] M. C. Jeruchim, P. Balaban, K. S. Shanmugan, *Simulation of communication systems*. New York: Plenum Press., 1992.
- [19] F. M. Gardner, J. D. Baker, *Simulation techniques*. New York: John Wiley & Sons, Inc., 1996.
- [20] C. E. Shannon, "A mathematical theory of communication," *The Bell System Technical Journal*, vol. 27, pp. 379–423, 623–656, July, October 1948.
- [21] X. Wang, "Advanced signal processing for wireless multimedia communications," *Informing science*, vol. 3, no. 1, 2000.
- [22] A. Hero, T. Chen, "Highlights of statistical signal and array processing," *IEEE Signal Processing Magazine*, pp. 21–64, Sept. 1998.
- [23] A. J. Viterbi, "Error bounds for convolutional codes and an asymptotically optimum decoding algorithm," *IEEE Trans. Inform. Theory*, vol. IT-13, no. 2, pp. 260–269, April 1967.
- [24] G. D. Forney, Jr., "The Viterbi algorithm," *Proc. IEEE*, vol. 61, no. 3, pp. 268–277, March 1973.

- [25] C. Berrou, A. Glavieux, "Near optimum error correcting coding and decoding: turbo-codes," *IEEE Trans. Commun.*, vol. 44, no. 10, pp. 1261–1271, Oct. 1996.
- [26] C. Berrou, A. Glavieux, P. Thitimajshima, "Near Shannon limit error-correcting coding and decoding: Turbo-codes. 1," *Communications, ICC'93 Geneva. Technical Program, Conference Record, IEEE International Conference on*, vol. 2, pp. 1064–1070, 1993.
- [27] R. M. Buehrer, A. G. Kogiantis, S. C. Liu, J. A. Tsai, and D. Uptegrove, "Intelligent antennas for wireless communications: Uplink," *Bell Labs Tech. Journal*, vol. 4, no. 3, pp. 73–103, July–Sept. 1999.
- [28] P. Vaidyanathan, *Multirate systems and filter banks*. Prentice Hall PTR, 1993.
- [29] B. D. Van Veen, K. M. Buckley, "Beamforming: a versatile approach to spatial filtering," *ASSP Magazine, IEEE*, vol. 5, no. 2, pp. 4–24, April 1988.
- [30] A. L. Swindlehurst, "Time delay and spatial signature estimation using known asynchronous signals," *IEEE Signal Processing Mag.*, vol. 46, no. 2, pp. 449–462, Feb. 1998.
- [31] D. Asztely, B. Ottersten, A. L. Swindlehurst, "A generalized array manifold model for local scattering in wireless communications," *Acoustics, Speech, and Signal Processing, 1997. ICASSP-97., 1997 IEEE International Conference on*, vol. 5, pp. 4021–4024, 1997.
- [32] H. Krim and M. Viberg, "Two decades of array signal processing research," *IEEE Signal Processing Mag.*, pp. 67–94, July 1996.
- [33] A. L. Swindlehurst, T. Kailath, "A performance analysis of subspace-based methods in the presence of model errors. i. the MUSIC algorithm," *IEEE Trans. Signal Processing*, vol. 40, no. 7, pp. 1758–1774, July 1992.
- [34] M. Viberg, B. Ottersten, "Sensor array processing based on subspace fitting," *IEEE Trans. Signal Processing*, vol. 39, no. 5, pp. 1110–1121, May 1991.
- [35] E. Moulines, P. Duhamel, J. F. Cardoso, S. Mayrargue, "Subspace methods for the blind identification of multichannel FIR filters," *IEEE Trans. Signal Processing*, vol. 43, no. 2, pp. 516–525, Feb. 1995.
- [36] R. Yonezawa, I. Chiba, "A combination of two adaptive algorithms SMI and CMA," *Special Issue on Adaptive Array Antenna Techniques for Advanced Wireless Communications, IEICE TRANS. Commun.*, vol. E84-B, no. 7, pp. 1768–1773.
- [37] J. F. Cardoso, A. Souloumiac, "Blind beamforming for non-Gaussian signals," *IEE proceedings-F*, vol. 140, no. 6, pp. 372–370, Dec. 1993.

- [38] J. Sheinvald, "On blind beamforming for multiple non-Gaussian signals and the constant-modulus algorithm," *IEEE Trans. Signal Processing*, vol. 46, no. 7, pp. 1878–1885, July 1998.
- [39] H. Bolcskel, A. J. Paulraj, K.V.S. Hari, R. U. Nabar, W. W. Lu, "Fixed broadband wireless access: state of the art, challenges, and future directions," *IEEE Commun. Mag.*, vol. 39, no. 1, pp. 100–108, Jan. 2001.
- [40] A. J. Viterbi, "Wireless digital communications: A view based on three lessons learned," *IEEE Commun. Mag.*, Sept. 1991.
- [41] N. Al-Dhahir, C. Fragouli, A. Stamoulis, W. Younis, R. Calderbank, "Space-time processing for broadband wireless access," *IEEE Commun. Mag.*, vol. 40, no. 9, pp. 136–142, Sept. 2002.
- [42] S. M. Alamouti, "A simple transmit diversity technique for wireless communications," *IEEE J. Select. Areas Commun.*, vol. 16, no. 8, pp. 1451–1458, Oct. 1998.
- [43] V. Tarokh, N. Seshadri, and A. R. Calderbank, "Space-time codes for high data rate wireless communication: performance criterion and code construction," *IEEE Trans. Inform. Theory*, vol. 44, no. 2, March 1998.
- [44] V. Tarokh, A. Naguib, N. Seshadri, and A. R. Calderbank, "Space-time codes for high data rate wireless communication: performance criterion in presence of channel estimation errors, mobility, and multiple paths," *IEEE Trans. Commun.*, vol. 47, no. 2, Feb. 1999.
- [45] T. H. Liew and L. Hanzo, "Space-time codes and concatenated channel codes for wireless communications," *Proc. IEEE*, vol. 90, no. 2, pp. 187–219, Feb. 2002.
- [46] V. Tarokh, H. Jafarkhani, A. R. Calderbank, "Space-time block codes from orthogonal designs," *IEEE Trans. Inform. Theory*, vol. 45, no. 5, pp. 1456–1467, July 1999.
- [47] B. M. Hochwald, T. L. Marzetta, T. J. Richardson, W. Sweldens, R. Urbanke, "Systematic design of unitary space-time constellations," *IEEE Trans. Inform. Theory*, vol. 46, no. 6, pp. 1962–1973, Sept. 2000.
- [48] B. L. Hughes, "Differential space-time modulation," *IEEE Trans. Inform. Theory*, vol. 46, no. 7, pp. 2567–2578, Nov. 2000.
- [49] E. G. Larsson, P. Stoica, J. Li, "On maximum-likelihood detection and decoding for space-time coding systems signal processing," *IEEE Trans. Commun.*, vol. 50, no. 4, pp. 937–944, April 2002.
- [50] S. Sandhu, R. Heath, A. Paulraj, "Space-time block codes versus space-time trellis codes," *Communications, IEEE International Conference on*, vol. 4, pp. 1132–1136, 2001.

- [51] B. M. Hochwald and W. Sweldens, "Differential unitary space-time modulation," *IEEE Trans. Commun.*, vol. 28, no. 12, pp. 2041–2045, Dec. 2000.
- [52] —, "Differential unitary space-time modulation," *IEEE Trans. Commun.*, vol. 48, no. 12, pp. 2041–2052, Dec. 2000.
- [53] B. L. Hughes, "Space-time group codes," *Thirty-Fourth Asilomar Conference*, vol. 1.1, pp. 699–704, 2000.
- [54] P. Li, K. B. Letaief, "Differential space-time multi-block decoding," *Wireless Communications and Networking Conference, IEEE*, vol. 1, pp. 239–243, 2002.
- [55] J. Liu, J. Li, H. Li and E. G. Larsson, "Differential space-code modulation for interference suppression," *IEEE Trans. Signal Processing*, vol. 49, no. 8, pp. 1786–1795, Aug. 2001.
- [56] J. Liu, E. G. Larsson, J. Li and H. Li, "High-rate differential space-code modulation for interference suppression," *Third IEEE signal processing workshop on signal advances in Wireless communications, Taiwan*, pp. 283–286, Mar. 2001.
- [57] P. Hoeher, "A statistical discrete-time model for the WSSUS multipath channel," *IEEE Trans. Veh. Technol.*, vol. 41, no. 4, pp. 461–468, Nov. 1992.
- [58] J. G. Proakis, *Digital communications, 3rd Ed.* McGraw-Hill., 1995.
- [59] K. Yu, B. Ottersten, "Models for MIMO propagation channels: a review," *Wirel. Commun. Mob. Comput.*, pp. 653–666, 2002.
- [60] D. Gesbert, H. Bolcskei, D. A. Gore, A. J. Paulraj, "Outdoor MIMO wireless channels: Models and performance predication," Jan. 2003. [Online]. Available: [http://www.ifi.uio.no/~gesbert/papers/mimo\\_final.pdf](http://www.ifi.uio.no/~gesbert/papers/mimo_final.pdf)
- [61] L. Tong, S. Perreau, "Multichannel blind identification: from subspace to maximum likelihood methods," *Proc. IEEE*, vol. 86, no. 10, pp. 1951–1968, Oct. 1998.
- [62] G. B. Giannakis, Y. Hua, P. Stoica and L. Tong, *Signal Processing Advances in Wireless and Mobile Communications*. Prentice Hall PTR, 2001, vol. 1,2.
- [63] Y. Hua, K. Abed-Meraim, M. Wax, "Blind system identification using minimum noise subspace," *IEEE Trans. Signal Processing*, vol. 45, no. 3, pp. 770–773, June 1997.
- [64] K. Abed-Meraim, W. Qiu, Y. Hua, "Blind system identification," *Proc. IEEE*, vol. 85, no. 8, pp. 1310–1322, Aug. 1997.
- [65] Z. Ding, L. Qiu, "Blind MIMO channel identification from second order statistics using rank deficient channel convolution matrix," *IEEE Trans. Signal Processing*, vol. 51, no. 2, pp. 535–544, Feb. 2003.



- [66] Z. Ding, "Matrix outer-product decomposition method for blind multiple channel identification," *IEEE Trans. Signal Processing*, vol. 45, no. 12, pp. 3053–3061, Dec. 1997.
- [67] D. Gesbert, P. Duhamel, S. Mayrargue, "Blind least-squares approaches for joint data/channel estimation," *Digital Signal Processing Workshop Proceedings*, pp. 450–453, 1996.
- [68] —, "On-line blind multichannel equalization," *IEEE Trans. Signal Processing*, vol. 85, no. 8, pp. 2307–2317, Sept. 1997.
- [69] J. Liang, Z. Ding, "Blind MIMO system identification based on cumulant subspace decomposition," *IEEE Trans. Signal Processing*, vol. 51, no. 6, pp. 1457–1465, June 2003.
- [70] S. Haykin, *Adaptive Filter Theory*, 3rd Ed. Prentice Hall, 1996.
- [71] B. Sklar, "Rayleigh fading channels in mobile digital communication systems. ii: Mitigation," *IEEE Commun. Mag.*, vol. 35, no. 9, pp. 148–155, Sept. 1997.
- [72] C. Tidestav, "The multivariable decision feedback equalizer: multiuser detection and interference rejection," Ph.D. dissertation, Uppsala University, Uppsala, 1999. [Online]. Available: <http://www.signal.uu.se/Publications/abstracts/a993.html>
- [73] A. M. Tehrani, "Space-time equalization in wireless systems with multiple transmit/receive array antennas," Ph.D. dissertation, Stanford University, November 2000.
- [74] A. Lozano, C. Papadias, "Layered space-time receivers for frequency-selective wireless channels," *IEEE Trans. Commun.*, vol. 50, no. 1, pp. 65–73, Jan. 2002.
- [75] H. Mathis, "Nonlinear functions for blind separation and equalization," Ph.D. dissertation, Swiss federal institute of technology, Zurich, 2001. [Online]. Available: [www.isi.ee.ethz.ch/publications/disseth/14313.pdf](http://www.isi.ee.ethz.ch/publications/disseth/14313.pdf)
- [76] C. R. Johnson, P. Schniter, T. J. Endres, J. D. Behm, D. R. Brown, R. A. Casas, "Blind equalization using the constant modulus criterion: A review," *Proc. IEEE*, vol. 86, no. 10, pp. 1927–1950, Oct. 1998.
- [77] L. J. Cimini, "Analysis and simulation of a digital mobile channel using orthogonal frequency division multiplexing," *IEEE Trans. Commun.*, vol. Com-33, no. 7, pp. 665–675, July 1985.
- [78] J. J. V. Beek, O. Edfors, M. Sandell, S. K. Wilson, P. O. Borjesson, "On channel estimation in OFDM systems," *IEEE VTC*, 45th, vol. 2, pp. 25–28, July 1995.

- [79] Y. Li, J. H. Winters, N. R. Sollenberger, "MIMO-OFDM for wireless communications: signal detection with enhanced channel estimation," *IEEE Trans. Commun.*, vol. 50, no. 9, pp. 1471–1477, Sept. 2002.
- [80] Y. Li, K. J. R. Liu, "Blind identification and equalization for multiple-input/multiple-output channels," *Global Telecommunications Conference, 1996. GLOBECOM '96*, vol. 3, no. 18-22, pp. 1789–1793, Nov. 1996.
- [81] H. Sampath, S. Talwar, J. Tellado, V. Erceg, A. Paulraj, "A fourth-generation MIMO-OFDM broadband wireless system: design, performance, and field trial results," *IEEE Commun. Mag.*, vol. 40, no. 9, pp. 143–149, Sep. 2002.
- [82] L. Tong, G. Xu, T. Kailath, "A new approach to blind identification and equalization of multipath channels," *Signals, Systems and Computers, 1991. 1991 Conference Record of the Twenty-Fifth Asilomar Conference on*, vol. 2, pp. 856–860, 1991.
- [83] ———, "Blind identification and equalization based on second-order statistics: A time domain approach," *IEEE Trans. Inform. Theory*, vol. 40, no. 2, pp. 340–349, Mar. 1994.
- [84] A. Gorokhov, M. Kristensson, B. Ottersten, "Robust blind second-order deconvolution," *IEEE Signal Processing Lett.*, vol. 6, no. 1, pp. 13–16, Jan. 1999.
- [85] F. Alberge, P. Duhamel, M. Nikolova, "Adaptive solution for blind identification equalization using deterministic maximum likelihood," *IEEE Trans. Signal Processing*, vol. 50, no. 4, pp. 923–936, April 2002.
- [86] G. B. Giannakis, C. Tepedelenlioglu, "Basis expansion models and diversity techniques for blind identification and equalization of time-varying channels," *Proc. IEEE*, vol. 86, no. 10, pp. 1969–1986, Oct. 1998.
- [87] A. J. van der Veen, S. Talwar and A. Paulraj, "A subspace approach to blind space-time signal processing for wireless communication systems," *IEEE Trans. Signal Processing*, vol. 45, no. 1, pp. 173–190, Jan. 1997.
- [88] T. L. Marzetta, "BLAST training: Estimating channel characteristics for high capacity space-time wireless," *Proc. of 37th Annual allerton conf. on Comm, Control, and Computing, Monticello, IL*, Sept. 1999.
- [89] Q. Shi, "OFDM in bandpass nonlinearity," *IEEE Trans. Consumer Electron.*, vol. 42, no. 3, pp. 253–258, Aug. 1996.
- [90] A. Czylik, "Degradation of multi-carrier and single carrier transmission with frequency domain equalization due to pilot-aided channel estimation and frequency synchronization," *GLOBECOM'97, IEEE*, vol. 1, pp. 27–31, 1997.

- [91] L. Deneire, "Training sequence versus cyclic prefix-a new look on single carrier communication," *IEEE Commun. Lett.*, vol. 5, no. 7, pp. 262–274, July 2001.
- [92] J. G. Proakis, D. G. Manolakis, *Digital Signal Processing principles, algorithms, and applications, 3rd Ed.* Prentice Hall, 1996.
- [93] L. L. Scharf, *Statistical signal processing-detection, estimation and time series analysis.* Addison-Wesley publishing company, 1990.
- [94] Y. Wang, Y. C. Pati, Y. M. Cho, A. Paulraj and T. Kailath, "A matrix factorization approach to signal copy of constant modulus signals arriving at an antenna array," *Proc. 28th Conf. Inform.Sci.Syst., Princeton, NJ*, pp. 178–183, Mar. 1994.
- [95] S. N. Diggavi, N. Al-Dhahir, A. Stamoulis, A. R. Calderbank, "Differential Space-Time Coding For frequency-Selective Channel," *IEEE Commun. Lett.*, vol. 6, no. 6, pp. 253–255, June 2002.
- [96] C. R. Rao, M. B. Rao, *Matrix algebra and its applications to statistics and econometrics.* World scientific publishing .Ltd., 1998.
- [97] S. M. Kay, *Fundamentals of statistical signal processing: estimation theory.* PTR Prentice hall, Englewood cliffs, NJ., 1993.
- [98] G. H. Golub, C. F. V. Loan, *Matrix computations, 2nd Ed.* The John Hopkins University Press, 1989.
- [99] S. Verdù, "Fifty years of Shannon theory," *IEEE Trans. Inform. Theory*, vol. 44, no. 6, pp. 2057–2078, Oct. 1998.
- [100] G. Ungerboeck, "Channel coding with multilevel/phase signals," *IEEE Trans. Inform. Theory*, vol. IT-28, no. 1, pp. 55–66, Jan. 1982.
- [101] G. D. Forney, Jr. and R. Gallager and G. R. Lang and F. M. Longstaff and S. U. Qureshi, "Efficient modulation for band-limited channels," *IEEE J. Select. Areas Commun.*, vol. SAC-2, no. 5, pp. 632–646, Jan. 1984.
- [102] R. Krishnamoorthy, "MIMO: The preferred choice for wireless last-mile access," *WCA technical symposium, San Jose*, Jan. 14-16 2002.
- [103] E. Telatar, "Capacity of multi-antenna Gaussian channels," *European Trans. on Telecommun.*, vol. 10, no. 6, pp. 585–595, Nov./Dec. 1999.
- [104] G. J. Foschini, G. D. Golden, R. A. Valenzuela, P. W. Wolniansky, "Simplified processing for high spectral efficiency wireless communication employing multi-element arrays," *IEEE J. Select. Areas Commun.*, vol. 17, no. 11, pp. 1841–1852, Nov. 1999.

- [105] G. J. Foschini and M. J. Gans, "On limits of wireless communications in a fading environment when using multiple antennas," *Wireless personal communications, Kluwer academic publishers*, vol. 6, pp. 311–335, 1998.
- [106] K. Liu and A. M. Sayeed, "Improved layered space-time processing in multiple antenna systems," *Proc. the 38th Annual Allerton Conference on Communication, Control and Computing*, Oct. 2001.
- [107] A. J. Paulraj, E. Lindskog, "Taxonomy of space-time processing for wireless networks," *IEE proc.-Radar, Sonar Navig.*, vol. 145, no. 1, pp. 25–31, Feb 1998.
- [108] J. P. Kermoal, P. E. Mogensen, S. H. Jensen, J. B. Andersen, F. Frederiksen, T. B. Sorensen, K.I. Pedersen, "Experimental investigation of multipath richness for multi-element transmit and receive antenna arrays," *VTC 2000-Spring Tokyo. IEEE 51st*, vol. 3, pp. 2004–2008, 2000.
- [109] D. Yoo and W. E. Stark, "Characterization of multipath fading channels," Feb. 2003. [Online]. Available: [www.eecs.umich.edu/~dyoo/publications/journal/yoo02B.pdf](http://www.eecs.umich.edu/~dyoo/publications/journal/yoo02B.pdf)
- [110] E. N. Onggosanusi, A. M. Sayeed, B. D. Van Veen, "Canonical space-time processing for wireless communications," *IEEE Trans. Commun. Technol.*, vol. 48, no. 10, pp. 1669–1680, Oct. 2000.
- [111] A. M. Sayeed, E. N. Onggosanusi, B. D. Van Veen, "A canonical space-time characterization of mobile wireless channels," *IEEE Communications Letters*, vol. 3, no. 4, pp. 94–96, April 1999.
- [112] J. B. Andersen, T. S. Rappaport, S. Yoshida, "Propagation measurements and models for wireless communications channels," *IEEE Commun. Mag.*, vol. 33, no. 1, pp. 42–49, Jan. 1995.
- [113] K. I. Pedersen, J. B. Andersen, J. P. Kermoal, P. Mogensen, "A stochastic multiple-input-multiple-output radio channel model for evaluation of space-time coding algorithms," *Vehicular Technology Conference, 2000. IEEE-VTS Fall VTC 2000. 52nd*, vol. 2, pp. 893–897, 2000.
- [114] R. Prasad, T. Ojanpera, "A survey on CDMA: evolution toward wideband CDMA," *Spread Spectrum Techniques and Applications, 1998. Proceedings.*, vol. 1, pp. 323–331, 1998.
- [115] T. S. Rappaport, S. Y. Seidel, K. Takamizawa, "Statistical channel impulse response models for factory and open plan building radio communicate system design," *IEEE Trans. Commun. Technol.*, vol. 39, no. 5, pp. 784–807, May 1991.
- [116] A. Dogandic and J. Jin, "Estimating statistical properties of MIMO fading channels," Jan. 2002. [Online]. Available: <http://clue.eng.iastate.edu/~ald/>

- [117] N. D. Sidiropoulos, R. Bro, G. B. Giannakis, "Parallel factor analysis in sensor array processing," *IEEE Trans. Signal Processing*, vol. 48, no. 8, pp. 2377–2388, Aug. 2000.
- [118] N. D. Sidiropoulos, G. B. Giannakis, R. Bro, "Blind PARAFAC receivers for DS-CDMA systems," *IEEE Trans. Signal Processing*, vol. 48, no. 8, pp. 810–823, Mar. 2000.
- [119] A. F. Naguib, N. Seshadri, A. R. Calderbank, "Increasing data rate over wireless channels," *IEEE Signal Processing Mag.*, vol. 17, no. 3, pp. 76–92, May 2000.
- [120] G. D. Forney, Jr., "Maximum-likelihood sequence estimation of digital sequences in the presence of intersymbol interference," *IEEE Trans. Inform. Theory*, vol. IT-18, no. 3, pp. 363–378, May 1972.
- [121] J. Hagenauer, P. Hoeher, "A Viterbi algorithm with soft-decision outputs and its applications," *IEEE Global Telecommunications Conference*, pp. 1680–1686, Oct. 1989.
- [122] B. L. Hughes, "Further results on differential space-time modulation," *IEEE Sensor Array and Multichannel Signal Processing Workshop*, pp. 163–167, 2000.
- [123] H. Liu, G. Xu, "A deterministic approach to blind symbol estimation," *IEEE Signal Processing Lett.*, vol. 1, no. 12, pp. 205–207, Dec. 1994.
- [124] G. B. Giannakis, "Blind equalization of time-varying channels: a deterministic multichannel approach," *Statistical Signal and Array Processing, 1996. Proceedings., 8th IEEE Signal Processing Workshop on*, pp. 180–183, 1996.
- [125] G. B. Giannakis, C. Tepedelenlioglu, "Direct blind equalizers of multiple FIR channels: a deterministic approach," *IEEE Trans. Signal Processing*, vol. 47, no. 1, pp. 62–74, Jan. 1999.
- [126] R. F. H. Fischer, C. Windpassinger, A. Lampe, J. B. Huber, "Tomlinson-Harashima precoding in space-time transmission for low-rate backward channel," *Broadband Communications, 2002. Access, Transmission, Networking. 2002 International Zurich Seminar on*, pp. 7–1–7–6, 2002.
- [127] M. Brookes, "Matrix reference manual," June 2001. [Online]. Available: <http://www.ee.ic.ac.uk/hp/staff/dmb/~matrix/intro.html>
- [128] H. Gazzah, P. Regalia, J. Delmas, K. Abed-meraim, "A blind multichannel identification algorithm robust to order overestimation," *IEEE Trans. Signal Processing*, vol. 50, no. 6, pp. 1449–1458, June 2002.
- [129] A. P. Liavas, "Least-squares channel equalization performance versus equalization delay," *IEEE Trans. Signal Processing*, vol. 48, no. 6, pp. 1832–1835, June 2000.

- [130] K. Abed-meraim, Y.Hua, P.loubaton , E. Moulines, "Subspace method for blind identification of multichannel FIR systems in noise field with unknown spatial covariance," *IEEE Signal Processing Lett.*, vol. 4, no. 5, pp. 135–137, May 1997.
- [131] A. P. Liavas, P.A. Regalia, J.P.Delmas, "Robustness of least-squares and subspace methods for blind channel identification /equalization with respect to effective channel undermodeling /overmodeling," *IEEE Trans. Signal Processing*, vol. 47, no. 6, pp. 1636–1645, June 1999.
- [132] Y. Hua, S. An, Y. Xiang, "Blind identification of FIR MIMO channels by decorrelating subcahnnels," *IEEE Trans. Signal Processing*, vol. 51, no. 5, pp. 1143–1155, May 2003.
- [133] A. Swami, G. B. Giannakis, G. Zhou, "Bibliography on higher-order statistics," *Signal processing*, vol. 60, no. 65-126, pp. 65–126, 1997.
- [134] Z. Zhang and J. Ilow, "Frequency domain equalization for MIMO space-time transmission with single carrier signaling," in *the IEEE International Symposium on Personal, Indoor, and Mobile Radio Communications, 'PIMRC 2003'*, Beijing, Sept. 2003.
- [135] —, "A receiver algorithm for unitary space-time differentially encoded transmissions of FIR multipath channels," in *IEEE International Workshop on Mobile and Wireless Communications Network, 2002*, Stockholm, Sweden, Sept., 2002, pp. 429–433.
- [136] —, "Frequency domain equalization with multiple receiving antennas for single carrier signaling," in *Communication Networks & Services Research (CNSR) 2003 Conference*, Moncton, New Brunswick, Canada, May 15-16, 2003.
- [137] —, "Multiwavelet-based fractal modulation," in *Proceedings of the IASTED International Conference on Wireless and Optical Communications*, Banff, Canada., July, 17-19, 2002.
- [138] —, "Signal reception for space-time differentially encoded transmissions over FIR rich-multipath channels," Dec., 2002, Submitted to EUROCHIP Journal on Applied Signal Processing.
- [139] —, "A differential space-time transceiver for unknown multi-path time-dispersive channels," Aug., 2003, Submitted to IEEE ISSPIT 2003, Darmstadt, Germany.